**Neurological Effects of Low-Level, Chronic**
**Domoic Acid Exposure in a Nonhuman Primate Model**

Rebekah Lee Petroff

A dissertation submitted
in partial fulfillment of the
requirements for the degree of

Doctor of Philosophy

University of Washington
2020

Reading Committee:
Dr. Thomas M. Burbacher, Chair
Dr. Elaine M. Faustman
Dr. Todd Richards

Program Authorized to Offer Degree:
Public Health – Environmental and Occupational Health Sciences

University of Washington

## Abstract

Neurological Effects of Low-Level, Chronic
Domoic Acid Exposure in a Nonhuman Primate Model

Rebekah Lee Petroff

Chair of the Supervisory Committee:
Thomas M. Burbacher
Environmental and Occupational Health Sciences

Global oceans play an important role in many aspects of human life. We build our homes on the shores, take our food from the waters, and create our economies from the wealth of resources in marine waters. There is a growing recognition, however, that certain species of marine algae produce potent toxins that can accumulate in seafood and pose health risks to human and wildlife populations. Domoic acid (DA), the focus of this dissertation, is produced by algae in the genus *Pseudo-nitzschia*. DA is a potent glutamate receptor agonist and neurotoxin, and high-dose exposure to this toxin has been associated with severe illness and permanent memory loss. Although there are strict regulatory limits preventing human exposures greater than 0.075-0.1 mg/kg, recent studies have suggested that repeated and chronic exposures below these levels may affect memory and learning in adults (Grattan et al., 2016, 2018).

The studies described in this dissertation took place as part of a larger investigation on the reproductive and developmental consequences of low-dose, chronic DA exposure during pregnancy in a nonhuman primate model (*Macaca fascicularis*). Early results from this study demonstrated that daily, oral exposure to 0.075 to 0.15 mg DA/kg/day for up to two years, induced symptoms in adults that were manifested as intention tremors (Burbacher et al., 2019). Given that previous studies have found oral doses up to ten times greater than those used in the present study were not overtly toxic, this observation was unexpected (Truelove et al., 1998). The three experiments detailed in Chapters 2, 3 and 4 were designed to further identify the brain's structural, physiological, and cellular effects in this unique cohort of animals and provide a greater understanding of the health risks associated with chronic, low-dose DA exposure.

In the first study, *in vivo* work using magnetic resonance imaging (MRI) demonstrated that the previously observed intention tremors were associated with white matter deficits in a key neural circuit involved in memory processing, including the fornix and internal capsule (Petroff et al., 2019). In the second study, electroencephalography (EEG) data were collected from sedated adult females, and results suggested subtle changes in power of DA-exposed animals that may be associated with neurophysiological changes (Petroff, et al., submitted). The final body of work in this dissertation integrates these findings by using *in vivo* MRI scans and *ex vivo* histopathology to understand the cellular level effects of low-level chronic exposure to DA. Study data revealed that animals exposed to DA and displaying clinical symptomology have a higher incidence of focal microglia reactions, which may be related to the observed decreases in white matter integrity and due to the activation of neuroinflammation pathways (Petroff et al., in preparation). Collectively, the studies described in this dissertation provide the first data on chronic, low-dose oral exposure in a preclinical nonhuman primate model and explore the consequences of DA on adult neurophysiology and macro and microstructural changes in the

brain. Vulnerable human populations, such as high-frequency shellfish consumers and coastal dwelling communities, may not be fully protected by existing guidelines and further longitudinal investigation is warranted to adequately protect public health.

**Table of Contents**

**List of Figures**

**List of Tables**

**Acknowledgements**

Acknowledgements alone could never express my gratitude to the innumerable kind and caring mentors, supporters, and loved ones that helped me through this dissertation. Regardless, here is my best attempt at it.

To Tom – thank you. You are one the most thoughtful and supportive mentors that I could have known. Working in your lab, teaching alongside you, and learning the ins and outs of how to be a professional, real-life scientist has given me the skills and knowledge I need to succeed in the future. You helped redirect my over-the-top enthusiasm for fun new ideas, shaping them into realistic and achievable goals. Your openness to new suggestions and patience while re-explaining concepts and ideas is, and will always be, deeply appreciated. Thank you for everything.

To Kim – thank you for teaching me compassion in science and life and pushing my writing to the next level. You taught me how to invite others in and approach difficult situations with the utmost level of care. Your time spent going above and beyond to check in or meticulously edit my many, many drafts is truly priceless to me. Your mentorship encouraged me throughout good times and bad, and my gratitude for you and your support is immeasurable.

Many other mentors helped along the way. Thank you to the plethora of other collaborators on this project – Drs. Todd Richards, Mike Murias, Jean Harry, Audrey Baldessari, and Nina Isoherranen. None of this research could have happened without your support. A special thank you goes to Todd for teaching me so much about a topic of which I knew so little. A wordy appreciation is heartfully extended to Jean, who let me crash in her lab for nearly a month and offered her very limited time to me, supporting my growth in this field.

Nearly every member of DEOHS Toxicology faculty facilitated my growth as a student, teacher and scientist, but a special acknowledgement is reserved for my other committee members, Elaine and Terry. Thank you for your mentorship and support in this research. Thank you, Kathi, for serving on my committee and supporting my studies. Thank you to Dave for

graciously acting as my GSR in this process. All of your recommendations and support helped shaped this dissertation and my growth as a scientist.

Thank you to all the other staff and student volunteers at the Washington National Primate Research Center for your help in conducting this research and teaching me new techniques. Brenda - you rock. You work so hand, and you taught me so much. You are caring, kind and one of the best friends and mentors that I could have asked for.

To all the staff and other students at DEOHS – thank you. I will miss sharing my experiences and growing with the caring community fostered in this department. A special thanks goes out to my other disserters, Team Tox, and WIPS ladies for the comradery and support throughout graduate school and life. You are all amazing people, and I could not have gotten through this without you.

Finally, thank you to all my non-academic supporters. To my friends and family, thank you for your love, support, and reminder of all the great things outside of academia. My parents and sisters especially. To Ben – your many homecooked meals and eternal loving patience with 2 am experimental timings and too many work weekends got me through this. I could not have asked for a better partner. Thank you.

**Funding**

Research in this dissertation could not have been completed without support from multiple institutions including the National Institute of Environmental Health Sciences (NIEHS, R01 ES023043), Washington National Primate Research Center (NIH grant: P51 OD010425), the University of Washington Interdisciplinary Center for Exposures, Diseases, Genomics and Environment (NIH P30ES007033), the Castner family and their generous gift, and the support from the Department of Environmental and Occupational Health Sciences at the University of Washington.

**Chapter 1: Introduction – Low-Level Exposure to the Common Marine Toxin, Domoic Acid, and Contemporay Risks to Human Health**

*A revised version of this chapter will be submitted for an invited review in Pharmacology and Therapeutics. The authors are:*

Rebekah Petroff,[1] Alicia Hendrix,[1] Kimberly S. Grant,[1,2] Thomas M. Burbacher [1,2,3]

[1] Department of Environmental and Occupational Health Sciences, University of Washington, Seattle, Washington, USA

[2] Center on Human Development and Disability, Seattle, Washington, USA

[3] Infant Primate Research Laboratory, Washington National Primate Research Center, Seattle, Washington, USA

Corresponding Author:

Rebekah Petroff

Department of Environmental and Occupational Health Sciences

School of Public Health, Box 357234

1959 NE Pacific Street

University of Washington

Seattle, WA 98195

petroffr@uw.edu

## 1.1 Oceans and Human Health

Oceans cover over 70% of the Earth's surface; we lean on them to supply our foods and medicines, while building our homes and recreational lives on shores and coastlines. Amidst the growing pressures of climate change and other anthropogenic strains, the health of our oceans is increasingly threatened. Many species of marine algae are an essential part of oceanic ecosystems, but some can produce dangerous toxins that pose a health risk to humans and wildlife alike. Domoic acid (DA), the cause of Amnesic Shellfish Poisoning (ASP) and the focus of this dissertation, is a common marine neurotoxin produced by algae in the genus *Pseudo-nitzschia*. This naturally occurring toxin concentrates in shellfish and finfish, where it can persist for weeks after an algal bloom subsides (Wekell et al., 1994b, 1994a). In recent years, record-breaking concentrations of DA in clams, mussels, oysters and Dungeness crab have been recorded, and exposures in coastal dwelling populations have become a significant public health concern (Du et al., 2016; Trainer and Hardy, 2015).

The use of DA was documented as early as 1958 in Japan, where it was characterized as an anti-parasitic treatment when administered in doses of 20 mg (Takemoto and Daigo, 1958). It was not until nearly thirty years later, when the potent neurotoxicity of the compound was fully revealed. On Prince Edward Island, Canada, over 150 people were sickened after consuming DA-contaminated shellfish (Perl et al., 1990b, 1990a). Of those who met the case definition (having gastrointestinal or neurological symptoms within 48 hrs after consuming mussels), most reported upset stomachs, vomiting and diarrhea that developed within 4-5 hours of exposure. Additionally, 18% were admitted to the hospital with seizures and a host of other neurological symptoms, which ranged from uncontrollable emotionality to coma. Four people died as a result of DA toxicity (Perl et al., 1990b).

The pressures of climate change are shifting the historical pattern of *Pseudo-nitzschia* algal blooms (McKibben et al., 2017) and contributing to larger, more severe, and longer lasting

blooms (Wells et al., 2015a, 2020). DA has now been documented in ocean waters around the globe (Bates et al., 2018) and in 2016, the largest DA bloom ever recorded extended from California to the Alaskan Peninsula (McCabe et al., 2016). When these ecological changes are considered in the context of increasing human reliance on seafood as a major source of dietary protein (FAO United Nations, 2013), there is heightened risk for human exposure to DA at or near the current regulatory limit (0.075 to 0.1 mg/kg/day) (Andjelkovic et al., 2012; Ferriss et al., 2017). Very little is known about the health effects of longer-term exposure near this limit, because most studies of DA effects have focused on using high doses to explore frank neurotoxicity (Lefebvre and Robertson, 2010). A few recent reports have indicated that long-term, low level DA exposures result in functional effects in adults. Studies with animal and human populations suggest that chronic DA exposures at low levels are associated with deficits in memory and upper limb tremors (Burbacher et al., 2019; Grattan et al., 2018, 2016; Lefebvre et al., 2017). Subsequently, there is concern that the current regulatory limits may not adequately protect sensitive populations. For example, new guidance in Washington State suggests limiting the consumption of razor clams for everyone, but particularly for “women who are or might become pregnant, nursing mothers, children, the elderly, and people with compromised renal function” (Washington State Department of Health, n.d.). A review of the studies that provide critical data regarding DA toxicity following acute, subacute, and chronic exposures is presented below.

### 1.3 Acute Human Exposures and Subsequent Environmental Regulation

As described earlier, the largest human episode of DA poisoning occurred in 1987 on Prince Edward Island, Canada and provided data on the acute health effects of DA at very high levels of exposure (60 to 290 mg/patient) (Perl et al., 1990b). In addition to a range of symptoms associated with overt illness, neuropsychological examinations of affected patients revealed a

unique pattern of functional losses consistent with anterograde amnesia (Todd, 1993). The term "Amnesic Shellfish Poisoning" is now widely used to refer to the clinical symptomology associated with acute DA toxicity (Perl et al., 1990a). Anterograde amnesia is characterized by the lack of ability to form new memories (Tulving, 1983), and, in more extreme DA poisoning cases, patients with amnesia had persistent and long-term memory deficits (Zatorre, 1990). One patient that initially survived the poisoning, but later developed temporal lobe epilepsy, died within a year (Cendes et al., 1995). Several individuals sickened by DA underwent magnetic resonance imaging (MRI), positron emission tomography (PET) scans, and electroencephalography (EEGs) assessments. MRI and PET results demonstrated that patients expressed acute neuronal death in the amygdala and parahippocampal gyrus, as well as moderate to severe disturbances in electrophysiology, namely spikes and seizure-like activity (Gjedde and Evans, 1990; Teitelbaum et al., 1990). Histopathological follow-up in deceased patients also reported injury to the amygdala and hippocampus, while identifying additional neuronal death and astrocyte reactivity in the amygdala, hippocampus, olfactory cortex, and thalamus (Carpenter, 1990). This pattern of damage mirrors that found in the hippocampal-anterior thalamus circuit, causing anterograde amnesia from other sources (Aggleton and Brown, 1999).

The severity of illness observed in DA-exposed patients prompted policy makers to develop regulations to protect shellfish consumers from high dose DA toxicity (Wekell et al., 2004). DA was undetectable in the blood and cerebral spinal fluid of patients by the time tests were performed in Canada, but concentrations in local shellfish ranged from 310 to 1280 ppm (Perl et al., 1990b). Additional dose-response calculations by investigators revealed that the lowest level of DA producing symptoms was 50 mg (Wright et al., 1990). By assuming a maximum one-meal seafood consumption of 200 g, and including a 12-fold safety factor, the final regulatory limit was set at 20 ppm in shellfish meat (Wekell et al., 2004). Since then,

research has estimated that the established regulatory limit in seafood is approximately equivalent to 0.075-0.1 mg/kg in adults (Mariën, 1996; Toyofuku, 2006). This limit, however, is based on information from a single episode of high-dose, catastrophic exposure and does not address the health risks associated with lower-dose, chronic exposure.

### 1.4 Chronic Exposure in Human and Wildlife Populations

*Humans*

In the decades following the poisoning event in Canada, research efforts have shifted to explore the health effects of more relevant environmental exposure scenarios. There is considerable interest in identifying populations at heightened risk from chronic, lower-dose exposure given the increasing prevalence of algal blooms that produce DA in global oceanic waters. Some cultural groups, such as coastal Native Tribes in the Pacific Northwest, regularly consume large amounts of seafood and may be chronically exposed to low-dose DA over years and even decades (Crosman et al., 2019). Given the potential for increased exposure in these groups, it is not surprising that a longitudinal study of DA exposure in humans is being conducted in Tribal Nations located on the coast of Washington State.

The Communities Advancing the Studies of Tribal Nations Across the Lifespan (CoASTAL) cohort was established in 2005, and consisted of 678 participants from three coastal tribes in Washington State (Tracy et al., 2016). Researchers used dietary records of the consumption rates of Pacific razor clams (*Siliqua patula*) and state-reported DA shellfish concentrations as a proxy for DA exposure (Fialkowski et al., 2010). Cognitive testing in this cohort revealed that adults consuming >15 razor clams per month had decreases in some aspects of memory compared to those who ate <15 clams per month, but these changes were not considered clinically significant (Grattan et al., 2016a). Slight performance decreases were observed in complex attention and concentration on the WAIS-III Digit Symbol Coding test and

memory on free and delayed recall tests. Follow-up studies in a smaller sub-sample found that difficulties with everyday memory were significantly associated with the frequent consumption of razor clams (Grattan et al., 2018). The overall results from this ground-breaking longitudinal study suggest that chronic exposure to DA at levels that are considered safe may disrupt memory in human adults.

*Sea Lions*

In addition to chronic exposures in humans, there are wildlife populations such as California sea lions (*Zalophus californianus*) exposed to DA on a regular basis. After acute, high-dose exposure, sea lions demonstrate marked symptomology similar to humans, including disorientation, seizures, coma and death (Gulland et al., 2002; Scholin et al., 2000). Chronic exposures in this species have been associated with deficits in spatial memory as well as damage to major white matter tracts in the brain (Cook et al., 2018, 2015). Sea lion studies are important but are limited in translational value because exposure levels cannot be well-characterized and are likely much higher than human exposures. Even with these caveats, continued efforts into the development of a translational serum-based antibody biomarker hold promise for the near future (Lefebvre et al., 2019, 2012). This biomarker has the potential to distinguish between short-term and chronic exposure and may eliminate current barriers in studying the chronic effects of DA in humans.

### 1.5 Domoic Acid Toxicity Mechanism

DA is a small, polar amino acid, structurally similar to the neurotoxin, kainic acid (KA), and the endogenous neurotransmitter, glutamate (Fig. 1.1) (Wright et al., 1989). Species of algae produce DA in combination with at least 10 other isomers, which have varying degrees of toxicity (Clayden et al., 2005; Wright et al., 1990). Once concentrated in shellfish tissue, DA

does not degrade easily, even with typical cooking and freezing methods (McCarron and Hess, 2006).

When contaminated seafood is consumed, DA is slowly absorbed in the gut, with a bioavailability of <10% (Iverson and Truelove, 1994; Jing et al., 2018; Truelove et al., 1997). It crosses the blood-brain barrier at a rate similar to sucrose (Preston and Hynie, 1991), where it binds to α-amino-3-hydroxy-5-methyl-4-isoxazolepropionic acid (AMPA) and kainic acid (KA) type glutamate receptors (Stewart et al., 1990), triggering a series of events typical of glutamate derived excitotoxicity (Fig. 1.2) (Wang and Qin, 2010). In cases of acute high-dose exposure, activated AMPA and KA receptors open, allowing an influx of $Na^{+}$ into the cell and the release of glutamate into the synapse. N-methyl-D-aspartic acid (NMDA) receptors are then indirectly activated via the released glutamate, and $Ca^{+2}$ ions subsequently flood into the cell. This potent activation causes the depolarization of the post-synaptic cell and leads to excessive production of reactive oxygen species (ROS) via the disruption of normal mitochondria function, ultimately activating necrotic cell death pathways.

Presently, the consensus on the mechanism of action at acute exposure levels (>100 µM in cell cultures) is well established, but lower level effects are not well understood. Currently it is thought that lower dose exposure may not involve the activation of NMDA type receptors, but instead produce lower amounts of ROS and activate the apoptotic cell death pathways. In primary mesencephalic cell cultures, the increase in ROS has been linked to low-level DA binding to AMPA and KA receptors, releasing enough $Ca^{+2}$ to interfere with mitochondrial function and increase ROS, but not enough $Ca^{+2}$ to release the neurotransmitter glutamate and involve additional signaling pathways (Radad et al., 2018). At moderate levels of exposure (~20 µM) in mixed cortical cultures, DA can induce high levels of cell death in the course of a 2-hr exposure, but exposures of ~10 µM are sufficient to induce similar levels of neuronal death after 2 hr exposure + 22 hr washout (Qiu et al., 2006). Additional experimentation with alternative

time courses of repeat exposures suggests that the severity of DA effects increase with the length of time exposed, but only in cases of low-dose exposures (Qiu et al., 2006).

Potential cell death compensatory mechanisms or other means of cell protection may include several different processes that are dependent on the dose and length of exposure. Low exposure (2 µM) to DA for 24 hrs causes some cell death in organotypic hippocampal slices, but also induces neurogenesis for up to a week post-exposure (Pérez-Gómez and Tasker, 2013, 2012). Prolonged exposure to extremely low levels (5-50 nM for up to ten days) does not cause overt death in neurons or glia *in vitro* rodent cultures of cerebral granule neurons, cortical neurons, and organotypic hippocampal slices (Giordano et al., 2013; Hiolski et al., 2016; Hogberg et al., 2011), but there are some differences in neuroelectrical function measured with microelectrode arrays of cortical neurons, which involves reductions of the inhibitory neurotransmitter, GABA (Hogberg et al., 2011), and the suppression of GABAergic neurons in hippocampal slices (Hiolski et al., 2016). Other low-level mechanisms of toxicity may involve the upregulation of neuroinflammation pathways; low-level exposure increases the production of ROS, and related protective mechanisms that help precondition the cultured cerebral granule neurons for future exposures (Giordano et al., 2013).

### 1.6 Laboratory Models of DA Exposure

The vast majority of what is known about DA neurotoxicity has been generated from studies of acute, high-dose exposure, but this scenario is not very relevant to human populations. Increasingly, the consequences of sub-acute exposures and, more recently, chronic exposures have been the focus of new experimental studies. As detailed in Table 1.1, exposure levels can vary widely across studies, depending on the experimental model and route of exposure used.

*Rodents: Pharmacokinetics*

Rodents have been used in deciphering the neurotoxic effects of DA since the first poisoning in 1987. Initial studies in mice reported neurotoxic symptoms of hind-limb scratching, seizures, and coma and helped reveal DA as the source of toxicity in humans (Iverson and Truelove, 1994). Early on, it was noted that rodents demonstrated a short half-life of DA in the body, with iv administered DA eliminated in urine within several hours (Suzuki and Hierlihy, 1993). Oral administration of rodents however, suggests that rats and mice display different kinetics than primate models, with a bioavailability of ~2% (Truelove et al., 1996) and a much higher resistance to toxic effects after oral exposures (Iverson and Truelove, 1994).

*Rodents: Short-Term, Subacute Studies*

Mice administered a single dose of 1-1.5 mg/kg DA ip do not display signs of overt toxicity (Baron et al., 2013) or histopathology (Vieira et al., 2015), and some research suggests that repeat exposure to 0.5-2 mg/kg ip does not change the toxic response (Peng et al., 1997). Single exposures in rats of 1 mg/kg ip demonstrates stark differences in spontaneous behavior that were not connected to any histopathological changes, suggesting that there may still be functional effects in absence of overt toxicity (Schwarz et al., 2014). Other research using a preconditioning paradigm (i.e. a very low DA dose followed by a higher dose of DA) have demonstrated that a single, nontoxic dose of DA can lessen the impact of repeated exposure to the toxin. Preconditioning with <0.25 mg/kg ip, at least 45 minutes before the administration of 2 mg DA/kg ip, reduced signs of typical DA neurotoxicity (Hesp et al., 2007; Sawant et al., 2010, 2008), suggesting a possible tolerance. This idea of tolerance is supported by observed reductions in the degree of spatial memory impairment following repeated exposures to 1-2 mg/kg ip in mice, compared with impairments in mice with a single exposure (Clayton et al., 1999).

*Rodents: Chronic Studies*

As detailed in Table 1.2, results from studies with repeat exposure to 2 mg DA/kg ip for longer time periods (1 month) suggest that key disruptions in cognition and behavior are caused by neuronal mitochondrial disruption (Lu et al., 2013, 2012; Wang et al., 2018; Wu et al., 2013). In a longer-term study with mice, chronic (25 weeks), low-level DA exposure (0.75 mg/kg/week ip) was associated with deficits in learning and memory, but effects were not observed after cessation of exposure (Lefebvre et al., 2017). These mice had no evidence of gross neuropathological injury, but the expression of glutamate vesicular transporters was increased in the hippocampus, which could potentially disrupt normal glutaminergic synapse function (Moyer et al., 2018).

Alternative routes of exposure have not been extensively utilized in chronic rodent studies. One long-term study in rodents demonstrated that rats orally administered DA at 0.1 and 0.5 mg/kg/day for over 2 months did not reveal signs of overt neurotoxicology or histopathology (Truelove et al., 1996). Another study aimed at assessing developmental toxicity also reported no signs of overt toxicity in the adult female dams chronically exposed to 1 and 3 mg DA/kg/day for nearly 3 weeks (Shiotani et al., 2017).

*Nonhuman Primates: Pharmacokinetics*

Perhaps the most relevant model to contemporary human exposures is research in the nonhuman primate monkey model. Early DA studies demonstrated that the pharmacokinetic properties of DA in monkeys closely mirror humans (Iverson and Truelove, 1994), and initial toxicity symptoms share similar onsets, around 4-5 hrs after consumption (Perl et al., 1990a; Tryphonas et al., 1990c). Recent pharmacokinetic research has used nonhuman primates to model oral exposures in humans, demonstrating that oral DA absorption, and thus peak

exposure, is highly limited (Jing et al., 2018). Bioavailability, however, is still moderate, at ~8% (Jing et al., 2018; Truelove et al., 1997).

*Nonhuman Primates: Chronic Studies*

Chronic toxicity studies in nonhuman primates are limited to two cohorts of animals. One study utilized oral doses of 0.5-0.75 mg/kg/day for 30 days in female macaques and did not reveal signs of overt toxicity, including clinical observations, hematological parameters, and histology of major organs (Truelove et al., 1997). A more recent longitudinal investigation was designed to explore the consequences of chronic, low-dose, oral DA exposure in adult female macaques before and during pregnancy (Burbacher et al., 2019). Animals in this cohort were exposed to 0.075-0.15 mg/kg/day for up to ten months at levels at or near the current regulatory limit. Systematic behavioral assessments revealed signs of neurotoxicity in DA-exposed females that were manifest as intention tremors (Burbacher et al., 2019). The results presented in this dissertation represent an expansion of the research findings in this unique group of animals and provide critical data on brain electrophysiology and histopathology in primates chronically exposed to low levels of DA.

## 1.7 Dissertation Aims

While the acute toxicity of DA is well understood, the effects from chronic, low-level DA exposure are still under investigation. As documented above, previous studies have reported neurological effects of DA following chronic low-level exposures. These effects, however, do not typically include gross signs of neurotoxicity or histopathology but rather encompass a variety of subtle functional and cellular changes in the brain that can significantly impact quality of life. Still, these effects are sparsely reported and bear additional investigation. The present

dissertation delves into this gap by evaluating the neurological effects of chronic, low-level domoic acid exposure in an adult, nonhuman primate model.

Research for this dissertation stems from a larger project using nonhuman primates to assess the maternal reproductive and offspring neurodevelopmental effects from chronic exposure to 0.075-0.15 mg/kg/day DA. As noted above, an unexpected neurological finding from this project was that DA-exposed adult macaques demonstrated novel signs of neurotoxicity – intention tremors when performing a reaching task during regular clinical assessments (Burbacher et al., 2019). DA is known epileptogen and can lead to seizures and gross neuronal damage (Teitelbaum et al., 1990). In animal models, assessment of tremors is limited and can be an inidcator of early signs of seizures or epilepsy (Authier et al., 2019). There are also numerous pathologies that have been associated with human tremors, including disrupted circuitry and cell damage in the brain stem, cerebellum, thalamus, frontal cortex, sensory cortex, and motor cortex (Brittain and Brown, 2013; Louis, 2014; Muthuraman et al., 2015). Additionally, DA has been known to cause atrophy and lesions at high doses in the hippocampus, amygdala, and thalamus (Teitelbaum et al., 1990). Research aims, therefore, were designed to assess global and targeted neurological changes associated with tremors as well as changes previously associated with chronic low-level exposure to DA. The three research aims are to:

1. Characterize injury in areas of the brain that are related to DA exposure and tremors using MRI.

2. Assess functional neuroelectric changes associated with DA exposure and tremors with EEGs.

3. Evaluate cellular changes in brain regions known to be affected by DA by conducting postmortem studies on brain tissue.

Research presented here used the same cohort of adult, female *Macaca fascicularis* monkeys, chronically exposed to 0, 0.075, and 0.15 mg/kg/day, for up to 2 years. Sample sizes for each study depended on available funding (Table 1.3). As detailed in Fig. 1.3, the first set of outcomes included MRIs and EEGs, which were conducted simultaneously, over a period of 5 months. Necropsies and histopathology were subsequently conducted over the following year.

The first analyses used MRI (including diffusion tensor imaging and magnetic resonance spectroscopy) to globally assess neurological injury in the brain related to DA exposure and tremors. Images were first reviewed for any gross lesions that could be the source of tremors. Global measures of structural changes were assessed to identify damage to the white matter (primarily axons and myelin). Concentrations of neurochemicals indicative of global brain damage was then assessed using spectroscopy.

At the same time, studies using EEGs were conducted to assess the functional changes associated with tremors and DA exposure. Power, a quantitative measure from EEGs that reflects the degree of signal generated across the brain was used in this analysis. This measure has been used to identify spectral changes in neurophysiological function in cases of DA-epilepsy (Sawant et al., 2010). Results from EEGs were analyzed to divulge functional electrical signaling changes after DA exposure and assess if tremors may be linked to power changes associated with epilepsy.

Finally, based on the initial global MRI studies, follow-up MRI analyses used volumetry to assess neuronal atrophy in the thalamus (an area of the brain associated with both tremor and DA injury) and hippocampus (the primary target of DA) and tractography to assess the strength and direction of white matter connectivity between these two regions. Any signs of macrostructural changes observed with these MRI methods were investigated using histology and immunohistochemistry to assess microstructural cellular damage and glia reactivity in these key regions associated with tremor and DA exposure.

Support for the studies described in this dissertation was provided by supplemental funding acquired through the National Institute of Environmental Health Sciences and the University of Washington's Interdisciplinary Center for Exposures, Diseases, Genomics and Environment.

### 1.8 Research Impact

Results from these studies are the first to assess the impacts from chronic, low-level exposures to DA on the primate brain. Using a translational, nonhuman primate model, the body of work described herein identifies subtle effects on the brain following chronic, low-level DA exposure and associated signs of behavioral neurotoxicity. Results from this dissertation provide new avenues for continued research in human populations and animal models to help determine the adequate regulatory protection from this common marine toxin.

### 1.9 References

Aggleton, J.P., Brown, M.W., 1999. Episodic memory, amnesia, and the hippocampal-anterior thalamic axis. Behav. Brain Sci. 22, 425–444. https://doi.org/10.1017/S0140525X99002034

Andjelkovic, M., Vandevijvere, S., Van Klaveren, J., Van Oyen, H., Van Loco, J., 2012. Exposure to domoic acid through shellfish consumption in Belgium. Environ. Int. 49, 115–119. https://doi.org/10.1016/j.envint.2012.08.007

Authier, S., Arezzo, J., Pouliot, M., Accardi, M. V., Boulay, E., Troncy, E., Dubuc Mageau, M., Tan, W., Sanfacon, A., Mignault Goulet, S., Paquette, D., 2019. EEG: Characteristics of drug-induced seizures in rats, dogs and non-human primates. J. Pharmacol. Toxicol. Methods 97, 52–58. https://doi.org/10.1016/j.vascn.2019.03.004

Baron, A.W., Rushton, S.P., Rens, N., Morris, C.M., Blain, P.G., Judge, S.J., 2013. Sex differences in effects of low level domoic acid exposure. Neurotoxicology 34, 1–8. https://doi.org/10.1016/j.neuro.2012.10.010

Bates, S.S., Hubbard, K.A., Lundholm, N., Montresor, M., Leaw, C.P., 2018. Pseudo-nitzschia, Nitzschia, and domoic acid: New research since 2011. Harmful Algae 79, 3–43. https://doi.org/10.1016/j.hal.2018.06.001

Brittain, J. S., & Brown, P. (2013). The many roads to tremor. Experimental Neurology, 250, 104–107. https://doi.org/10.1016/j.expneurol.2013.09.012

Burbacher, T., Grant, K., Petroff, R., Crouthamel, B., Stanley, C., McKain, N., Shum, S., Jing, J., Isoherranen, N., 2019. Effects of chronic, oral domoic acid exposure on maternal reproduction and infant birth characteristics in a preclinical primate model. Neurotoxicol. Teratol. 440354. https://doi.org/10.1101/440354

Carpenter, S., 1990. The human neuropathology of encephalopathic mussel toxin poisoning. Symp. Domoic Acid Toxic. 73–34.

Cendes, F., Andermann, F., Carpenter, S., Zatorre, R.J., Cashman, N.R., 1995. Temporal lobe epilepsy caused by domoic acid intoxication: Evidence for glutamate receptor–mediated excitotoxicity in humans. Ann. Neurol. 37, 123–126. https://doi.org/10.1002/ana.410370125

Clayden, J., Read, B., Hebditch, K.R., 2005. Chemistry of domoic acid, isodomoic acids, and their analogues. Tetrahedron 61, 5713–5724. https://doi.org/10.1016/j.tet.2005.04.003

Clayton, E.C., Peng, Y.G., Means, L.W., Ramsdell, J.S., 1999. Working memory deficits induced by single but not repeated exposures to domoic acid. Toxicon 37, 1025–39.

Cook, P.F., Berns, G.S., Colegrove, K., Johnson, S., Gulland, F.M.D., 2018. Postmortem DTI reveals altered hippocampal connectivity in wild sea lions diagnosed with chronic toxicosis from algal exposure. J. Comp. Neurol. 526, 216–228. https://doi.org/10.1002/cne.24317

Cook, P.F., Reichmuth, C., Rouse, A.A., Libby, L.A., Dennison, S.E., Carmichael, O.T., Kruse-Elliott, K.T., Bloom, J., Singh, B., Fravel, V.A., Barbosa, L., Stuppino, J.J., Van Bonn, W.G., Gulland, F.M.D., Ranganath, C., 2015. Algal toxin impairs sea lion memory and hippocampal connectivity, with implications for strandings. Science. 350, 1545–1547. https://doi.org/10.1126/science.aac5675

Crosman, K.M., Petrou, E.L., Rudd, M.B., Tillotson, M.D., 2019. Clam hunger and the changing ocean: Characterizing social and ecological risks to the Quinault razor clam fishery using participatory modeling. Ecol. Soc. 24. https://doi.org/10.5751/ES-10928-240216

Du, X., Peterson, W., Fisher, J., Hunter, M., Peterson, J., 2016. Initiation and development of a toxic and persistent Pseudo-nitzschia bloom off the Oregon coast in spring/summer2015. PLoS One 11, e0163977. https://doi.org/10.1371/journal.pone.0163977

FAO United Nations, 2013. The state of world fisheries and aquaculture, 2012. https://doi.org/10.5860/choice.50-5350

Ferriss, B.E., Marcinek, D.J., Ayres, D., Borchert, J., Lefebvre, K.A., 2017. Acute and chronic dietary exposure to domoic acid in recreational harvesters: A survey of shellfish consumption behavior. Environ. Int. 101, 70–79. https://doi.org/10.1016/j.envint.2017.01.006

Fialkowski, M.K., McCrory, M.A., Roberts, S.M., Tracy, J.K., Grattan, L.M., Boushey, C.J., 2010. Evaluation of dietary assessment tools used to assess the diet of adults participating in the Communities Advancing the Studies of Tribal Nations Across the Lifespan cohort. J. Am. Diet. Assoc. 110, 65–73. https://doi.org/10.1016/j.jada.2009.10.012

Giordano, G., Kavanagh, T.J., Faustman, E.M., White, C.C., Costa, L.G., 2013. Low-level domoic acid protects mouse cerebellar granule neurons from acute neurotoxicity: Role of glutathione. Toxicol. Sci. 132, 399–408. https://doi.org/10.1093/toxsci/kft002

Gjedde, A., Evans, A.C., 1990. PET studies of domoic acid poisoning in humans: Excitotoxic destruction of brain glutamatergic pathways, revealed in measurements of glucose metabolism by positron emission tomography. Symp. Domoic Acid Toxic. 105–109. https://doi.org/10.2174/1568026616666160405

Grattan, L.M., Boushey, C.J., Liang, Y., Lefebvre, K.A., Castellon, L.J., Roberts, K.A., Toben, A.C., Morris, J.G.J., 2018. Repeated dietary exposure to low levels of domoic acid and problems with everyday memory: Research to public health outreach. Toxins. 10, 103. https://doi.org/10.3390/toxins10030103

Grattan, L.M., Boushey, C.J., Tracy, K., Trainer, V.L., Roberts, S.M., Schluterman, N., Morris, J.G.J., 2016. The association between razor clam consumption and memory in the CoASTAL cohort. Harmful Algae 57, 20–25. https://doi.org/10.1016/j.hal.2016.03.011

Gulland, F.M.D., Haulena, M., Fauquier, D., Langlois, G., Lander, M.E., Zabka, T.S., Duerr, R., 2002. Domoic acid toxicity in Californian sea lions (Zalophus californianus): Clinical signs. Vet. Rec. 150, 475–480. https://doi.org/doi:10.1136/vr.150.15.475

Hesp, B.R., Clarkson, A.N., Sawant, P.M., Kerr, D.S., 2007. Domoic acid preconditioning and seizure induction in young and aged rats. Epilepsy Res. 76, 103–112. https://doi.org/10.1016/j.eplepsyres.2007.07.003

Hiolski, E.M., Ito, S., Beggs, J.M., Lefebvre, K.A., Litke, A.M., Smith, D.R., 2016. Domoic acid disrupts the activity and connectivity of neuronal networks in organotypic brain slice cultures. NeuroToxicology 56, 215–224. https://doi.org/10.1016/j.neuro.2016.08.004

Hiolski, E.M., Kendrick, P.S., Frame, E.R., Myers, M.S., Bammler, T.K., Beyer, R.P., Farin, F.M., Wilkerson, H., Smith, D.R., Marcinek, D.J., Lefebvre, K.A., 2014. Chronic low-level domoic acid exposure alters gene transcription and impairs mitochondrial function in the CNS. Aquat. Toxicol. 155, 151–159. https://doi.org/10.1016/j.aquatox.2014.06.006

Hogberg, H.T., Sobanski, T., Novellino, A., Whelan, M., Weiss, D.G., Bal-Price, A.K., 2011. Application of micro-electrode arrays (MEAs) as an emerging technology for developmental neurotoxicity: Evaluation of domoic acid-induced effects in primary cultures of rat cortical neurons. Neurotoxicology 32, 158–168. https://doi.org/10.1016/j.neuro.2010.10.007

Iverson, F., Truelove, J., 1994. Toxicology and seafood toxins: Domoic acid. Nat. Toxins 2, 334–339. https://doi.org/10.1002/nt.2620020514

Iverson, F., Truelove, J., Nera, E., Tryphonas, L., Campbell, J., Lok, E., 1989. Domoic acid poisoning and mussel-associated intoxication: Preliminary investigations into the response of mice and rats to toxic mussel extract. Food Chem. Toxicol. 27, 377–384. https://doi.org/10.1016/0278-6915(89)90143-9

Jing, J., Petroff, R., Shum, S., Crouthamel, B., Topletz, A.R., Grant, K.S., Burbacher, T.M., Isoherranen, N., 2018. Toxicokinetics and physiologically based pharmacokinetic modeling of the shellfish toxin domoic acid in nonhuman primates. Drug Metab. Dispos. 46, 155–165. https://doi.org/10.1124/dmd.117.078485

Lefebvre, K.A., Frame, E.R., Gulland, F.M.D., Hansen, J.D., Kendrick, P.S., Beyer, R.P., Bammler, T.K., Farin, F.M., Hiolski, E.M., Smith, D.R., Marcinek, D.J., 2012. A novel antibody-based biomarker for chronic algal toxin exposure and sub-acute neurotoxicity. PLoS One 7, 1–7. https://doi.org/10.1371/journal.pone.0036213

Lefebvre, K.A., Kendrick, P.S., Ladiges, W., Hiolski, E.M., Ferriss, B.E., Smith, D.R., Marcinek, D.J., 2017. Chronic low-level exposure to the common seafood toxin domoic acid causes cognitive deficits in mice. Harmful Algae 64, 20–29. https://doi.org/10.1016/j.hal.2017.03.003

Lefebvre, K.A., Noren, D.P., Schultz, I.R., Bogard, S.M., Wilson, J., Eberhart, B.T.L., 2007. Uptake, tissue distribution and excretion of domoic acid after oral exposure in coho salmon (Oncorhynchus kisutch). Aquat. Toxicol. 81, 266–274. https://doi.org/10.1016/j.aquatox.2006.12.009

Lefebvre, K.A., Robertson, A., 2010. Domoic acid and human exposure risks: A review. Toxicon 56, 218–230. https://doi.org/10.1016/j.toxicon.2009.05.034

Lefebvre, K.A., Tilton, S.C., Bammler, T.K., Beyer, R.P., Srinouanprachan, S., Stapleton, P.L., Farin, F.M., Gallagher, E.P., 2009. Gene expression profiles in zebrafish brain after acute exposure to domoic acid at symptomatic and asymptomatic doses. Toxicol. Sci. 107, 65–77. https://doi.org/10.1093/toxsci/kfn207

Lefebvre, K.A., Yakes, B.J., Frame, E., Kendrick, P., Shum, S., Isoherranen, N., Ferriss, B.E., Robertson, A., Hendrix, A., Marcinek, D.J., Grattan, L.M., 2019. Discovery of a potential human serum biomarker for chronic seafood toxin exposure using an SPR biosensor. Toxins (Basel). 11, 293. https://doi.org/10.3390/toxins11050293

Louis, E. D. (2014). Understanding essential tremor: Progress on the biological front. Neurol Neuroscience Rep, 14(6), 450. https://doi.org/10.1080/10810730902873927.Testing

Lu, J., Wu, D. -m., Zheng, Y. -l., Hu, B., Cheng, W., Zhang, Z. -f., Li, M.-Q., 2013. Troxerutin counteracts domoic acid-induced memory deficits in mice by inhibiting CCAAT/enhancer binding protein β-mediated inflammatory response and oxidative stress. J. Immunol. 190, 3466–3479. https://doi.org/10.4049/jimmunol.1202862

Lu, J., Wu, D., Zheng, Y., Hu, B., Cheng, W., Zhang, Z., 2012. Purple sweet potato color attenuates domoic acid-induced cognitive deficits by promoting estrogen receptor-α-mediated mitochondrial biogenesis signaling in mice. Free Radic. Biol. Med. 52, 646–659. https://doi.org/10.1016/j.freeradbiomed.2011.11.016

Mariën, K., 1996. Establishing tolerable dungeness crab (Cancer magister) and razor clam (Siliqua patula) domoic acid contaminant levels. Environ. Health Perspect. 104, 1230–6. https://doi.org/10.1289/ehp.961041230

McCabe, R.M., Hickey, B.M., Kudela, R.M., Lefebvre, K.A., Adams, N.G., Bill, B.D., Gulland, F.M.D., Thomson, R.E., Cochlan, W.P., Trainer, V.L., 2016. An unprecedented coastwide toxic algal bloom linked to anomalous ocean conditions. Geophys. Res. Lett. 43, 10,366-10,376. https://doi.org/10.1002/2016GL070023

McCarron, P., Hess, P., 2006. Tissue distribution and effects of heat treatments on the content of domoic acid in blue mussels, Mytilus edulis. Toxicon 47, 473–479. https://doi.org/10.1016/j.toxicon.2006.01.004

McKibben, S.M., Peterson, W., Wood, A.M., Trainer, V.L., Hunter, M., White, A.E., 2017. Climatic regulation of the neurotoxin domoic acid. Proc. Natl. Acad. Sci. 114, 239–244. https://doi.org/10.1073/pnas.1606798114

Moyer, C.E., Hiolski, E.M., Marcinek, D.J., Lefebvre, K.A., Smith, D.R., Zuo, Y., 2018. Repeated low level domoic acid exposure increases CA1 VGluT1 levels, but not bouton density, VGluT2 or VGAT levels in the hippocampus of adult mice. Harmful Algae 79, 74–86. https://doi.org/10.1016/j.hal.2018.08.008

Muthuraman, M., Deuschl, G., Anwar, A. R., Mideksa, K. G., Von Helmolt, F., & Schneider, S. A. (2015). Essential and aging-related tremor: Differences of central control. Movement Disorders, 30(12), 1673–1680. https://doi.org/10.1002/mds.26410

Nakajima, S., Potvin, J.L., 1992. Neural and behavioural effects of domoic acid, an amnesic shellfish toxin, in the rat. Can. J. Psychol. 46, 569–581. https://doi.org/10.1037/h0084334

Peng, Y.G., Clayton, E.C., Means, L.W., Ramsdell, J.S., 1997. Repeated independent exposures to domoic acid do not enhance symptomatic toxicity in outbred or seizure-sensitive inbred mice. Fundam. Appl. Toxicol. 40, 63–67. https://doi.org/10.1093/toxsci/40.1.63

Pérez-Gómez, A., Tasker, R.A., 2013. Transient domoic acid excitotoxicity increases BDNF expression and activates both MEK- and PKA-dependent neurogenesis in organotypic hippocampal slices. BMC Neurosci. 14, 72. https://doi.org/10.1186/1471-2202-14-72

Pérez-Gómez, A., Tasker, R.A., 2012. Enhanced neurogenesis in organotypic cultures of rat hippocampus after transient subfield-selective excitotoxic insult induced by domoic acid. Neuroscience 208, 97–108. https://doi.org/10.1016/j.neuroscience.2012.02.003

Perl, T.M., Bedard, L., Kosatsky, T., Hockin, J.C., Todd, E.C., McNutt, L.A., Remis, R.S., 1990a. Amnesic shellfish poisoning: a new clinical syndrome due to domoic acid. Canada Dis. Wkly. Rep. 16 Suppl 1, 7–8.

Perl, T.M., Bedard, L., Kosatsky, T., Hockin, J.C., Todd, E.C.D., 1990b. An outbreak of toxic encephalopathy caused by eating mussels contaminated with domoic acid. N. Engl. J. Med. 322, 1775–1780. https://doi.org/10.1056/NEJM199006213222504

Preston, E., Hynie, I., 1991. Transfer constants for blood-brain barrier permeation of the neuroexcitatory shellfish toxin, domoic acid. Can. J. Neurol. Sci. 18, 39–44.

Qiu, S., Pak, C.W., Currás-Collazo, M.C., 2006. Sequential involvement of distinct glutamate receptors in domoic acid-induced neurotoxicity in rat mixed cortical cultures: Effect of multiple dose/duration paradigms, chronological age, and repeated exposure. Toxicol. Sci. 89, 243–256. https://doi.org/10.1093/toxsci/kfj008

Radad, K., Al-Shraim, M., Al-Emam, A., Moldzio, R., Rausch, W.D., 2018. Neurotoxic effects of domoic acid on dopaminergic neurons in primary mesencephalic cell culture. Folia Neuropathol. 56, 39–48. https://doi.org/10.5114/fn.2018.74658

Sawant, P.M., Holland, P.T., Mountfort, D.O., Kerr, D.S., 2008. In vivo seizure induction and pharmacological preconditioning by domoic acid and isodomoic acids A, B and C. Neuropharmacology 55, 1412–1418. https://doi.org/10.1016/j.neuropharm.2008.09.001

Sawant, P.M., Mountfort, D.O., Kerr, D.S., 2010. Spectral analysis of electrocorticographic activity during pharmacological preconditioning and seizure induction by intrahippocampal domoic acid. Hippocampus 20, 994–1002. https://doi.org/10.1002/hipo.20698

Scholin, C.A., Gulland, F., Doucette, G.J., Benson, S., Busman, M., Chavez, F.P., Cordaro, J., DeLong, R., De Vogelaere, A., Harvey, J., Haulena, M., Lefebvre, K., Lipscomb, T., Loscutoff, S., Lowenstine, L.J., Marin, R., Miller, P.E., McLellan, W.A., Moeller, P.D.R., Powell, C.L., Rowles, T., Silvagni, P., Silver, M., Spraker, T., Trainer, V., Van Dolah, F.M., 2000. Mortality of sea lions along the central California coast linked to a toxic diatom bloom. Nature 403, 80–84. https://doi.org/10.1038/47481

Schwarz, M., Jandová, K., Struk, I., Marešová, D., Pokorný, J., Riljak, V., 2014. Low dose domoic acid influences spontaneous behavior in adult rats. Physiol. Res. 63, 369–376. https://doi.org/932636 [pii]

Shiotani, M., Cole, T.B., Hong, S., Park, J.J.Y., Griffith, W.C., Burbacher, T.M., Workman, T., Costa, L.G., Faustman, E.M., 2017. Neurobehavioral assessment of mice following repeated oral exposures to domoic acid during prenatal development. Neurotoxicol. Teratol. 64, 8–19. https://doi.org/10.1016/J.NTT.2017.09.002

Sobotka, T.J., Brown, R., Quander, D.Y., Jackson, R., Smith, M., Long, S.A., Barton, C.N., Rountree, R.L., Hall, S., Eilers, P., Johannessen, J.N., Scallet, A.C., 1996. Domoic acid: Neurobehavioral and neurohistological effects of low-dose exposure in adult rats. Neurotoxicol. Teratol. 18, 659–670. https://doi.org/10.1016/S0892-0362(96)00120-1

Stewart, G.R., Zorumski, C.F., Price, M.T., Olney, J.W., 1990. Domoic acid: A dementia-inducing excitotoxic food poison with kainic acid receptor specificity. Exp. Neurol. 110, 127–138. https://doi.org/10.1016/0014-4886(90)90057-Y

Suzuki, C., Hierlihy, S., 1993. Renal Clearance of Domoic Acid in the Rat. Food Chem. Toxicol. 31, 701–706.

Takemoto, T., Daigo, K., 1958. Constituents of Chondria armata. Chem. Pharm. Bull. 6, 578–580. https://doi.org/10.1248/cpb.6.578b

Teitelbaum, J., Zatorre, R.J., Carpenter, S., Gendron, D., Cashman, N.R., 1990. Neurological Sequelae of Domoic Acid Intoxication. Symp. Domoic Acid Toxic. 16, 9–12. https://doi.org/10.2174/13816128236661701241

Todd, E.C.D., 1993. Domoic Acid and Amnesic Shellfish Poisoning - A Review. J. Food Prot. 56, 69–83. https://doi.org/10.4315/0362-028x-56.1.69

Toyofuku, H., 2006. Joint FAO/WHO/IOC activities to provide scientific advice on marine biotoxins (research report). Mar. Pollut. Bull. 52, 1735–1745. https://doi.org/10.1016/j.marpolbul.2006.07.007

Tracy, K., Boushey, C.J., Roberts, S.M., Morris, J.G., Grattan, L.M., 2016. Communities advancing the studies of Tribal nations across their lifespan: Design, methods, and baseline of the CoASTAL cohort. Harmful Algae 57, 9–19. https://doi.org/10.1016/j.hal.2016.03.010

Trainer, V., Hardy, F., 2015. Integrative Monitoring of Marine and Freshwater Harmful Algae in Washington State for Public Health Protection. Toxins (Basel). 7, 1206–1234. https://doi.org/10.3390/toxins7041206

Truelove, J., Mueller, R., Pulido, O., Iverson, F., 1996. Subchronic toxicity study of domoic acid in the rat. Food Chem. Toxicol. 34, 525–529. https://doi.org/10.1016/0278-6915(96)81814-X

Truelove, J., Mueller, R., Pulido, O., Martin, L., Fernie, S., Iverson, F., 1997. 30-day oral toxicity study of domoic acid in cynomolgus monkeys: Lack of overt toxicity at doses approaching the acute toxic dose. Nat. Toxins 5, 111–114. https://doi.org/10.1002/nt.5

Tryphonas, L., Truelove, J., Iverson, F., 1990a. Acute Neurotoxicity of Domoic Acid in Cynomolgus Monkeys (M. fascicularis). Toxicol. Pathol. 18, 297–303. https://doi.org/10.1177/019262339001800101

Tryphonas, L., Truelove, J., Iverson, F., Todd, E.C.D., Nera, E., 1990b. Neuropathology of Experimental Domoic Acid Poisoning in Nonhuman Primates and Rats. Symp. Domoic Acid Toxic. 78–81.

Tryphonas, L., Truelove, J., Todd, E.C.D., Nera, E., Iverson, F., 1990c. Experimental oral toxicity of domoic acid in cynomolgus monkeys (Macaca fascicularis) and rats. Food Chem. Toxicol. 28, 707–715. https://doi.org/10.1016/0278-6915(90)90147-F

Tulving, E., 1983. Elements of Episodic Memory. Can. Psychol. 26, 351.

Vieira, A.C., Alemañ, N., Cifuentes, J.M., Bermúdez, R., Peña, M.L., Botana, L.M., 2015. Brain pathology in adult rats treated with domoic acid. Vet. Pathol. 52, 1077–1086. https://doi.org/10.1177/0300985815584074

Wang, D., Zhao, J., Li, S., Shen, G., Hu, S., 2018. Quercetin attenuates domoic acid-induced cognitive deficits in mice. Nutr. Neurosci. 21, 123–131. https://doi.org/10.1080/1028415X.2016.1231438

Wang, Y., Qin, Z.H., 2010. Molecular and cellular mechanisms of excitotoxic neuronal death. Apoptosis 15, 1382–1402. https://doi.org/10.1007/s10495-010-0481-0

Washington State Department of Health, n.d. Domoic Acid in Razor Clams [WWW Document]. URL https://www.doh.wa.gov/CommunityandEnvironment/Shellfish/RecreationalShellfish/Illnesses/Biotoxins/DomoicAcidinRazorClams (accessed 5.10.20).

Wekell, J.C., Gauglitz, E.J., Barnett, H.J., Hatfield, C.L., Eklund, M., 1994a. The occurrence of domoic acid in razor clams (Siliqua patula), Dungeness crab (Cancer magister), and achovies (Engraulis mordax). J. Shellfish Res. 13, 587–593. https://doi.org/10.2983/035.029.0302

Wekell, J.C., Gauglitz, E.J., Barnett, H.J., Hatfield, C.L., Simons, D., Ayres, D., 1994b. Occurrence of domoic acid in Washington State razor clams (Siliqua patula) during 1991-1993. Nat. Toxins 2, 197–205. https://doi.org/10.1002/nt.2620020408

Wekell, J.C., Jurst, J., Lefebvre, K. a, 2004. The origin of the regulatory limits for PSP and ASP toxins in shellfish. J. Shellfish Res. 23, 927–930.

Wells, M.L., Karlson, B., Wulff, A., Kudela, R., Trick, C., Asnaghi, V., Berdalet, E., Cochlan, W., Davidson, K., De Rijcke, M., Dutkiewicz, S., Hallegraeff, G., Flynn, K.J., Legrand, C.,

Paerl, H., Silke, J., Suikkanen, S., Thompson, P., Trainer, V.L., 2020. Future HAB science: Directions and challenges in a changing climate. Harmful Algae 91, 101632. https://doi.org/10.1016/j.hal.2019.101632

Wells, M.L., Trainer, V.L., Smayda, T.J., Karlson, B.S.O., Trick, C.G., Kudela, R.M., Ishikawa, A., Bernard, S., Wulff, A., Anderson, D.M., Cochlan, W.P., 2015. Harmful algal blooms and climate change: Learning from the past and present to forecast the future. Harmful Algae 49, 68–93. https://doi.org/10.1016/j.hal.2015.07.009

Wright, J.L.C., Bird, C.J., de Freitas, A.S., Hampson, D., McDonald, J., Quilliam, M.A., 1990. Chemistry, biology, and toxicology of domoic acid and its isomers. Canada Dis. Wkly. Rep. 16 Suppl 1, 21–26.

Wright, J.L.C., Boyd, R.K., de Freitas, A.S.W., Falk, M., Foxall, R.A., Jamieson, W.D., Laycock, M. V., McCulloch, A.W., McInnes, A.G., Odense, P., Pathak, V.P., Quilliam, M.A., Ragan, M.A., Sim, G., Thibault, P., Walter, J.A., 1989. Identification of domoic acid, a neuroexcitatory amino acid, in toxic mussels from eastern Prince Edward Island. Can. J. Chem. 67, 481–490. https://doi.org/10.1139/v89-075

Wu, D., Lu, J., Zhang, Y., Zheng, Y., Hu, B., Cheng, W., Zhang, Z., Li, M., 2013. Ursolic acid improves domoic acid-induced cognitive deficits in mice. Toxicol. Appl. Pharmacol. 271, 127–136. https://doi.org/10.1016/j.taap.2013.04.038

Zatorre, R., 1990. Memory Loss Following Domoic Acid Intoxication from Ingestion of Toxic Mussels. Symp. Domoic Acid Toxic. 101–103.

## 1.10 Tables and Figures

***Table 1.1: Approximate Single-Dose Toxic Levels of DA in Adult Animals and Humans***

| | Oral | | Intraperitoneal | | Intravenous | |
|---|---|---|---|---|---|---|
| **Fish** | | | | | | |
| *Acute Effects* | --- | | 0.8-1.2 mg/g | Lefebvre et al., 2009 | --- | |
| *Sub-Acute Toxicity* | --- | | 0.003-0.5 mg/g | Hiolski et al., 2014; Lefebvre et al., 2009, 2007 | --- | |
| *No Effects* | <10-13 mg/kg | Lefebvre et al., 2007 | <0.003 mg/g | Lefebvre et al., 2007 | --- | |
| **Mice** | | | | | | |
| *Acute Effects* | 35 mg/kg | Iverson et al., 1989 | >2.3 mg/kg | Iverson et al., 1989 | --- | |
| *Sub-Acute Toxicity* | --- | | --- | | --- | |
| *No Effects* | 28 mg/kg | Iverson et al., 1989 | 0.6 mg/kg | Iverson et al., 1989 | --- | |
| **Rats** | | | | | | |
| *Acute Effects* | 80 mg/kg | Iverson et al., 1989 | 2 mg/kg | Iverson et al., 1989 | 0.5 mg/kg | Nakajima and Potvin, 1992 |
| *Sub-Acute Toxicity* | >60 mg/kg | Tryphonas et al., 1990c | 1 mg/kg | Schwarz et al., 2014 | --- | |
| *No Effects* | <60 mg/kg | Iverson et al., 1989 | <0.2 mg/kg | Sobotka et al., 1996 | --- | |
| **Monkeys** | | | | | | |
| *Acute Effects* | 5 mg/kg | Tryphonas et al., 1990c | 4 mg/kg | Tryphonas et al., 1990a | 0.025 mg/kg | Tryphonas et al., 1990b, 1990c |
| *Sub-Acute Toxicity* | --- | | --- | | --- | |
| *No Effects* | 0.5 mg/kg | Iverson and Truelove, 1994 | 0.5 mg/kg | Tryphonas et al., 1990b | 0.005 mg/kg | Jing et al., 2018 |
| **Humans** | | | | | | |
| *Acute Effects* | 1 mg/kg | Perl et al., 1990b | --- | | --- | |
| *Sub-Acute Toxicity* | | | --- | | --- | |
| *No Effects* | 0.2 mg/kg | Perl et al., 1990b | --- | | --- | |

***Table 1.2: Laboratory Models with Chronic, Low-Dose DA Exposures***

| Study | Model | DA Dose | Length of Exposure | Findings |
|---|---|---|---|---|
| Lefebvre et al., 2017 | Mice | 0.75 mg/kg ip | 1x/week, up to 25 weeks | Adult deficits in spatial memory that were recoverable after 9 weeks post-last dose |
| Shiotani et al., 2017 | Rats | 1-3 mg/kg, oral | 1x/day, for 7 days | No observable effects in adults |
| Burbacher et al., 2019 | Monkeys | 0.075-0.15 mg/kg, oral | 1x/day, for up to 10 months | Increased intention tremors in exposed adults |

***Table 1.3: Sample Sizes for Each Assessment***

| DA Dose Group (mg/kg/day) | Total (n) | MRI (n) | EEG (n) | Postmortem (n) |
|---|---|---|---|---|
| 0.00 | 10 | 6 | 8 | 8 |
| 0.075 | 10 | 2 | 6 | 7 |
| 0.15 | 11 | 4 | 6 | 7 |

*Total reflects the overall number of females/group in the parent study. MRI (magnetic resonance imaging) outcomes used a subset of animals to assess global white matter structure and neurochemicals (Chapter 2), as well as gray matter structure volume and white matter connectivity (Chapter 4). EEG (electroencephalography) used a larger subset, including the MRI animals and is found in Chapter 3. Postmortem studies used histology and immunohistochemistry on the largest subset of animals, encompassing all the animals from the EEG subset. This work is found in Chapter 4.*

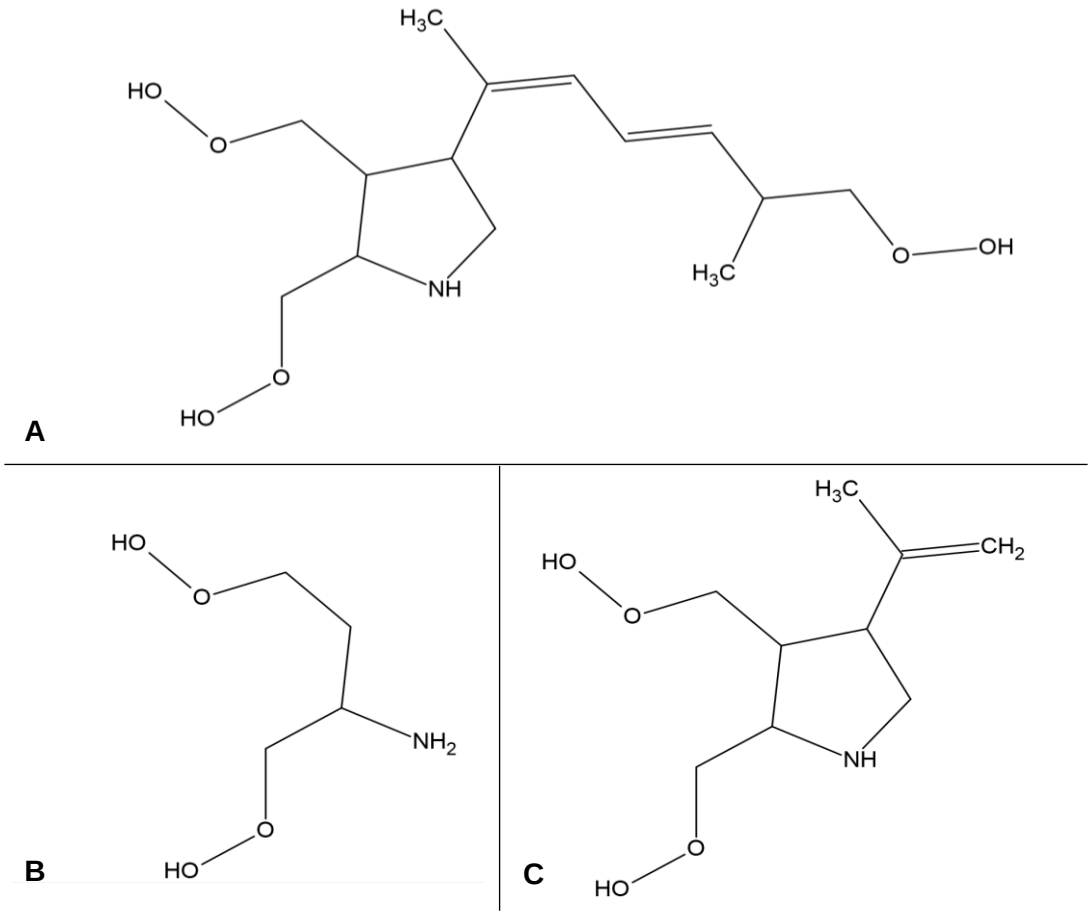


*Figure 1.1: Chemical structures of domoic acid and analogues. A) Domoic acid; B) Glutamate; C) Kainic Acid*

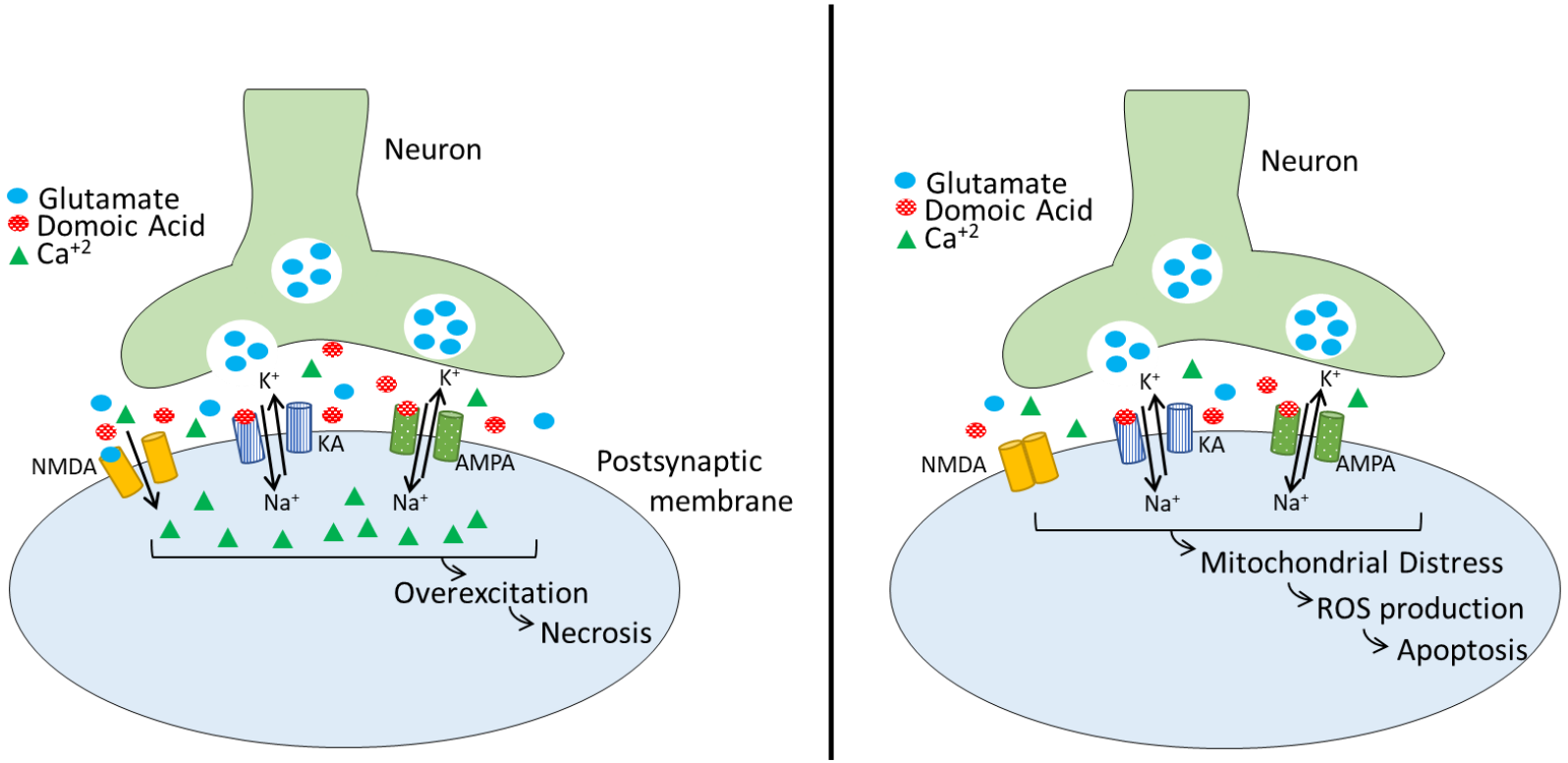


*Figure 1.2: Proposed mechanism of action for domoic acid. LEFT: Acute exposures to DA to bind to KA and AMPA type glutamate receptors, resulting in an influx of $Na^+$ into the postsynaptic membrane and the release of glutamate into the synapse. Glutamate activates NMDA receptors, allowing an influx of $Ca^{+2}$, and leading to necrotic cell death. RIGHT: Lower level exposures do not involve the NMDA receptors, and therefore, leads to mitochondrial distress, the production of ROS, and apoptosis. $Ca^{+2}$ = calcium, $Na^+$ = sodium, $K^+$ = potassium, DA = domoic acid, APMA = α-amino-3-hydroxy-5-methyl-4-isoxazolepropionic acid, KA = kainic acid, NMDA = N-methyl-D-aspartic acid, ROS = reactive oxygen species.*

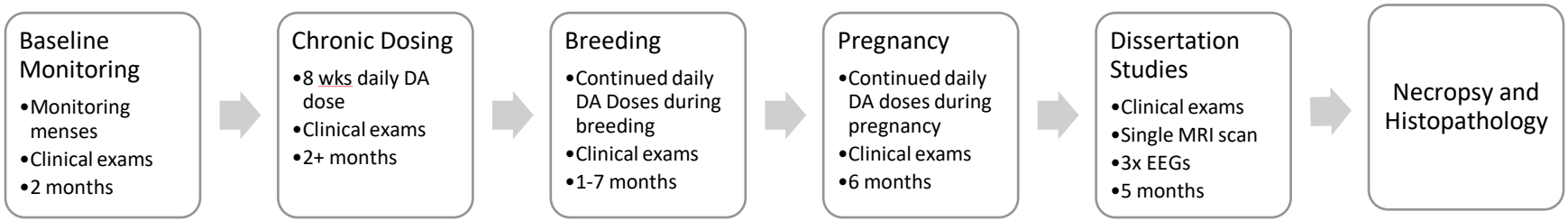


*Figure 1.3: Timeline of dissertation project*

**Chapter 2: Chronic, Low-Level Oral Exposure to Marine Toxin, Domoic Acid, Alters Whole Brain Morphometry in Nonhuman Primates**

*This chapter was published in NeuroToxicology. The authors are:*

Petroff, R.,[1] Richards, T.,[2,3] Crouthamel, B.,[1] McKain, N.,[1] Stanely, C.,[1] Grant, K.S.,[1,2] Shum, S.,[4] Jing, J.,[4] Isoherranen, N., [2,4] Burbacher, T.M.[1,2,5]

[1] Department of Environmental and Occupational Health Sciences, University of Washington, Seattle, Washington, USA

[2] Center on Human Development and Disability, Seattle, Washington, USA

[3] Department of Radiology, University of Washington, Seattle, Washington, USA

[4] Department of Pharmaceutics, University of Washington, Seattle, Washington, USA

[5] Infant Primate Research Laboratory, Washington National Primate Research Center, Seattle, Washington, USA

Corresponding Author:

Rebekah Petroff

Department of Environmental and Occupational Health Sciences

School of Public Health, Box 357234

1959 NE Pacific Street

University of Washington

Seattle, WA 98195

petroffr@uw.edu

**2.1 Abstract**

Domoic acid (DA) is an excitatory neurotoxin produced by marine algae and responsible for Amnesiac Shellfish Poisoning in humans. Current regulatory limits (~0.075-0.1 mg/kg/day) protect against acute toxicity, but recent studies suggest that the chronic consumption of DA below the regulatory limit may produce subtle neurotoxicity in adults, including decrements in memory. As DA-algal blooms are increasing in both severity and frequency, we sought to better understand the effects of chronic DA exposure on reproductive and neurobehavioral endpoints in a preclinical nonhuman primate model. To this end, we initiated a long-term study using adult, female *Macaca fascicularis* monkeys exposed to daily, oral doses of 0.075 or 0.15 mg/kg of DA for a range of 321-381, and 346-554 days, respectively. This time period included a pre-pregnancy, pregnancy, and postpartum period. Throughout these times, trained data collectors observed intentional tremors in some exposed animals during biweekly clinical examinations. The present study explores the basis of this neurobehavioral finding with in vivo imaging techniques, including diffusion tensor magnetic resonance imaging and spectroscopy. Diffusion tensor analyses revealed that, while DA exposed macaques did not significantly differ from controls, increases in DA-related tremors were negatively correlated with fractional anisotropy, a measure of structural integrity, in the internal capsule, fornix, pons, and corpus callosum. Brain concentrations of lactate, a neurochemical closely linked with astrocytes, were also weakly, but positively associated with tremors. These findings are the first documented results suggesting that chronic oral exposure to DA at concentrations near the current human regulatory limit are related to structural and chemical changes in the adult primate brain.

**Keywords:** Domoic acid; neurotoxicity; diffusion tensor imaging; magnetic resonance spectroscopy; fractional anisotropy; chronic exposure

## 2.2 Introduction

Domoic acid (DA) is an excitatory neurotoxin produced by marine algae in the genus *Pseudo-nitzschia* and found in ocean waters around the world. DA can accumulate in many types of seafood, including razor clams, scallops, oysters, mussels, anchovies, sardines, and crabs (Andjelkovic et al., 2012; Lefebvre et al., 2002; Trainer et al., 2007; Wekell et al., 1994a). When DA-contaminated seafoods are consumed, people may experience symptoms that include gastrointestinal distress, seizures, and the disruption of memory processes, collectively known as the clinical syndrome, Amnesic Shellfish Poisoning (Perl et al., 1990a; Perl et al., 1990b). The largest known DA human poisoning episode occurred in 1987 on Prince Edward Island, Canada, where over 150 people became ill and four died after consuming DA-contaminated mussels. Clinical T2-weighted magnetic resonance (MR) imaging shortly before the death of intoxicated adults displayed stark atrophy of the hippocampus (Cendes et al., 1995). Post-mortem histology in affected patients suggested that DA excitotoxicity was associated with gross necrosis, astrocytosis, and atrophy, primarily in the limbic system and temporal lobe of the brain, including the hippocampus, amygdala, and thalamus (Carpenter, 1990), and similar effects have been documented in a number of model animals and sentinel species after acute DA poisoning (McHuron et al., 2013; Silvagni et al., 2005; Tryphonas et al., 1990c; Vieira et al., 2015). Since 1987, there have been no documented cases of human DA poisonings, but toxic algal blooms have been increasing in both severity and frequency (Smith et al., 2018a; Wells et al., 2015b). This oceanographic change has been linked to many causal factors, including both seasonal upwelling (Du et al., 2016; Schnetzer et al., 2013; Seubert et al., 2013; Smith et al., 2018b) and shifting ocean temperatures (McCabe et al., 2016; McKibben et al., 2017; Zhu et al., 2017).

To protect human health, the US Food and Drug Administration has established an action level of 20 ppm in shellfish tissue (US Food and Drug Administration, 2011). This

regulatory limit has been officially accepted for commercial and recreational shellfish harvesting in coastal US states (California Office of Health and Environmental Assessment, 1991; Washington Department of Fish and Wildlife, n.d.), as well as in the European Union (O'Mahony, 2018) and Canada (Canadian Food Inspection Agency, 2011). When DA concentrations are at or above 20 ppm in these locations, beaches are closed to shellfish harvesting and commercial fisheries suspend operations (Wekell et al., 2004). The 20 ppm action level was established after the 1987 poisoning, when it was estimated that people showing symptoms of toxicity consumed approximately 200 mg DA. Follow-up studies have calculated that the regulatory limit is equivalent to approximately 0.075-0.10 mg DA/kg bodyweight in a normal, human adult (Mariën, 1996; Toyofuku, 2006). This regulatory limit was, however, only established on acute toxicity data and, in recent years, there has been a growing number of studies documenting the health effects of chronic low-level DA exposure. Data from rodent laboratory research with adult animals suggest that chronic, low-dose exposure can result in short-term, yet recoverable, deficits in cognition (Lefebvre et al., 2017). Human epidemiological findings from a coastal cohort of adult Native Americans in Washington State link the consumption of >15 razor clams/month (a proxy for low-level, chronic DA exposure) to decreased performance on several different memory exams (Grattan et al., 2016a, 2018). Cognitive deficits from these epidemiological studies were severe enough to interfere with daily living skills. Collectively, these data suggest that chronic exposure to DA, at environmentally relevant levels of exposure, may have significant consequences on the central nervous system.

One opportunity with which the effects of chronic DA exposure on health and behavior are studied has been sentinel marine species, naturally exposed to DA through the consumption of contaminated seafood (Bossart, 2011). Elevated levels of DA in plasma and urine have been documented in a variety of animals (Lefebvre et al., 2016), but DA toxicity has been most well-defined in California sea lions. Many afflicted animals display symptoms that are similar to those

observed in acutely poisoned humans, including changes in cognition, seizures, and, in the case of sea lions, a death rate exceeding 50% (Gulland et al., 2002; Scholin et al., 2000). Sickened animals exhibit signs of gliosis and neuronal necrosis in patterns similar to human DA toxicity cases, with damage primarily in the hippocampus and dentate gyrus (Silvagni et al., 2005). Importantly for the present study, researchers have connected chronic DA toxicosis in sea lions to differences in the structural integrity of the brain, using diffusion tensor imaging (DTI) (Cook et al., 2018). DTI is a model used with diffusion-weighted imaging (DWI), a variation of MR imaging that measures the diffusion rate and anisotropy, or the degree of directionality, of water in tissues. These measures can be used to estimate changes in the density or integrity of axon bundles and myelin, as well as changes in glial cells or extracellular fluids. Cook and colleagues conducted a post-mortem DTI analysis of sea lions diagnosed with DA toxicosis and found decreased anisotropy in the fornix, a white matter tract connecting the hippocampus and thalamus. These data demonstrate a link between oral DA exposure and changes in the microscopic architecture of the mammalian brain, but the translational value of these studies is difficult to ascertain due to differences in neuroanatomy and the lack of quantifiable dose-response data.

The study described in this paper offers an innovative approach to examine the effects of lower level DA exposure by linking behavioral intentional tremors in a nonhuman primate model with in vivo changes in brain structure. Macaques utilized in the present research were selected from a larger, longitudinal reproductive and developmental study (Burbacher et al., 2019). In the parent study, adult female macaque monkeys were chronically exposed to 0.0, 0.075 or 0.15 mg/kg/day oral DA prior to, during, and post pregnancy. These exposures were selected to mirror estimates of DA exposure in humans who consumed shellfish with elevated levels of DA below the regulatory threshold (Ferriss et al., 2017; Kumar et al., 2009). Long term exposure in this investigation yielded unanticipated signs of neurotoxicity in the adult females in

the form of subtle intentional tremors during a reaching and grasping task (Burbacher et al., 2019). Subsequently, the aim of the present imaging study was to explore how the observed intentional tremors in DA-exposed animals were related to changes in brain structure and neurochemistry in vivo. Individuals were selected based on individual tremor and dose status and underwent a single, sedated MR scan with DTI to measure whole brain, voxel-wise diffusion measures. We additionally conducted MR spectroscopy to measure neurochemical concentrations of n-acetyl aspartate (NAA), choline, creatinine, glutamate/glutamine (Glx), and lactate, and captured T1- and T2-weighted images to survey for gross lesions. Results from this translational study represent the first presentation of data that describe in vivo structural changes in nonhuman primates after chronic, oral DA exposure at levels close to real-world human exposures.

### 2.3 Methods

*Study Animals*

Macaques for the present study were selected from a larger study aimed at investigating the reproductive and developmental effects of chronic, low-level oral exposure to DA (Burbacher et al., 2019). Thirty-two healthy, adult female *Macaca fascicularis* were enrolled in the larger reproductive and developmental study. All animals were housed in the Infant Primate Research Laboratory at the Washington National Primate Research Center, paired with a grooming contact social partner, and allowed unrestricted access to water. Monkeys were fed with Purina High Protein Monkey Diet (St. Louis, MO) biscuits twice a day and provided extensive enrichment (fresh produce, toys, movies/music, and frozen foraging treats). All animal procedure guidelines followed the Animal Welfare Act and the Guide for Care and Use of Laboratory Animals of the National Research Council and protocols were approved by the University of Washington Institutional Animal Care and Use Committee.

Animals were pseudo-randomly assigned to one of three treatment groups: control (n=10), 0.075 (n=11), or 0.15 (n=11) mg/kg/day of DA (BioVectra, Charlottetown, PE, Canada). Blinded testers used positive reinforcement techniques to train macaques to drink from a syringe, complete a battery of clinical assessments to monitor toxicity, and undergo unsedated saphenous blood draws (Burbacher et al., 2004). After training was complete, all experimental procedures were conducted for a 2-month pre-exposure period. During this period, animals were dosed daily with a 5% sucrose solution. Daily, oral exposure to DA was initiated after this 2-month run-in period, and blinded testers orally administered 1 ml of either 0 (n=10), 0.075 (n=11), or 0.15 (n=11) mg/kg of DA in 5% sugar water for at least 2 months. All dosing solutions were quality controlled by measuring DA concentrations via validated LC-MS/MS methods (Shum et al., 2018). After at least two months of exposure, enrolled females were bred with treatment naïve males, and dosing continued throughout breeding and pregnancy. Dosing then was continued postpartum, through the MR imaging.

Plasma DA concentrations were monitored with unsedated blood draws from the saphenous vein, taken 5 hours after dosing. Blood was drawn into sodium heparin tubes and centrifuged at 3,000 *g*. Plasma was separated, stored at -20° C, and analyzed using the methods detailed in Shum et al., 2018. Before pregnancy, average plasma DA concentrations were 1.31 ng/ml for the 0.075 mg/kg/day DA group and 3.42 ng/ml for the 0.15 mg/kg/day DA exposure group. No DA was detected in the vehicle dosed control animals. Twenty-eight females conceived, 9 in the control group, 9 in the 0.075 mg/kg/day DA exposure group, and 10 in the 0.15 mg/kg/day DA exposure group. Mean blood DA concentrations during pregnancy were 0.93 ng/ml (SE: 0.22) and 2.93 ng/ml (SE: 0.38) for the 0.075 and 0.15 mg/kg/day DA exposure groups, respectively.

Throughout the study, general health was monitored daily by clinical staff and weights were recorded weekly. Trained and reliable examiners conducted clinical assessments on all

dams at least three times per week. Clinical exams were designed to detect behavioral changes in study animals and included visual orientation and tracking, as well as fine motor and tremor assessments. To assess tremors, blinded testers offered individuals a small treat approximately 6-8 inches from the front of the individual homecage, requiring full extension of the individual's arm. Testers administered three trials/session, at least three days/week. An animal was considered positive for tremors on any test session if a tester noted the presence of tremors during the reach on at least 2 of the 3 trials. All testers maintained a minimum reliability score of 80% with the primary tester, repeated every 6-8 months. One female in the 0.075 mg/kg/day DA exposure group was dropped from the study after a single breeding due to amenorrhea. In addition, a female in the control group was dropped from the tremor assessment analysis after an MRI revealed a lesion in the temporal lobe (see below for additional details).

Previous reported results from the tremor assessment (Burbacher et al., 2019) revealed a significant increase in tremors in the 0.15 mg/kg/day DA exposure group, when tremor increase scores (tremor rates observed over the entire DA exposure period up to delivery minus the tremor rates observed during the pre-exposure period) were compared across DA exposure groups (see Fig. 2.1). The average tremor increase scores for the 3 DA exposure groups were 5.6% (SE: 1.4%) for the controls, 17.7% (SE: 4.1%) for the 0.075 mg/kg/day DA exposure group, and 30.5% (SE: 8.3%) for the 0.15 mg/kg/day DA exposure group.

Enrolled individuals were selected from the larger reproductive and developmental study for MR imaging to compare a subgroup of control females not exhibiting tremors (n=6) to DA exposed females exhibiting tremors (n=6) (Table 2.1). Selected females included four females from the 0.15 mg/kg/day DA exposure group, two from the 0.075 mg/kg/day DA exposure group and six from the control group. The average age of females selected from the DA exposed and control groups was 8 years and the average weight 4.1 kg. The average duration of DA exposure for the DA exposed females was 419 days.

An additional control female that exhibited a high rate of tremors throughout the study was examined separately to investigate other potential structural brain changes in a non-DA exposed female exhibiting tremors (see Table 2.1).

*MR Image Acquisition and Parameters*

Each female underwent a single, sedated MR scan. Less than 30 days before the scan, females were required to meet health standards on a physical exam conducted by clinical veterinary staff. MR image data were acquired on a Philips 3T Achieva (version 5.17) and a custom made 8-channel rf head coil that was developed by Dr. Cecil Hayes and optimized for the small primate head. Females were pre-anesthetized with ketamine (5-10 mg/kg i.m.) and atropine (0.04 mg/kg i.m.) and maintained on inhaled sevoflurane (0.8 - 2.5%) and 100% oxygen. Females were placed in the scanner in prone position, and the coil was arranged over the head. Oxygen saturation levels and single-channel ECG were monitored with an MRI-compatible device (InvivoPrecess™) and temperature was maintained with warm packs. Diffusion weighted images were acquired with the following parameters: spin-echo echo-planar pulse sequence with diffusion gradients, repetition time 5500 ms, echo time 77.98 ms, reconstructed matrix 128x128, number of slices 44, resolution/voxel size 0.78x0.78x1.5mm, 64 different diffusion weighted directions and one non-diffusion volume at Blip right, b value 1500, 5 different diffusion weighted directions and one non-diffusion volume at Blip left, which where compatible with FSL's topup and eddy software.

Additionally, both a T1-weighted and a T2-weighted image were captured to allow for detection of lesions. The 3-D, high-resolution, T1-weighted MPRAGE images were acquired with a multishot turbo field echo (TFE) pulse sequence and an inversion prepulse (1,151 ms delay); repetition time (TR)/echo time (TE) = 14 s/7.1 ms; 130 axial slices; acquisition matrix 208 x 141 x 130; acquisition voxel size 0.48 x0.53 X1.0 mm; reconstructed voxel size 0.39 x 0.39 x

0.5 mm; slice over sample factor = 2; sense factor = 2 in the foot-head direction; turbo factor = 139; number of signaling averages = 1;TFE shots = 65, and acquisition time = 3 min 14 s. A 2-D, high-resolution, T2-weighted images were acquired with a multishot turbo spin-echo (TSE) pulse sequence; repetition time (TR)/echo time (TE) = 7374 ms/80 ms; 24 axial slices; acquisition matrix 208 x 179 x 24; reconstructed voxel size 0.446 x 0.446 x 2 mm; turbo factor = 15; sense factor of 2 in the right left direction, number of signaling averages = 2; and acquisition time = 2 min 42 s.

*T1-Weighted and T2-Weighted Image Analysis*

Trained testers inspected each slice of T1- and T2-weighted images for abnormalities and lesions in FSLeyes (McCarthy, 2018). Any hypointensities on T1-weighted images and hyperintensities on T2-weighted identified on any single slice were verified as lesions by a second, independent MRI-expert.

*Diffusion Weighted Image Processing and Analysis*

Whole brain, voxel-wise DTI measures were obtained in *FSL* (Jenkinson et al., 2012), using a method that is similar to tract-based spatial statistics, but allows for better alignment (C. G. Schwarz et al., 2014). Diffusion images were processed using *FSL*'s *topup* software and *FSL*'s *eddy* software to minimize distortion from eddy currents and head motion (Andersson et al., 2003; Smith et al., 2004), The FSL program, *dtifit* (https://fsl.fmrib.ox.ac.uk/fsl/fslwiki/FDT), was used to reconstruct the diffusion tensor for each voxel, and the matrix was diagonalized to obtain tensor eigenvalues, L1, L2, L3. Outcomes of interest included voxel-wise fractional anisotropy (FA), a measure of the directionality of water diffusion and white matter integrity, mean diffusivity (MD, MD=(L1 + L2 + L3)/3), axial diffusivity (AD, AD=L1), and radial diffusivity (RD, RD=(L2+L3)/2). Software *buildtemplate*, part of Advanced Normalization Tools (ANTs)

(Avants et al., 2011), was used to coregister individual FA maps to a target brain, chosen at random from among all scanned individuals. The locations of TFCE significant voxels (from FSL *randomise* software) were identified using the macaque NeuroMaps atlas (Dubach and Bowden, 2009; Rohlfing et al., 2012).

*MR Spectroscopy*

MR spectroscopy data were acquired using the same scanner and rf coil described above with the following parameters: PRESS pulse sequence, repetition time 2000 ms, echo time 32 ms, number of FID points 2048, number of averages 48, voxel size 15x15x15 mm and voxel place centered over right thalamus (and including other brain regions) as shown in Fig. 2.2. MR spectroscopy spar/sdat files were processed using software *LCmodel* written by Provencher (Provencher, 1993), using both water-suppressed MRS and non-water suppressed MRS files as inputs (Fig. 2.3). Absolute concentrations of n-acetyl aspartate (NAA), choline, creatinine, glutamate/glutamine (Glx), and lactate were obtained by scaling the in vivo spectrum to the unsuppressed water peak. Concentrations were corrected for cerebral spinal fluid (CSF) volume before statistical analysis.

*Statistical Methods*

***Behavioral Tremors***: Tremor scores for the subjects in the present study were calculated during baseline and during the exposure period by dividing the total number of sessions recorded as positive for tremors by the total number of sessions tested. The baseline or pre-exposure period included all clinical sessions from 2 months prior to the first day of exposure through the day before exposure. The exposed tremor score used in all analyses included all clinical observation sessions from day 1 of exposure to the day of imaging. To assess the normality of the exposed tremor scores distribution, a Shapiro-Wilk test was used.

***DTI***: FSL software *randomise*, a method that uses 500 random permutations and threshold-free cluster enhancement (TFCE) that corrects for multiple voxel comparisons, was first used to assess group-wise differences between control and exposed groups and then to compute brain-wide correlations of DTI measures and individual tremor score at the time of the scan (Table 2.1) (Smith and Nichols, 2009; Winkler et al., 2014). Tremor scores were centered/demeaned around the mean tremor score of all animals by subtracting the mean from the individual score, in accordance with the use of this software program. Any significant correlations in either the TFCE *randomise* software analysis was visually identified in the brain as a cluster in FSLeyes. Diffusion measures from individual voxels within significant clusters were then correlated to the demeaned tremor scores, using the nonparametric Spearman rank method. Because significant clusters were analyzed on a whole-brain level, p-values from the Spearman correlations in individual voxels are not included in the present manuscript.

***MRS:*** Group-wise differences in concentrations of NAA, choline, creatinine, Glx, and lactate were first compared between exposure groups using a Welch's t-test in R (R Core Team, 2020). A follow-up analysis used Spearman's correlation in R to assess the correlation between each neurochemical and individual tremor scores (R Core Team, 2020).

## 2.4 Results

*Behavioral Tremors*

Tremors were observed rarely during testing sessions prior to DA exposure (see Table 2.1, average n sessions=35). The % of sessions that tremors were observed during DA exposure for females selected from the DA exposure groups ranged from 29% to 79%, with an average and SE of 44% ± 9% sessions (n sessions ranged from 117 to 236). The % of sessions that tremors were observed during the DA exposure period for females selected from the control

group ranged from 1% to 9%, with an average and SE of 4.5% ± 1.3% (n sessions ranged from 134 to 293).

The % of sessions tremors were observed during the DA exposure period up to MR scans (tremor scores) were not normally distributed (W=0.845, p=0.031), thus nonparametric Spearman's correlations were used for the analysis of MR measures.

*Lesion Identification*

Visual inspection of T1- and T2-weighted images revealed that, while there were no lesions in the low-tremoring, controls or high-tremoring, exposed primates (data not shown), the high-tremoring control female (Table 2.1) had a significant lesion in the right temporal lobe (Fig. 2.5). Diffusion Tensor Imaging (DTI) and Magnetic Resonance Spectroscopy (MRS) measures for this individual are denoted by a star in Fig. 2.6 and 2.7.

*Diffusion Weighted Images*

Using a threshold-free cluster enhancement (TFCE) based analysis, we found that there were no differences in whole-brain DTI measures when using group-wise analysis to compare exposed macaques to controls (fractional anisotropy, p=0.132; axial diffusivity, p=0.392; radial diffusivity, p=0.432; mean diffusivity, p=0.414). Follow-up correlation analysis between whole-brain DTI measures and tremor scores from the 12 scans revealed a significant negative correlation between tremor scores and fractional anisotropy (FA) (p=0.048, Fig. 2.7). Clusters of FA that were significantly related to tremor scores were observed bilaterally in the anterior internal capsule and fornix. Correlations revealed strong relationships in these regions, as well as with smaller clusters observed in the pons and corpus callosum (Fig. 2.7). Axial (p=0.178), radial (p=0.218), and mean diffusivity (p=0.232) were not correlated with tremor scores.

*MR Spectroscopy*

MR spectroscopy concentrations were obtained from each female, centered on the right thalamus. There were no significant differences in neurochemical concentrations between DA exposed and control females (Welch's t-test; n-acetyl aspartate (NAA), p=0.924; choline, p= 0.691; creatinine, p=0.086; glutamate/glutamine (Glx), p=0.852; lactate, p=0.908). In addition, CSF-corrected measures for NAA, choline, creatinine, and Glx were not significantly correlated with tremor scores. Lactate concentration, however, was positively correlated with tremor scores, but measurements were highly variable (Fig. 2.8, p=0.048).

## 2.5 Discussion

DA is a known neurotoxin, but few studies have investigated the effects of chronic, low-level exposure to this toxin in any model. This study is the first to use DTI and whole brain analysis in a nonhuman primate model chronically exposed to oral, low-dose DA. We used a TFCE approach with DTI to detect differential clusters of significance, a method that has been shown to have increased sensitivity over other voxel-based analysis methods (Smith and Nichols, 2009) and was untargeted and unbiased. While this approach lowered our ability to detect smaller changes in DTI measures, it allowed us to visualize other structural changes in areas not previously known to be affected by DA. Within the sample of 6 macaque monkeys chronically exposed to low-levels of DA and 6 non-exposed controls, we did not find any changes in DTI measures when comparing DA-exposed macaques to the control group. However, decreased FA, a measure of tissue integrity, was significantly correlated with increased intentional tremors, but no other diffusion measure was found to be related to tremors. While the fornix, the major white matter tract connecting the hippocampus, the primary target of DA, was affected, there were also other areas of the brain that showed significantly changed FA, including the internal capsule, brainstem, and corpus callosum. Additionally, we

found a correlation between tremors and increased lactate in the thalamus. These data collectively show that adult nonhuman primates exposed to chronic, oral, low levels of DA have neurological damage that can be observed through changes in behavior, neurochemical concentrations, and neurological structural integrity.

The observed increases in intentional tremors have only been documented in our model, possibly due to the limited number of chronic, oral DA exposure studies. The only other published study to examine chronic oral exposures in a preclinical model used exposure levels of 0.5 and 0.75 mg/kg in macaque monkeys and did not report any significant behavioral or physiological effects after 30 days of repeated exposure (Truelove et al., 1997). It should be further noted that standardized observations, such as those included in the current study, were not utilized in Truelove et al. Other short-term observational and histopathological studies have demonstrated that higher levels of oral exposure (5-10 mg/kg in monkeys and 30-80 mg/kg in rodents) are typically associated with acute symptomology (i.e. scratching, vomiting, shaking/seizures, death) and severe neuronal damage and gliosis primarily in the hippocampus (Iverson et al., 1989; Tryphonas et al., 1990c), outcomes not observed in our model. In this research by Tryphonas and colleagues, individual variability in response was noted in both behavioral responses and pathological findings but was ultimately attributed to the differences in dose consumed, due to individual variation in vomiting onset and severity (Tryphonas et al., 1990). Within our study, we did not observe DA related vomiting, but we still found substantial variability in DA symptomology (tremors), suggesting that there may be hypo- and hyper-responders to DA. This type of interindividual variation is not uncommon in both pharmacological and toxicological responses after exposure to xenobiotics and may be due to variety of factors, such as genetic variation or individual pharmacokinetic differences (Thummel and Lin, 2014). Additionally, while our procedure for detecting tremors was a valid assay for monitoring the low-level neurotoxic response to DA, it may not be sensitive enough to detect the

most subtle of behavioral tremors. Overall, our results suggest that chronic, low-level oral exposure below levels previously shown to be asymptomatic are related to variable, yet significant increases in behavioral tremors.

The present results also suggest that these tremors are connected with decreased FA in several areas of the nonhuman primate brain. FA is a measure of the directionality of water in the brain and ranges in values from 0 (no directionality or equally restricted in all directions) to 1 (fully restricted in one direction). Especially in white matter tracts, FA is typically high and reflects overall axonal integrity (Beaulieu, 2002). It has been suggested that low FA scores are indicative of either direct damage to the myelin/axonal tracts or the replacement of axonal bundles with other cells (i.e. gliosis) (Alba-Ferrara and de Erausquin, 2013; Budde et al., 2011; Garcia-Lazaro et al., 2016; Smith et al., 2006). Significant clusters of decreased FA in tremoring, exposed animals were observed in both the right and left anterior internal capsule and fornix, and smaller clusters were found in the brainstem and the corpus callosum. The internal capsule is a complex bundle of fibers that are essential to motor function (Morecraft et al., 2002), and these fibers include projections that connect the thalamus to the prefrontal cortex, projections from the basal ganglia, and frontopontine fibers that connect the frontal cortex and brain stem (Schmahmann et al., 2004). The pons of the brain stem was also found to have small clusters of decreased FA, possibly in relation to the neurological damage observed in the internal capsule fibers. Clusters of decreased FA were also observed in the fornix, the white matter tract that connects to the hippocampus, the limbic structure responsible for memory and the primary target structure of DA toxicity (Jeffery et al., 2004), and the corpus callosum, the major white matter structure that connects the left and right hemispheres of the brain and is integral to processing stimulation from a multitude of senses (Fabri, 2014). Decreased FA in any of these regions can contribute to a host of neurological phenotypes, but

continued research is necessary to understand the underlying connection between the observed behavioral phenotype of intentional tremors to FA deficits across these major brain structures.

In our study, no other diffusion measures, including axial, radial, and mean diffusivity, were changed in relation to tremors. Previous imaging studies have suggested that axial diffusivity reflects acute axonal damage, such as beading (Budde and Frank, 2010) or swelling (Dickson et al., 2007), whereas changes in radial diffusivity are symptomatic of demyelination (Song et al., 2002). Other studies have implicated that when FA is decreased, but mean diffusivity is unchanged, there may be other types of neuronal damage, such as axonal degeneration or an associated glial response, as a cause (Werring et al., 2000). Given our results in FA changes, we propose that there may be axonal degeneration or an increased glial cell response, but not acute axonal damage in primates chronically exposed to low-levels of this increasingly prevalent marine neurotoxin.

Although there are currently no other whole brain DTI analyses in any animal model or human studies of DA exposure, other studies in DA-exposed humans and sea lions have shown that acute DA exposures can produce hippocampal lesions and atrophy as visualized with T2-weighted MR images (Cendes et al., 1995; Montie et al., 2010). Importantly, we did not detect any visible lesions on T1- and T2-weighted images in either the high-tremoring, DA exposed macaques or the low-tremoring control animals, but we did confirm the presence of a lesion on the high-tremoring, control. This finding suggests that tremoring observed in DA exposed animals may be connected with low-level, neurological damage that is not highly visible on T1- or T2-weighted MR images. The only other DTI study conducted in DA-exposed mammals was a post-mortem targeted diffusion analysis in the brains of sea lions that were chronically afflicted with symptoms of DA poisoning (2018). Authors of this MR study used T2-weighted and DTI analyses to assess volumetric and structural changes in the brain. In this study, a limited number of brain regions were selected for analysis, and results showed that FA in the fornix,

hippocampus, and tracts connecting the hippocampus and thalamus was decreased in DA poisoned animals. These results are similar to those observed in the fornix in our model but were obtained from sea lions demonstrating frank neurotoxicity with visible T2-weighted hippocampal damage, thus suggesting neurological damage that was more severe than the subtle tremors observed in our study. Neurological effects in the fornix, as observed in our study, are also consistent with the published literature, as DA is known to primarily target the hippocampus, resulting in diminished memory. While the present research did not include any examination of cognition, other non-DA, DTI studies in humans have connected decreases in FA to reduced working memory and cognitive performance (Nusbaum et al., 2001; Schulze et al., 2011; Takeuchi et al., 2011).

Our spectroscopy analysis calculated concentrations of several neurochemicals in a voxel placed over the thalamus and adjacent areas of the brain. These data showed that concentrations of NAA, choline, creatinine, lactate and Glx were unchanged in relation to exposure status. NAA, choline, creatinine, and Glx did not correlate with increasing tremors, but lactate was significantly increased with increased tremoring in our cohort. Lactate is an important chemical in the brain, with several multifaceted roles including as: fuel for the brain (Boumezbeur et al., 2010; Smith et al., 2003); signaling for redox cycling and gene expression (Brooks, 2009); and conducting normal astrocyte and myelinating oligodendrocyte functions (Rinholm and Bergersen, 2014). It should be noted, however, that the observed correlation between lactate and tremors was variable ($r=0.58$, $p=0.048$), so further investigations are needed to confirm this.

The neurological damage observed in this study revealed new brain areas that are potential targets of DA, but it should be noted that the present study is exploratory and the first of its kind. Additional research should be conducted in other preclinical models, using both male and female animals, to verify these results and better understand the biochemical and cellular

mechanisms underlying the observed changes in FA and lactate. Future research may also be directed at investigating the relationship between FA and DA-related deficits in memory. These results, however, remain compelling for humans who are regularly exposed to DA. Our nonhuman primate model is highly translatable to humans, sharing close similarities in brain structure, connectivity, and function (Passingham, 2009). In addition to our model, we also chose to give exposures orally and near the current regulatory limits (Mariën, 1996; Wekell et al., 2004), to bring strong environmental relevance to the study. These results may be particularly significant to already vulnerable communities that have close cultural connections to various types of seafood, such as some coastal Native American Tribes, where up to 84% of people regularly consume razor clams (Boushey et al., 2016). As DA algal blooms continue to increase in frequency and severity around the globe, it is imperative that we continue to advance our understanding of the health consequences associated with chronic, low-level intake of this marine biotoxin.

### 2.6 Acknowledgements

We would like to thank Mr. Tim Wilbur for this help with the RF coil and MR scanning, as well as staff and volunteers at the Washington National Primate Research Center and University of Washington Diagnostics Imaging Sciences Center for their skill and technical assistance with this research.

### 2.7 References

Alba-Ferrara, L. M., & de Erausquin, G. A. (2013). What does anisotropy measure? Insights from increased and decreased anisotropy in selective fiber tracts in schizophrenia. Frontiers in Integrative Neuroscience, 7, 9. https://doi.org/10.3389/fnint.2013.00009

Andersson, J. L. R., Skare, S., & Ashburner, J. (2003). How to correct susceptibility distortions in spin-echo echo-planar images: Application to diffusion tensor imaging. NeuroImage, 20(2), 870–888. https://doi.org/10.1016/S1053-8119(03)00336-7

Andjelkovic, M., Vandevijvere, S., Van Klaveren, J., Van Oyen, H., & Van Loco, J. (2012). Exposure to domoic acid through shellfish consumption in Belgium. Environment International, 49, 115–119. https://doi.org/10.1016/j.envint.2012.08.007

Avants, B. B., Tustison, N. J., Song, G., Cook, P. A., Klein, A., & Gee, J. C. (2011). A reproducible evaluation of ANTs similarity metric performance in brain image registration. NeuroImage, 54(3), 2033–2044. https://doi.org/10.1016/j.neuroimage.2010.09.025

Beaulieu, C. (2002, November). The basis of anisotropic water diffusion in the nervous system - A technical review. NMR in Biomedicine, Vol. 15, pp. 435–455. https://doi.org/10.1002/nbm.782

Bossart, G. D. (2011). Marine mammals as sentinel species for oceans and human health. Veterinary Pathology, 48(3), 676–690. https://doi.org/10.5670/oceanog.2006.77

Boumezbeur, F., Petersen, K. F., Cline, G. W., Mason, G. F., Behar, K. L., Shulman, G. I., & Rothman, D. L. (2010). The contribution of blood lactate to brain energy metabolism in humans measured by dynamic 13C nuclear magnetic resonance spectroscopy. Journal of Neuroscience, 30(42), 13983–13991. https://doi.org/10.1523/JNEUROSCI.2040-10.2010

Boushey, C. J., Delp, E. J., Ahmad, Z., Wang, Y., Roberts, S. M., & Grattan, L. M. (2016). Dietary assessment of domoic acid exposure: What can be learned from traditional methods and new applications for a technology assisted device. Harmful Algae, 57(B), 51–55. https://doi.org/10.1016/j.hal.2016.03.013

Brooks, G. A. (2009, December 1). Cell-cell and intracellular lactate shuttles. Journal of Physiology, Vol. 587, pp. 5591–5600. https://doi.org/10.1113/jphysiol.2009.178350

Budde, M. D., & Frank, J. A. (2010). Neurite beading is sufficient to decrease the apparent diffusion coefficient after ischemic stroke. Proceedings of the National Academy of Sciences, 107(32), 14472–14477. https://doi.org/10.1073/pnas.1004841107

Budde, M. D., Janes, L., Gold, E., Turtzo, L. C., & Frank, J. A. (2011). The contribution of gliosis to diffusion tensor anisotropy and tractography following traumatic brain injury: Validation in the rat using Fourier analysis of stained tissue sections. Brain, 134(8), 2248–2260. https://doi.org/10.1093/brain/awr161

Burbacher, T., Grant, K., Petroff, R., Crouthamel, B., Stanley, C., McKain, N., Shum, S., Jing, J., Isoherranen, N. (2019). Effects of Chronic, Oral Domoic Acid Exposure on Maternal Reproduction and Infant Birth Characteristics in a Preclinical Primate Model. Neurotoxicology and Teratology, 440354. https://doi.org/10.1101/440354

Burbacher, T. M., Grant, K. S., Shen, D. D., Sheppard, L., Damian, D., Ellis, S., & Liberato, N. (2004). Chronic maternal methanol inhalation in nonhuman primates (Macaca fascicularis): Reproductive performance and birth outcome. Neurotoxicology and Teratology, 26(5), 639–650. https://doi.org/10.1016/j.ntt.2004.06.001

California Office of Health and Environmental Assessment. (1991). Natural Marine Toxins: PSP and Domoic Acid California's Mussel Quarantine Natural Marine Toxin Monitoring Program. 1–4.

Canadian Food Inspection Agency. (2011). Canadian Shellfish Sanitation Program: Manual of Operations. 1–139. Retrieved from http://www.inspection.gc.ca/food/fish-and-seafood/manuals/canadian-shellfish-sanitation-program/eng/1351609988326/1351610579883?chap=0

Carpenter, S. (1990). The Human Neuropathology of Encephalopathic Mussel Toxin Poisoning. Symposium Domoic Acid Toxicity, 73–34.

Cendes, F., Andermann, F., Carpenter, S., Zatorre, R. J., & Cashman, N. R. (1995). Temporal lobe epilepsy caused by domoic acid intoxication: Evidence for glutamate receptor–mediated excitotoxicity in humans. Annals of Neurology, 37(1), 123–126. https://doi.org/10.1002/ana.410370125

Cook, P. F., Berns, G. S., Colegrove, K., Johnson, S., & Gulland, F. M. D. (2018). Postmortem DTI reveals altered hippocampal connectivity in wild sea lions diagnosed with chronic toxicosis from algal exposure. Journal of Comparative Neurology, 526(2), 216–228. https://doi.org/10.1002/cne.24317

Dickson, T. C., Chung, R. S., McCormack, G. H., Staal, J. A., & Vickers, J. C. (2007). Acute reactive and regenerative changes in mature cortical axons following injury. NeuroReport, 18(3), 283–288. https://doi.org/10.1097/WNR.0b013e3280143cdb

Du, X., Peterson, W., Fisher, J., Hunter, M., & Peterson, J. (2016). Initiation and development of a toxic and persistent Pseudo-nitzschia bloom off the Oregon coast in spring/summer2015. PLoS ONE, 11(10), e0163977. https://doi.org/10.1371/journal.pone.0163977

Dubach, M. F., & Bowden, D. M. (2009). BrainInfo online 3D macaque brain atlas: a database in the shape of a brain. Society for Neuroscience Annual Meeting, Chicago, IL, Abstract No. 199.5. Retrieved from https://scalablebrainatlas.incf.org/docs/dubach_bowden_sfn2009.pdf

Fabri, M. (2014). Functional topography of the corpus callosum investigated by DTI and fMRI. World Journal of Radiology, 6(12), 895. https://doi.org/10.4329/wjr.v6.i12.895

Ferriss, B. E., Marcinek, D. J., Ayres, D., Borchert, J., & Lefebvre, K. A. (2017). Acute and chronic dietary exposure to domoic acid in recreational harvesters: A survey of shellfish consumption behavior. Environment International, 101, 70–79. https://doi.org/10.1016/j.envint.2017.01.006

Garcia-Lazaro, H. G., Becerra-Laparra, I., Cortez-Conradis, D., & Roldan-Valadez, E. (2016). Global fractional anisotropy and mean diffusivity together with segmented brain volumes assemble a predictive discriminant model for young and elderly healthy brains: A pilot study at 3T. Functional Neurology, 31(1), 39–46. https://doi.org/10.11138/FNeur/2016.31.1.039

Grattan, L.M., Boushey, C.J., Liang, Y., Lefebvre, K.A., Castellon, L.J., Roberts, K.A., Toben, A.C., Morris, J.G.J., 2018. Repeated dietary exposure to low levels of domoic acid and problems with everyday memory: Research to public health outreach. Toxins. 10, 103. https://doi.org/10.3390/toxins10030103

Grattan, L.M., Boushey, C.J., Tracy, K., Trainer, V.L., Roberts, S.M., Schluterman, N., Morris, J.G.J., 2016. The association between razor clam consumption and memory in the CoASTAL cohort. Harmful Algae 57, 20–25. https://doi.org/10.1016/j.hal.2016.03.011

Gulland, F. M. D., Haulena, M., Fauquier, D., Langlois, G., Lander, M. E., Zabka, T. S., & Duerr, R. (2002). Domoic acid toxicity in Californian sea lions (Zalophus californianus): clinical signs. Veterinary Record, 150, 475–480. https://doi.org/doi:10.1136/vr.150.15.475

Iverson, F., Truelove, J., Nera, E., Tryphonas, L., Campbell, J., & Lok, E. (1989). Domoic acid poisoning and mussel-associated intoxication: Preliminary investigations into the response of mice and rats to toxic mussel extract. Food and Chemical Toxicology, 27(6), 377–384. https://doi.org/10.1016/0278-6915(89)90143-9

Jeffery, B., Barlow, T., Moizer, K., Paul, S., & Boyle, C. (2004). Amnesic shellfish poison. Food and Chemical Toxicology, 42(4), 545–557. https://doi.org/10.1016/j.fct.2003.11.010

Jenkinson, M., Beckmann, C. F., Behrens, T. E. J., Woolrich, M. W., & Smith, S. M. (2012, August 15). FSL. NeuroImage, Vol. 62, pp. 782–790. https://doi.org/10.1016/j.neuroimage.2011.09.015

Kumar, K. P., Kumar, S. P., & Nair, G. A. (2009). Risk assessment of the amnesiac shellfish poison, domoic acid, on animals and humans. Journal of Environmental Biology, 30(May), 319–325. https://doi.org/DOI 10.1016/j.automatica.2013.03.005

Lefebvre, K. A., Kendrick, P. S., Ladiges, W., Hiolski, E. M., Ferriss, B. E., Smith, D. R., & Marcinek, D. J. (2017). Chronic low-level exposure to the common seafood toxin domoic acid causes cognitive deficits in mice. Harmful Algae, 64, 20–29. https://doi.org/10.1016/j.hal.2017.03.003

Lefebvre, K. A., Quakenbush, L., Frame, E., Huntington, K. B., Sheffield, G., Stimmelmayr, R., … Gill, V. (2016). Prevalence of algal toxins in Alaskan marine mammals foraging in a changing arctic and subarctic environment. Harmful Algae, 55, 13–24. https://doi.org/10.1016/j.hal.2016.01.007

Lefebvre, K. A., Silver, M., Coale, S. L., & Tjeerdema, R. S. (2002). Domoic acid in planktivorous fish in relation to toxic Pseudo-nitzschia cell densities. Marine Biology, 140(3), 625–631. https://doi.org/10.1007/s00227-001-0713-5

Mariën, K. (1996). Establishing tolerable dungeness crab (Cancer magister) and razor clam (Siliqua patula) domoic acid contaminant levels. Environmental Health Perspectives, 104(11), 1230–1236. https://doi.org/10.1289/ehp.961041230

McCabe, R. M., Hickey, B. M., Kudela, R. M., Lefebvre, K. A., Adams, N. G., Bill, B. D., … Trainer, V. L. (2016). An unprecedented coastwide toxic algal bloom linked to anomalous ocean conditions. Geophysical Research Letters, 43(19), 10,366-10,376. https://doi.org/10.1002/2016GL070023

McCarthy, P. (2018). FSLeyes. https://doi.org/10.5281/ZENODO.1887737

McHuron, E. A., Greig, D. J., Colegrove, K. M., Fleetwood, M., Spraker, T., Gulland, F. M. D., … Frame, E. R. (2013). Domoic acid exposure and associated clinical signs and histopathology in Pacific harbor seals (Phoca vitulina richardii). Harmful Algae, 23, 28–33. https://doi.org/10.1016/j.hal.2012.12.008

McKibben, S. M., Peterson, W., Wood, A. M., Trainer, V. L., Hunter, M., & White, A. E. (2017). Climatic regulation of the neurotoxin domoic acid. Proceedings of the National Academy of Sciences, 114(2), 239–244. https://doi.org/10.1073/pnas.1606798114

Montie, E. W., Wheeler, E., Pussini, N., Battey, T. W. K., Barakos, J., Dennison, S., … Gulland, F. M. D. (2010). Magnetic resonance imaging quality and volumes of brain structures from live and postmortem imaging of California sea lions with clinical signs of domoic acid toxicosis. Diseases of Aquatic Organisms, 91(3), 243–256. https://doi.org/10.3354/dao02259

Morecraft, R. J., Herrick, J. L., Stilwell-Morecraft, K. S., Louie, J. L., Schroeder, C. M., Ottenbacher, J. G., & Schoolfield, M. W. (2002). Localization of arm representation in the corona radiata and internal capsule in the non-human primate. Brain, 125(1), 176–198. https://doi.org/10.1093/brain/awf011

Nusbaum, A. O., Tang, C. Y., Buchsbaum, M. S., Tsei Chung Wei, & Atlas, S. W. (2001). Regional and global changes in cerebral diffusion with normal aging. American Journal of Neuroradiology, 22(1), 136–142. Retrieved from http://www.ncbi.nlm.nih.gov/pubmed/11158899

O'Mahony, M. (2018, March 10). EU regulatory risk management of marine biotoxins in the marine bivalve mollusc food-chain. Toxins, Vol. 10. https://doi.org/10.3390/toxins10030118

Passingham, R. (2009, February). How good is the macaque monkey model of the human brain? Current Opinion in Neurobiology, Vol. 19, pp. 6–11. https://doi.org/10.1016/j.conb.2009.01.002

Perl, T. M., Bedard, L., Kosatsky, T., Hockin, J. C., & Todd, E. C. D. (1990). An Outbreak of Toxic Encephalopathy Caused by Eating Mussels Contaminated with Domoic Acid. New England Journal of Medicine, 322(25), 1775–1780. https://doi.org/10.1056/NEJM199006213222504

Perl, T. M., Bedard, L., Kosatsky, T., Hockin, J. C., Todd, E. C., McNutt, L. A., & Remis, R. S. (1990). Amnesic shellfish poisoning: a new clinical syndrome due to domoic acid. Canada Diseases Weekly Report, 16 Suppl 1, 7–8. Retrieved from http://www.ncbi.nlm.nih.gov/pubmed/2101742

Provencher, S. W. (1993). Estimation of metabolite concentrations from localized in vivo proton NMR spectra. Magnetic Resonance in Medicine, 30(6), 672–679. https://doi.org/10.1002/mrm.1910300604

R Core Team. (2020). R: A language and environment for statistical computing. https://doi.org/http://www.R-project.org/

Rinholm, J. E., & Bergersen, L. H. (2014, September 12). White matter lactate - Does it matter? Neuroscience, Vol. 276, pp. 109–116. https://doi.org/10.1016/j.neuroscience.2013.10.002

Rohlfing, T., Kroenke, C. D., Sullivan, E. V., Dubach, M. F., Bowden, D. M., Grant, K. A., & Pfefferbaum, A. (2012). The INIA19 template and NeuroMaps atlas for primate brain image parcellation and spatial normalization. Frontiers in Neuroinformatics, 6(NOV), 27. https://doi.org/10.3389/fninf.2012.00027

Schmahmann, J. D., Rosene, D. L., & Pandya, D. N. (2004). Motor projections to the basis pontis in Rhesus monkey. Journal of Comparative Neurology, 478(3), 248–268. https://doi.org/10.1002/cne.20286

Schnetzer, A., Jones, B. H., Schaffner, R. A., Cetinic, I., Fitzpatrick, E., Miller, P. E., … Caron, D. A. (2013). Coastal upwelling linked to toxic Pseudo-nitzschia australis blooms in Los Angeles coastal waters, 2005-2007. Journal of Plankton Research, 35(5), 1080–1092. https://doi.org/10.1093/plankt/fbt051

Scholin, C. A., Gulland, F., Doucette, G. J., Benson, S., Busman, M., Chavez, F. P., … Van Dolah, F. M. (2000). Mortality of sea lions along the central California coast linked to a toxic diatom bloom. Nature, 403(6765), 80–84. https://doi.org/10.1038/47481

Schulze, E. T., Geary, E. K., Susmaras, T. M., Paliga, J. T., Maki, P. M., & Little, D. M. (2011). Anatomical correlates of age-related working memory declines. Journal of Aging Research, 2011, 606871. https://doi.org/10.4061/2011/606871

Schwarz, C. G., Reid, R. I., Gunter, J. L., Senjem, M. L., Przybelski, S. A., Zuk, S. M., … Jack, C. R. (2014). Improved DTI registration allows voxel-based analysis that outperforms Tract-Based Spatial Statistics. NeuroImage, 94, 65–78. https://doi.org/10.1016/j.neuroimage.2014.03.026

Seubert, E. L., Gellene, A. G., Howard, M. D. A., Connell, P., Ragan, M., Jones, B. H., … Caron, D. A. (2013). Seasonal and annual dynamics of harmful algae and algal toxins revealed through weekly monitoring at two coastal ocean sites off southern California, USA. Environmental Science and Pollution Research, 20(10), 6878–6895. https://doi.org/10.1007/s11356-012-1420-0

Shum, S., Kirkwood, J. S., Jing, J., Petroff, R., Crouthamel, B., Grant, K. S., … Isoherranen, N. (2018). Validated HPLC-MS/MS method to quantify low levels of domoic acid in plasma and urine after subacute exposure. ACS Omega, 3(9), 12079–12088. https://doi.org/10.1021/acsomega.8b02115

Silvagni, P. A., Lowenstine, L. J., Spraker, T., Lipscomb, T. P., & Gulland, F. M. D. (2005). Pathology of domoic acid toxicity in California sea lions (Zalophus californianus). Veterinary Pathology, 42(2), 184–191. https://doi.org/10.1354/vp.42-2-184

Smith, D., Pernet, A., Hallett, W. A., Bingham, E., Marsden, P. K., & Amiel, S. A. (2003). Lactate: A preferred fuel for human brain metabolism in vivo. Journal of Cerebral Blood Flow and Metabolism, 23(6), 658–664. https://doi.org/10.1097/01.WCB.0000063991.19746.11

Smith, J., Connell, P., Evans, R. H., Gellene, A. G., Howard, M. D. A., Jones, B. H., … Caron, D. A. (2018). A decade and a half of Pseudo-nitzschia spp. and domoic acid along the coast of southern California. Harmful Algae, 79, 87–104. https://doi.org/10.1016/j.hal.2018.07.007

Smith, J., Gellene, A. G., Hubbard, K. A., Bowers, H. A., Kudela, R. M., Hayashi, K., & Caron, D. A. (2018). Pseudo-nitzschia species composition varies concurrently with domoic acid concentrations during two different bloom events in the Southern California Bight. Journal of Plankton Research, 40(1), 1–17. https://doi.org/10.1093/plankt/fbx069

Smith, S. M., Jenkinson, M., Johansen-Berg, H., Rueckert, D., Nichols, T. E., Mackay, C. E., … Behrens, T. E. J. (2006). Tract based spatial statistics: Voxelwise analysis of multi-subjects diffusion data. NeuroImage, 31(4), 1487–1505. https://doi.org/10.1016/j.neuroimage.2006.02.024

Smith, S. M., Jenkinson, M., Woolrich, M. W., Beckmann, C. F., Behrens, T. E. J., Johansen-Berg, H., … Matthews, P. M. (2004). Advances in functional and structural MR image analysis and implementation as FSL. NeuroImage, 23(SUPPL. 1), S208–S219. https://doi.org/10.1016/j.neuroimage.2004.07.051

Smith, S. M., & Nichols, T. E. (2009). Threshold-free cluster enhancement: Addressing problems of smoothing, threshold dependence and localisation in cluster inference. NeuroImage, 44(1), 83–98. https://doi.org/10.1016/j.neuroimage.2008.03.061

Song, S. K., Sun, S. W., Ramsbottom, M. J., Chang, C., Russell, J., & Cross, A. H. (2002). Dysmyelination revealed through MRI as increased radial (but unchanged axial) diffusion of water. NeuroImage, 17(3), 1429–1436. https://doi.org/10.1006/nimg.2002.1267

Takeuchi, H., Taki, Y., Sassa, Y., Hashizume, H., Sekiguchi, A., Fukushima, A., & Kawashima, R. (2011). Verbal working memory performance correlates with regional white matter structures in the frontoparietal regions. Neuropsychologia, 49(12), 3466–3473. https://doi.org/10.1016/j.neuropsychologia.2011.08.022

Toyofuku, H. (2006). Joint FAO/WHO/IOC activities to provide scientific advice on marine biotoxins (research report). Marine Pollution Bulletin, 52(12), 1735–1745. https://doi.org/10.1016/j.marpolbul.2006.07.007

Trainer, V., Cochlan, W. P., Erickson, A., Bill, B. D., Cox, F. H., Borchert, J. A., & Lefebvre, K. A. (2007). Recent domoic acid closures of shellfish harvest areas in Washington State inland waterways. Harmful Algae, 6(3), 449–459. https://doi.org/10.1016/j.hal.2006.12.001

Truelove, J., Mueller, R., Pulido, O., Martin, L., Fernie, S., & Iverson, F. (1997). 30-day oral toxicity study of domoic acid in cynomolgus monkeys: Lack of overt toxicity at doses approaching the acute toxic dose. Natural Toxins, 5(3), 111–114. https://doi.org/10.1002/nt.5

Tryphonas, L., Truelove, J., Todd, E. C. D., Nera, E., & Iverson, F. (1990). Experimental oral toxicity of domoic acid in cynomolgus monkeys (Macaca fascicularis) and rats. Food and Chemical Toxicology, 28(10), 707–715. https://doi.org/10.1016/0278-6915(90)90147-F

US Food and Drug Administration. (2011). Fish and Fishery Products Hazards and Controls Guidance. Retrieved from https://www.fda.gov/downloads/food/guidanceregulation/ucm252395.pdf

Vieira, A. C., Alemañ, N., Cifuentes, J. M., Bermúdez, R., Peña, M. L., & Botana, L. M. (2015). Brain Pathology in Adult Rats Treated With Domoic Acid. Veterinary Pathology, 52(6), 1077–1086. https://doi.org/10.1177/0300985815584074

Washington Department of Fish and Wildlife. (n.d.). Domoic Acid - A major concern to Washington state's shellfish lovers. Retrieved January 1, 2016, from Fishing and Shellfishing website: http://wdfw.wa.gov/fishing/shellfish/razorclams/domoic_acid.html

Wekell, J. C., Gauglitz, E. J., Barnett, H. J., Hatfield, C. L., & Eklund, M. (1994). The occurrence of domoic acid in razor clams (Siliqua patula), Dungeness crab (Cancer magister), and achovies (Engraulis mordax). Journal of Shellfish Research, 13(2), 587–593. https://doi.org/10.2983/035.029.0302

Wekell, J. C., Jurst, J., & Lefebvre, K. a. (2004). The origin of the regulatory limits for PSP and ASP toxins in shellfish. Journal of Shellfish Research, 23(3), 927–930.

Wells, M. L., Trainer, V. L., Smayda, T. J., Karlson, B. S. O., Trick, C. G., Kudela, R. M., … Cochlan, W. P. (2015). Harmful algal blooms and climate change: Learning from the past and present to forecast the future. Harmful Algae, 49, 68–93. https://doi.org/10.1016/j.hal.2015.07.009

Werring, D. J., Toosy, A. T., Clark, C. A., Parker, G. J. M., Barker, G. J., Miller, D. H., & Thompson, A. J. (2000). Diffusion tensor imaging can detect and quantify corticospinal tract degeneration after stroke. Journal of Neurology Neurosurgery and Psychiatry, 69(2), 269–272. https://doi.org/10.1136/jnnp.69.2.269

Winkler, A. M., Ridgway, G. R., Webster, M. A., Smith, S. M., & Nichols, T. E. (2014). Permutation inference for the general linear model. NeuroImage, 92, 381–397. https://doi.org/10.1016/j.neuroimage.2014.01.060

Zhu, Z., Qu, P., Fu, F., Tennenbaum, N., Tatters, A. O., & Hutchins, D. A. (2017). Understanding the blob bloom: Warming increases toxicity and abundance of the harmful bloom diatom Pseudo-nitzschia in California coastal waters. Harmful Algae, 67, 36–43. https://doi.org/10.1016/j.hal.2017.06.004

## 2.8 Tables and Figures

***Table 2.1: Characteristics of Individuals Selected for MRI Study.***

| ID | Dose (mg/kg/day) | Days Exposed to DA at MRI | Age (years) | Weight (kg) | % Tremors Pre-Exposure^ | % Tremors Exposure to MRI |
|---|---|---|---|---|---|---|
| 1 | 0.150 | 363 | 11.58 | 4.80 | 8 | 32 |
| 2 | 0.150 | 546 | 8.08 | 4.30 | 0 | 25 |
| 3 | 0.150 | 554 | 7.94 | 4.10 | 0 | 65 |
| 4 | 0.150 | 346 | 8.27 | 3.05 | 15 | 79 |
| 5 | 0.075 | 381 | 7.96 | 3.95 | 0 | 26 |
| 6 | 0.075 | 321 | 7.52 | 4.40 | 5 | 39 |
| Mean | | 419 | 8.6 | 4.1 | 5 | 44 |
| 7 | 0.000 | 0 | 9.24 | 5.12 | 0 | 2 |
| 8 | 0.000 | 0 | 7.91 | 3.59 | 0 | 3 |
| 9 | 0.000 | 0 | 7.93 | 3.99 | 0 | 1 |
| 10 | 0.000 | 0 | 8.43 | 5.23 | 3 | 9 |
| 11 | 0.000 | 0 | 8.14 | 4.36 | 0 | 4 |
| 12 | 0.000 | 0 | 7.44 | 3.34 | 0 | 8 |
| Mean | | 0 | 8.2 | 4.3 | 1 | 5 |
| 13* | 0.000 | 0 | 8.46 | 3.06 | 20 | 64 |

*^ % sessions tremors observed on total sessions tested during a 2-month period immediately preceding the start of exposure.*
*# % sessions tremors observed on total sessions tested from day 1 of exposure to MR scan.*
** Indicates high-tremoring, control animal, excluded from analyses*

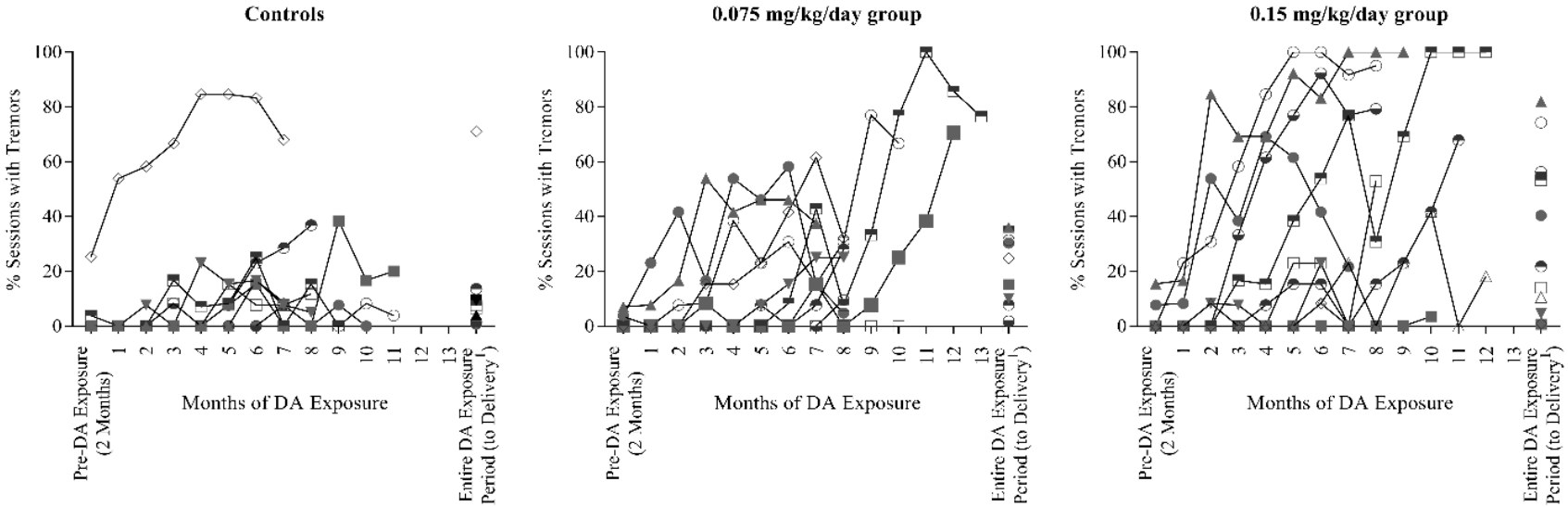


*Figure 2.1: Overall tremors. % of sessions arm/hand tremors observed on reaching task during 2-month pre-exposure period, monthly during DA exposure period and over entire DA exposure period to delivery[1,2]*

*[1]End of breeding for females who did not conceive*

*[2]Reprinted from Neurotoxicology and Teratology, 72, Burbacher, T.M., Grant, K.S., Petroff, R., Shum, S., Crouthamel, B., Stanley, C., McKain, N., Jing, J., Isoherranen, N., Effects of oral domoic acid exposure on maternal reproduction and infant birth characteristics in a preclinical nonhuman primate model, Pages 10-21, Copyright (2019), with permission from Elsevier.*

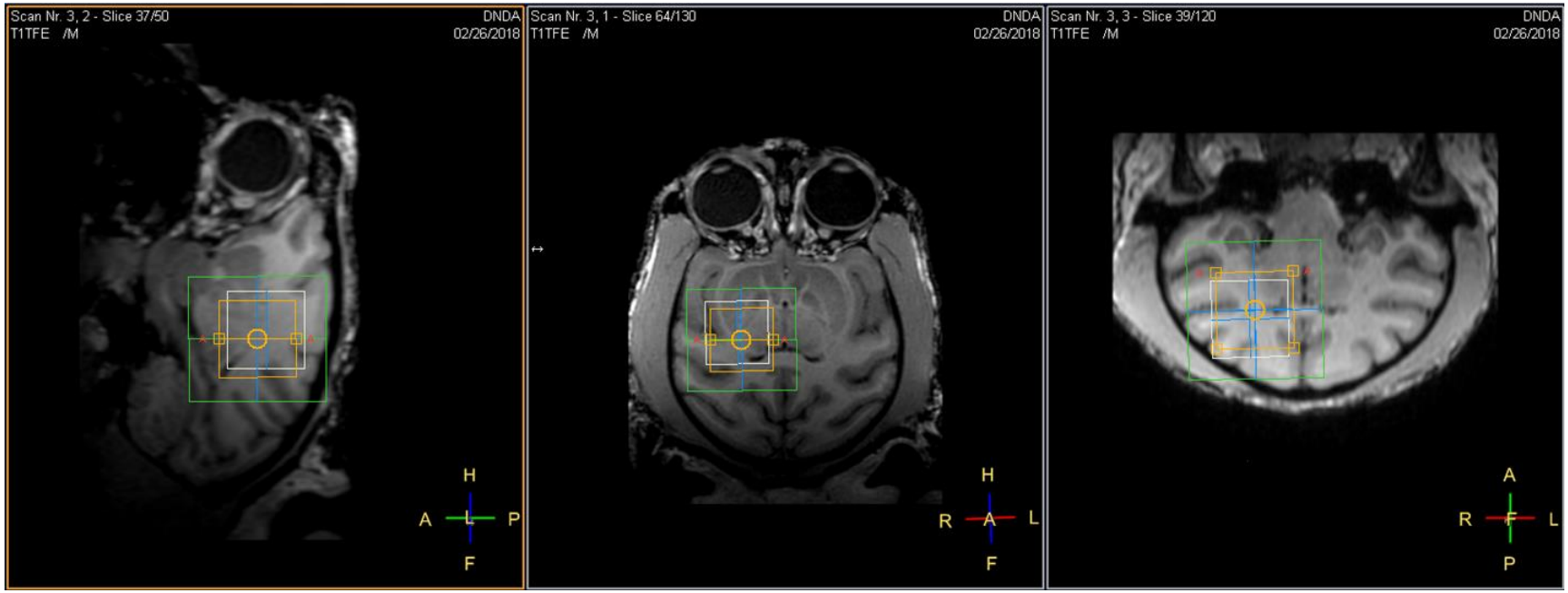


*Figure 2.2: MRS voxel placement. Placement of voxel for MR spectroscopy measurement was centered on the right thalamus.*

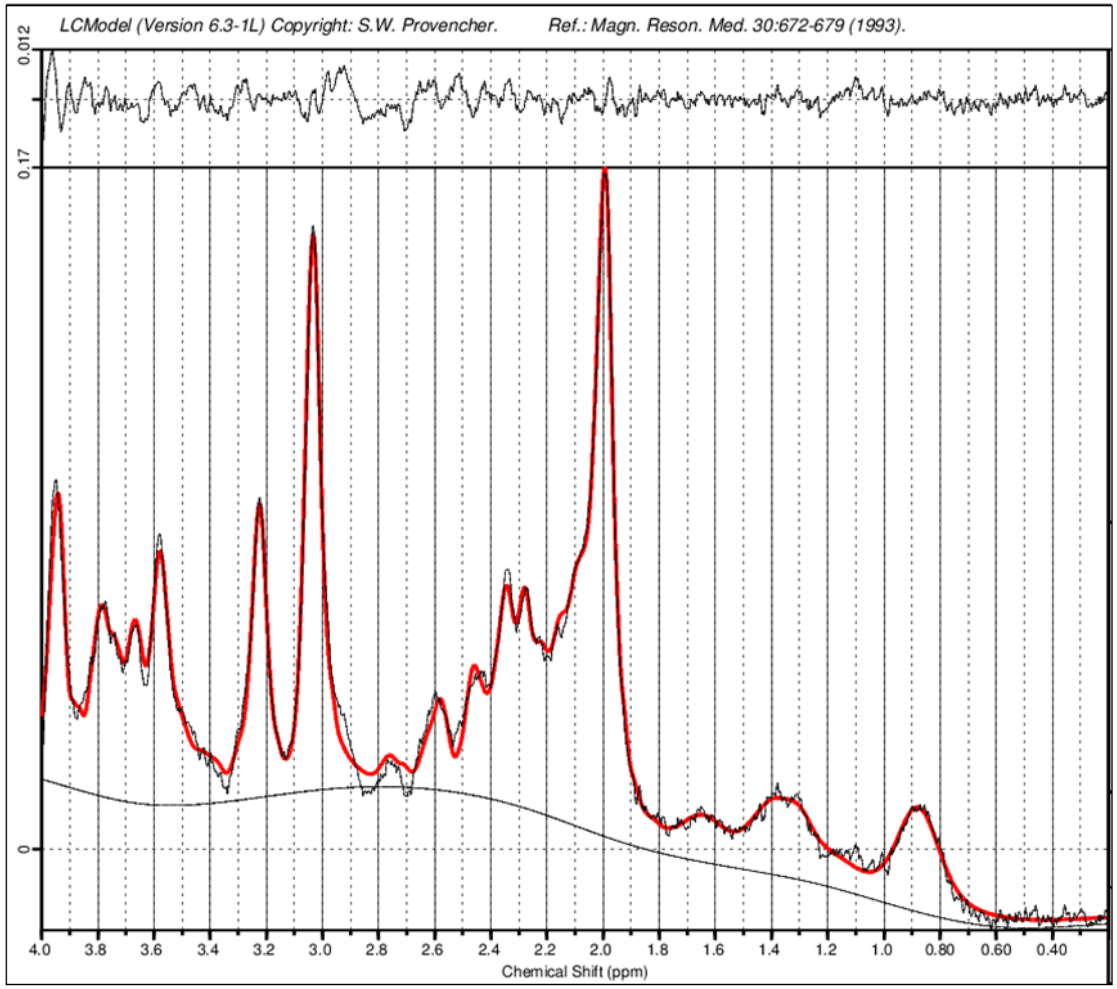


*Figure 2.3: LCmodel fit. LCmodel fitting of the neurochemical spectrum from the voxel placement shown in Fig. 2.2. Smoothed, fitted curve is overlayed on measured spectrum. Differences between the fitted model and true spectrum shown by the curve on top.*

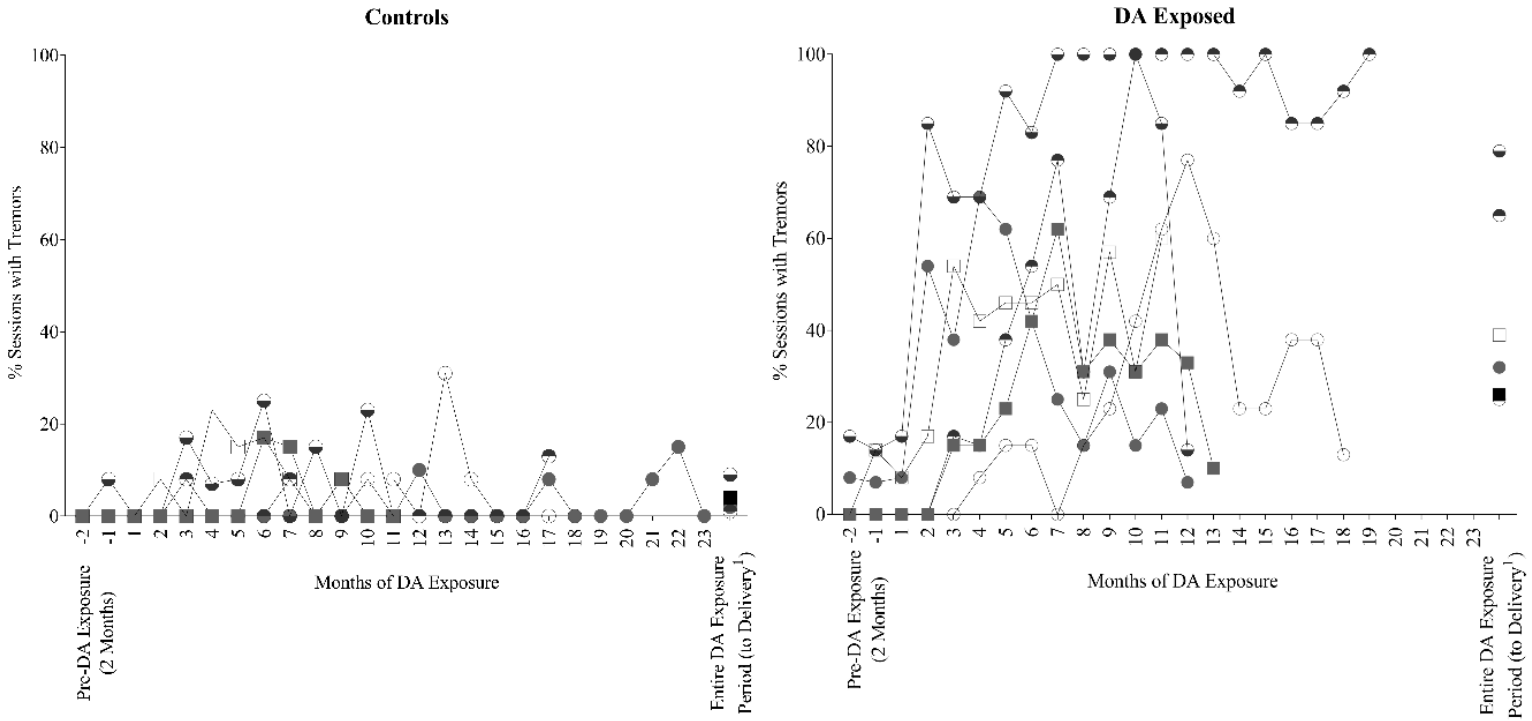


*Figure 2.4: MRI tremors. % of sessions arm/hand tremors for the imaging study animals observed on reaching task monthly during pre-DA exposure period, DA exposure period and over entire DA exposure period to MR study for subset of females selected for MR study.*

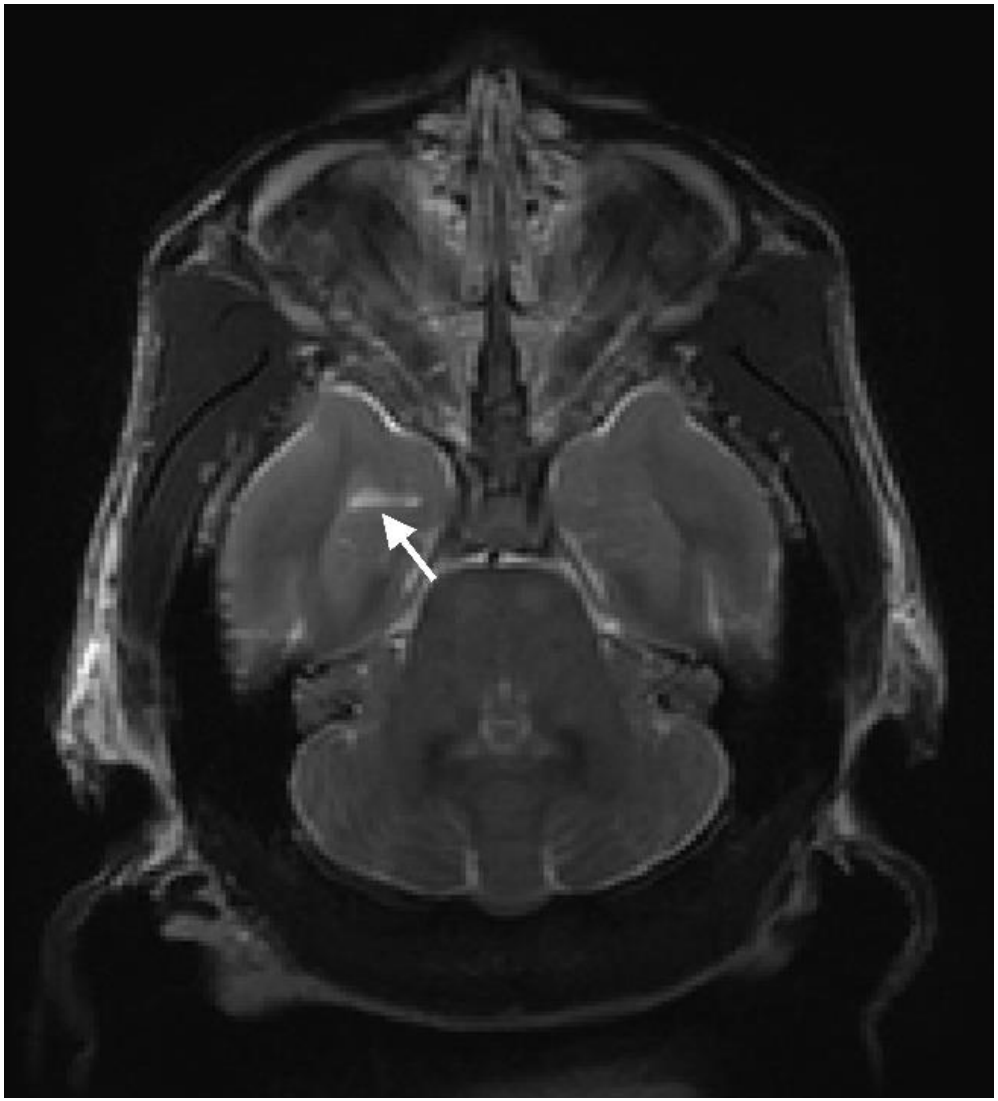

*Figure 2.5: Lesion detection. T2-weighted horizontal image from the high tremoring, control animal. Lesion indicated with the arrow is located in the right temporal lobe, near the fornix and hippocampus.*

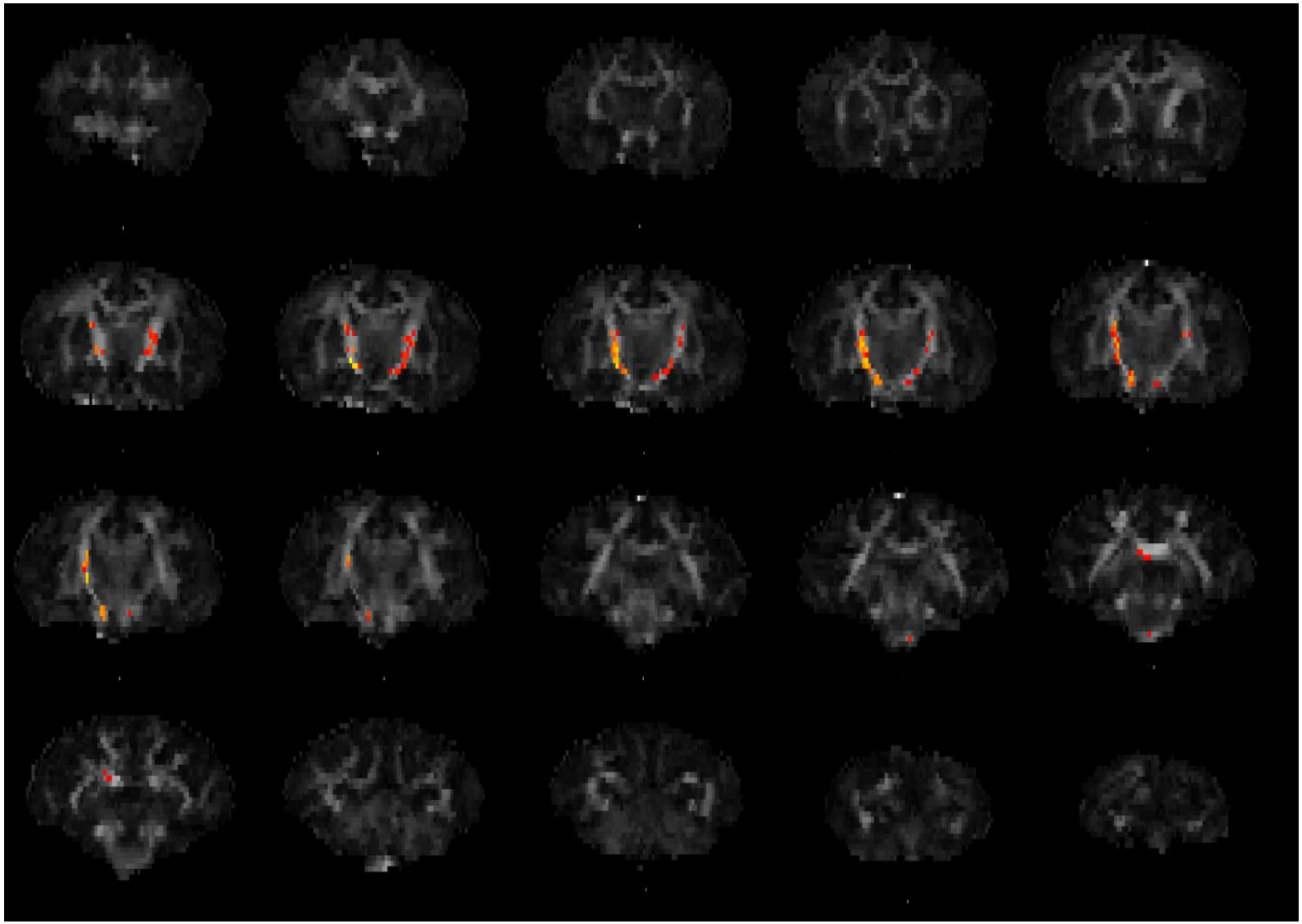

*Figure 2.6: FA averages. Sequential coronal slices from anterior to posterior, of average FA across all individuals included in the analysis. Significant clusters ($p<0.05$) are superimposed in red-yellow.*

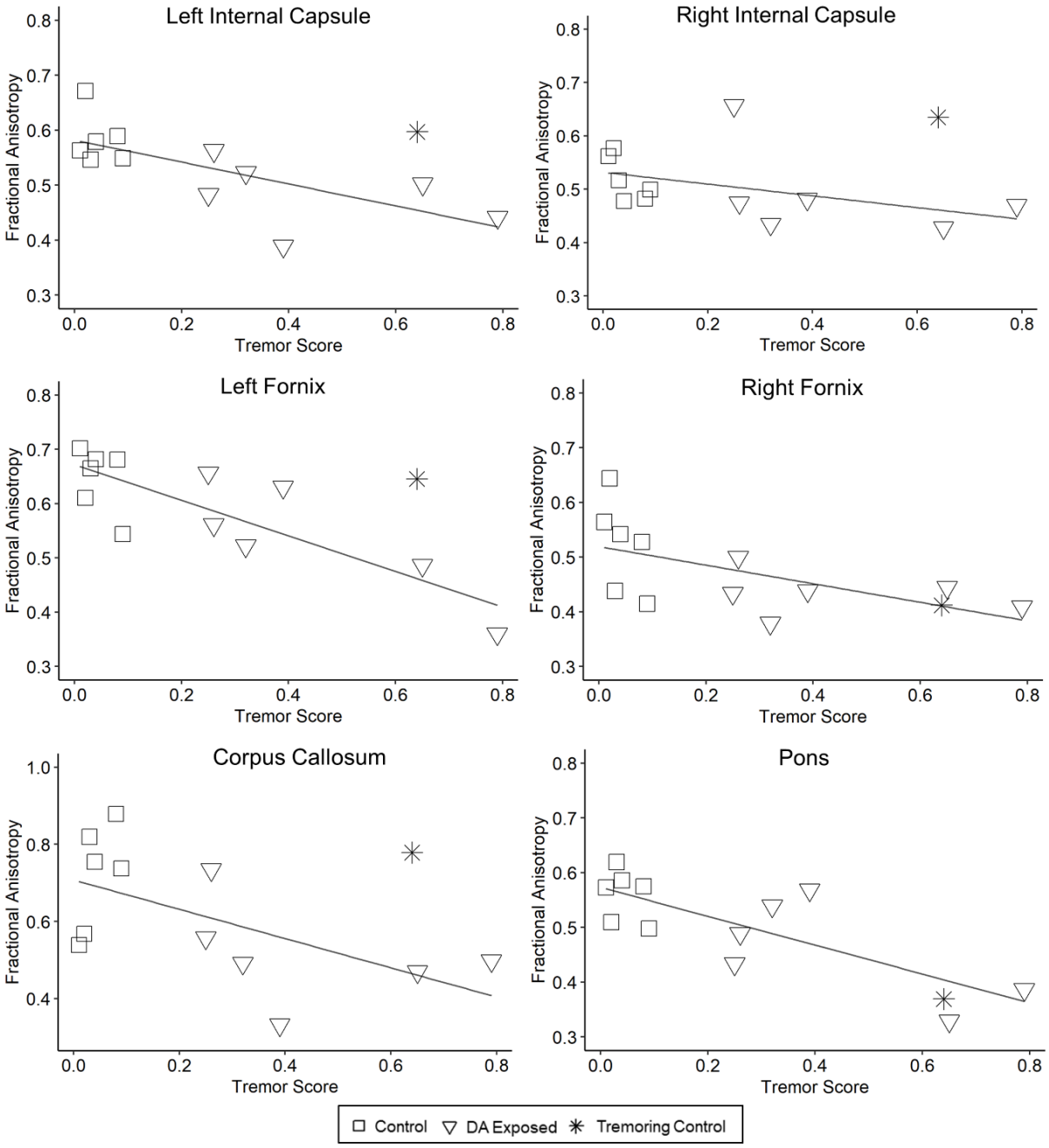


*Figure 2.73: FA and tremor correlations. Brain regions with significant Spearman correlations (rho) for tremor scores and FA. Each correlation represents a single coordinate in the brain from the designated brain region. Control females are represented by squares, exposed females are shown as triangles. Star denotes the high tremoring control female not included in the correlation analysis.*

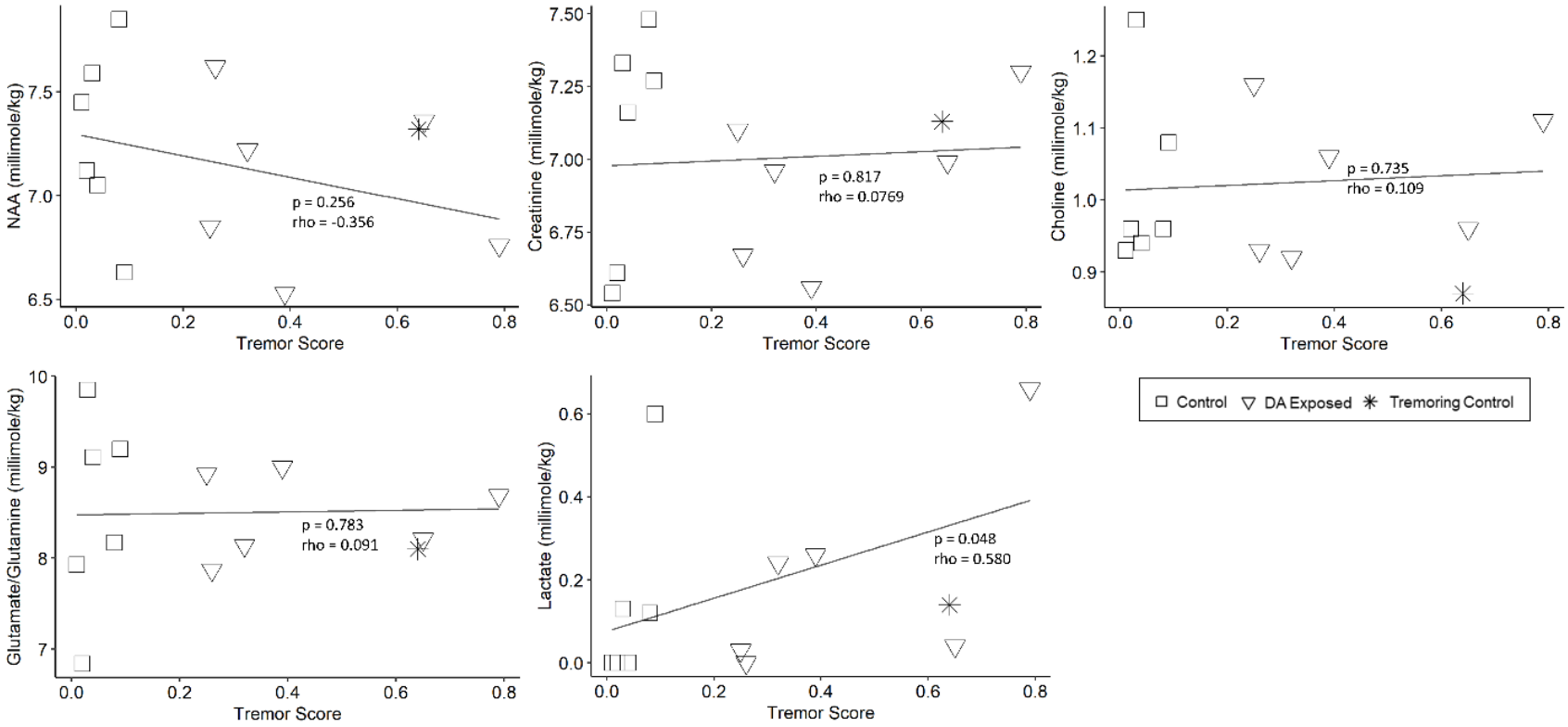


*Figure 2.8: Neurochemical and tremor correlations. Spearman correlation of CSF-corrected neurochemical concentrations and individual tremor scores. Control females are represented by the squares, exposed females are represented by the triangles. Individual denoted by a star is the high tremoring control female, not included in the analyses.*

**Chapter 3: Power spectrum analysis of EEG in a translational nonhuman primate model after chronic exposure to low levels of the common marine neurotoxin, domoic acid**

*This chapter has been submitted for publication in NeuroToxicology. The authors are:*

Petroff, R.,[1] Murias, M.,[2,3] Grant, K.S.,[1] Crouthamel, B.,[1] McKain, N.,[1] Shum, S.,[4] Jing, J.,[4] Isoherranen, N., [4,5] Burbacher, T.M.[1,5,6]

[1] Department of Environmental and Occupational Health Sciences, University of Washington, Seattle, Washington, USA

[2] Department of Medical Social Sciences, Northwestern University, Chicago, IL, USA

[3] Institute for Innovations in Developmental Sciences (DevSci), Northwestern University, Chicago, IL, USA

[4] Department of Pharmaceutics, University of Washington, Seattle, Washington, USA

[5] Center on Human Development and Disability, Seattle, Washington, USA

[6] Infant Primate Research Laboratory, Washington National Primate Research Center, Seattle, Washington, USA

Corresponding Author:

Rebekah Petroff

Department of Environmental and Occupational Health Sciences

School of Public Health, 357234

1959 NE Pacific Street

University of Washington

Seattle, WA 98195

petroffr@uw.edu

**3.1 Abstract**

Domoic acid (DA), the focus of this research, is a marine neurotoxin and epileptogen produced by *Pseudo-nitzschia* algae and found in finfish and shellfish across the globe. The current regulatory limit for DA consumption (20 ppm in shellfish meat) was set to protect humans from acute toxic effects, but there is a growing body of evidence suggesting that regular consumption of DA contaminated seafood below permissible levels may lead to subtle neurological health effects in adults. The present research uses a translational nonhuman primate model to assess neurophysiological changes after chronic exposure to DA near the regulatory limit. Sedated electroencephalography (EEG) was used in 20 healthy adult female *Macaca fascicularis*, orally administered 0.075 and 0.15 mg DA/kg/day for nearly 1 year. Paired video and EEG recordings were cleaned, and a Fast Fourier Transformation was applied to EEG recordings to assess power differences in frequency bands from 1-20 Hz. When DA exposed animals were compared to controls, power was significantly decreased in the delta band (1-4 Hz, $p<0.005$) but significantly increased in the alpha band (5-8 Hz, $p<0.005$), and theta band (9-12 Hz, $p<0.01$). The power differences were not dose dependent, related to the duration of DA exposure, or subtle clinical symptoms of DA exposure (intention tremors). Alterations of power in these bands have been associated with a host of clinical symptoms, such as deficits in memory and neurodegenerative diseases, and ultimately could provide new insight into the subclinical toxicity of chronic, low-dose DA exposure on the adult primate brain.

**Keywords:** Domoic acid; electroencephalography; nonhuman primate; chronic exposure; power spectrum density

### 3.2 Introduction

Over the past several decades, a rapidly changing global environment has led to increasing algal blooms worldwide (Wells et al., 2020). While some blooms may not impact human or wildlife health, other blooms contain algal toxins that can cause health effects in mammalian species (Backer and Miller, 2016; Berdalet et al., 2015; Grattan et al., 2016b). One algal toxin of emerging concern is domoic acid (DA), a small, excitatory amino acid produced by marine algae in the genus *Pseudo-nitzschia*.

DA is a glutamate receptor agonist that primarily binds with high affinity to 2-amino-3-hydroxy-5-methyl-isoxazole-4-propionic acid (AMPA) and kainic acid (KA) type receptors and causes typical glutamate excitotoxity (Debonnel et al., 1989; Stewart et al., 1990). Its toxicity was not documented until 1987, when a mass poisoning occurred, afflicting over 100 people with seizures, memory loss, and death (Cendes et al., 1995; Perl et al., 1990a, 1990b). At high levels, DA targets the temporal lobe, with gross neurotoxicity (necrosis and vacuolization) observed in the hippocampus, thalamus, and amygdala (Carpenter, 1990; Cendes et al., 1995). In subacute studies, DA induces status epilepticus in rats when administered 1 mg/kg/h ip for 3-5 hrs (Muha and Ramsdell, 2011; Tiedeken and Ramsdell, 2013). DA has also been associated with an elevated risk of developing adult epilepsy or spontaneous seizures in naturally exposed sea lions (Ramsdell and Gulland, 2014). In these models, there is extensive neuronal damage, possibly attributable to the injury during seizures. Additionally, a number of reports detail that chronic exposure to very low levels (below the current regulatory limit) of DA is associated with memory deficits in humans (Grattan et al., 2018, 2016a).

Current regulatory limits in North America close fisheries at 20 ppm DA in shellfish, thus constraining environmentally relevant exposures (Wekell et al., 2004). This threshold was estimated from the DA level that caused the first clinical symptoms in humans (~200 ppm) with a 12-fold safety factor (Perl et al., 1990b). Estimates suggest that, with the 20 ppm limit for

shellfish, an adult consumes 0.075-0.1 mg DA/kg bodyweight per meal of seafood (Mariën, 1996; Toyofuku, 2006). Since 1987, there has been no documentation of acute human DA toxicity, but environmental factors are changing today's oceans. In the last 30 years, there has been an increase in the frequency, severity and duration of toxic algal blooms, including DA blooms (McKibben et al., 2017; Wells et al., 2015a). These changing DA algal bloom dynamics could lead to more frequent exposures to levels of DA at or below the current regulatory limit.

While seizures and other abnormal limb activities after DA exposure have been well documented in acutely exposed laboratory and wildlife animals alike (Dakshinamurti et al., 1991; Fujita et al., 1996; Iverson et al., 1989; Ramsdell and Gulland, 2014; Tryphonas et al., 1990b), it remains unclear if lower level exposures to DA may have effects on neuroelectrophysiology. In the present investigation, we used electroencephalography (EEG) in a cohort of adult, female *Macaca fascicularis* chronically exposed to 0.075 and 0.15 mg DA/kg/day to investigate the effects of DA on the power spectrum of neuroelectric activity measured by EEG.

EEG signals reflect the total amount of neuroelectric activity generated in the cortex, with contributing noise from the skull, scalp, dura, and surrounding electrical interference. Power is a quantitative EEG (qEEG) measure that originates from the signaling of large, pyramidal neurons in the cortex, hippocampus and amygdala (Kirschstein and Köhling, 2009) and uses the Fast Fourier Transformation to describe the strength of the signal at a given frequency, and frequencies are often divided into bands, which typically include delta (1-4 Hz), theta (5-8 Hz), alpha (9-12 Hz), and beta (13-20 Hz). Dramatic increases in power are frequently observed in epilepsy, but, in silent epilepsy and absence seizures (i.e. petit mal seizures), these increases can be mild and within normal parameters (Clemens et al., 2000). Alternatively, discordant changes in bands can be indicative of psychiatric disorders, neurodegenerative disease, or the engagement of specific tasks, such as in memory and learning challenges (Harmony, 2013;

Newson and Thiagarajan, 2019). Thus, even subtle changes in EEG bandpower may be indicative of larger neuroelectrical aberrations. The goals of this study were to employ noninvasive EEG methods in sedated animals to evaluate differences in EEG bandpower after chronic exposure to DA near the human regulatory limit.

### 3.3 Methods

*Animals and Study Protocol*

For this study, a subset of 20 adult female *Macaca fascicularis* were selected from the cohort described in Burbacher et al., 2019. Age ranged between 6 and 11 years (mean: 7 years), and weight ranged between 2.8 and 4.8 kg (mean: 3.5 kg). Animals were singly housed in stainless steel cages, which provided visual and grooming contact with an adjacent animal, in the Infant Primate Research Center at the Washington National Primate Research Center. Room temperature was maintained at approximately 24°C, with a 12-hour light-dark cycle. All animals were fed Purina Monkey Chow twice daily and were supplied with regular environmental enrichment that included fresh fruit and vegetables, frozen foraging treats, and cereals, grains, and other treats. Animal protocols strictly adhered to the Animal Welfare Act and the Guide for Care and Use of Laboratory Animals of the National Research Council and protocols were approved by the University of Washington Institutional Animal Care and Use Committee.

Original study procedures and exposure monitoring protocols are described in detail in Burbacher et al. (2019). In brief, animals were exposed to either 0 (n=7), 0.075 (n=6), or 0.15 (n=8) mg/kg DA/day via an oral solution of 5% sucrose water for 306 to 596 days (mean: 429.6 ± SEM: 22.7), during which all but one female conceived and delivered a single infant (see Supplement 2.1). Testers performed clinical assessments at least 3x/week to track animal's ability to visually orient and track a small piece of fresh produce, and then fully extend an arm to

retrieve the treat. During the reaching task, hand/arm tremors were recorded as either present or absent. Testers were blind to the animal's assignment and maintained an 80% reliability with the primary tester.

*Experimental Design*

All adult females underwent three sedated EEGs, for a total of 60 recordings. EEGs were conducted in the morning. The first and second EEGs were recorded 1.5 hours post dosing, and the third EEG was recorded 24 hours post-dosing. Each EEG occurred a minimum of 3 days apart, to assure the animal was fully recovered before undergoing sedation again. Animals were sedated for EEGs with 4 mg/kg im Telozol®, a combination of tiletamine and zolazepam (Zoetis Services LLC, Parsippany, NJ, USA), and monitored until fully sedate. Once sedated, animals were removed from the homecage and brought to a quiet testing suite for EEG acquisition. Females were prepped and closely monitored throughout EEG acquisition, as described below.

*EEG Procedures and Acquisition*

EEGs were acquired using an Avatar EEG 4000 Series Recorder (Avatar EEG Solutions Inc., Calgary, AB, Canada), equipped with eight 6-mm gold electrodes. Electrode cables were braided together to minimize sources of noise and cleaned with an alcohol wipe before each use. After the subject was fully sedated, the head was shaved and cleaned with alcohol, before applying electrodes with Ten20 conductive paste (Weaver and Company, Aurora, CO, USA) in approximation to the international 10-20 system locations F3/F4, T3/T4, P3/P4. A reference electrode was applied in the center of the head, and a ground electrode was applied to the left mid-back. Electrodes application was typically achieved within 15 minutes of sedation. All EEG sessions were paired with video monitoring to ensure that any movement during the session

would be removed during preprocessing. EEGs were recorded for a minimum of 20 minutes or until the animal was waking from sedation. All impedances were kept below <100 kΩ and were checked at the beginning of the session and at least once during the session after electrodes had settled. Once the recording was complete, all electrode paste was removed, and the animal was returned to her homecage and monitored until fully awake.

*EEG Processing and Power Calculation*

Recordings were processed and analyzed in Matlab using the FieldTrip toolkit and a standardized method to analyze power from EEG recordings (Oostenveld et al., 2011; "Time-frequency analysis using Hanning window, multitapers and wavelets," 2013). To minimize differences in sedation state, a 2-3-minute window was identified in all recordings at the same time post administration of the sedative (24 minutes post-injection). Once this window was identified, EEG recordings were synced with the paired video, and any segment with noticeable head movement, large facial movement (e.g. yawning), or electrode wire movement were removed from the recording, using the *ft_databrowser* function. Two independent, blinded testers reviewed each recording for epileptic and spike activity. After checking for epileptic activity, recordings were converted into Matlab files and preprocessed with *ft_preprocessing* to remove higher order trends from the data. Recordings were then divided into 1-second segments, and the *ft_rejectvisualartifact* graphical user interface was used to visually inspect the variance of each segment. Any segment outside of the normal variance in that recording was removed from further analysis. Whole recordings were excluded if: 1) the animal was resistant to sedation or 2) if more than 25% of total time was removed from the EEG. For each animal, the first EEG recording that met these criteria was used for analysis. All recordings from a single animal in the control group was rejected due to a lack of sedation on all 3 EEG

recordings. Thus, the animals included in the analysis were 6 control animals, 6 in the 0.075 mg/kg group, and 8 in the 0.15 mg/kg group.

After preprocessing, recordings were unblinded and then band pass filtered at 50 Hz to remove harmonics. Timeseries data were segmented into 1-second epochs. Absolute and relative power (% of total power observed in each frequency) was calculated with FieldTrip function *ft_freqanalysis* using a Hanning window and with multitapered Fast Fourier Transformation, yielding power values expressed in 1 Hz frequency bands from 1-50 Hz.

*Statistical Analysis*

To understand if exposure to DA affected the distribution of power, FieldTrip's *ft_freqstatistics* function was used. This uses nonparametric Monte Carlo simulation with a two-tail correction to estimate the significant probabilities of difference in power distributions between dose groups. The two-tailed alpha was set at 0.05, and distributions were compared at each channel and frequency from 1-50 Hz.

To compare frequency bands that have previously been shown to be affected by DA, three tests were conducted in R (R Core Team, 2018) using data averaged across the entire primate head. Frequency bands of interest included delta (1-4 Hz), theta (5-8 Hz), alpha (9-12 Hz), and beta (13-20 Hz). First, to assess if any exposure to DA affected power, a two-sample t-test was used to compare the total average power in each band of the control animals and the exposed animals. A Bonferroni correction was applied to the p-values from the four bands of interest. Secondly, a repeated measures ANOVA was used to assess whether the DA effects observed on the total average power in each band were dose dependent. Finally, a Spearman correlation was used to assess the association between tremor scores and power in the bands of interest, with tremor score as the ranked predictor variable. Differences were considered

significant only when the coefficient confidence interval did not include 0 and the Bonferroni adjusted p-value was less than 0.05

### 3.4 Results

After artifact removal and visual inspection of the EEG recordings, 13 of the 60 total EEGs were excluded, primarily due to an animal's lack of sedation during the recording (see exclusion criteria above). Overall, recordings were clean, without many artifacts, and amplitudes were low, as expected for sedated recordings (Supplement 3.2). No epileptic or spike activity was identified on any recording. On two recordings from one control animal, we captured distinct electrooculographic (EOG) artifacts across multiple sessions, which, to the best of our knowledge, have not been documented in this species before (Supplement 3.3). When observed, the EOG artifact occurred simultaneously on all channels. Notably, paired video-capture did not show any signs of body movement or eye blinking, but only displayed subtle, closed-eyelid movements.

Unsurprisingly and likely due to volume conduction across the small primate head, power distributions across all animals were highly similar on all electrodes on the same side of the head, and somewhat similar between each hemisphere (Fig. 3.1). Using a Monte Carlo simulation to compare the absolute and relative power spectrum between exposed and control groups across all frequencies, we found that there were no significant differences in the overall distributions between dose groups ($p>0.05$) (Fig. 3.1).

The results of the t-test examining the total average power in each band indicated that there were significant differences between the DA exposed and control groups for all bands except the beta band (delta (1-4 Hz) adjusted-p= 0.005, theta (5-8 Hz) adjusted-p =0.002, alpha (9-12 Hz) adjusted-p=0.009, beta (13-20 Hz) adjusted-p=0.53, see Fig. 3.2). The results of the follow-up analysis, assessing the dose-response relationship, did not indicate that the DA

exposure effects were dose dependent for any of the bands (repeated measures ANOVA, p=0.43, F=0.87, see Fig. 3.3). The results of the final analysis did not indicate a significant relationship between tremor scores and power for any of the bands (p>0.1, all tests, see Fig. 3.4).

### 3.5 Discussion

Domoic acid (DA) is a common marine algal neurotoxin that is becoming more widespread under changing oceanic conditions (Wells et al., 2020). It is well documented that acute exposure to DA (>1 mg/kg) can cause seizures and epilepsy (Cendes et al., 1995; Fujita et al., 1996; Gulland et al., 2002; Teitelbaum et al., 1990) and increased electroencephalography (EEG) power in all frequencies have been documented in humans, sea lions, and rodents after acute DA exposure (Cendes et al., 1995; Fujita et al., 1996; Gulland et al., 2002; Teitelbaum et al., 1990). Despite these clear effects at high levels, there is presently little research regarding changes in EEG following long-term exposure to DA at levels near the human regulatory limit (0.075-0.1 mg/kg). Recent evidence from human and animal models suggests that chronic, low-level DA exposure may be related to other subtle neurological changes in motor responses and challenges with regular daily activities (Burbacher et al., 2019; Grattan et al., 2018, 2016a; Lefebvre et al., 2017).

The present research used EEG to assess chronic, low-level neuroelectric power effects in the nonhuman primate model, *Macaca fascicularis*, exposed to 0.075-0.15 mg DA/kg/day. Results from a power spectrum analysis demonstrated that animals exposed to DA have decreased power in the delta band and increased power in the alpha and theta bands. No DA effects were observed in the high frequency beta band. These changes in electrophysiology were not dose dependent or related to clinical symptomology (intention tremors) previously reported in some of the DA exposed females. Proportionately, animals with the highest median

power in delta had the lowest median power in all other bands and tended to be in the control group (n=5/10). Similarly, animals with the lowest median delta power had the highest median power in other bands, and most were exposed animals (n=8/10).

EEG power is a quantitative measure that reflects the action and signaling of large, pyramidal neurons in the cortex, hippocampus and amygdala (Kirschstein and Köhling, 2009). Power can be divided into several frequency bands, each related to many different cognitive and neurological functions. The delta band is comprised of brain oscillations from the slowest frequency band in the EEG assessment and typically ranges from 0-4 Hz, and dominates deep sleep and basic homeostatic resting states (Başar et al., 1999; Knyazev, 2012). Delta also reflects most inhibitory responses of functional processing (Herrmann et al., 2016). Theta is comprised of oscillations in the 5-8 Hz range, and alpha ranges from 9-12 Hz. These two closely connected bands are often connected to memory and cognition, but frequently operate in opposite directions during tasks (i.e. when one increases, the other decreases) (Herrmann et al., 2016; Klimesch, 1999). Beta rhythms are between 13 and 20 Hz and have been linked to sensory and motor tasks and processing. While each band is often known for specific processing tasks, broad spectral changes across several bands have been identified as collectively reflective of performance on memory and learning tests (Finnigan and Robertson, 2011) and many psychiatric disorders (Newson and Thiagarajan, 2019), even during resting states. DA exposed macaques had decreased delta power in EEGs, and increased power in the theta and alpha bands. Decreases in low frequency power have been observed in neurodegenerative diseases, including Parkinson and Alzheimer's disease (Bosboom et al., 2009; Poza et al., 2007); whereas increases in higher frequencies have been linked to psychiatric disorders, such as depression (Hinrikus et al., 2009).

These findings bear careful interpretation, because it is not clearly evident how the different power bands are translated across individuals and across species. Previous EEG

research in *Macaca fascicularis* suggests that most resting EEG activity lies in the delta band, which aligns with our findings (Authier et al., 2009). In humans, however, resting-state EEG power is much more broadly distributed across bands (Hooper, 2005). Additionally, we used a sedative that contains two active ingredients: tiletamine, a relative of ketamine, and zolazepam, a benzodiazepine. These two sedatives interact with the NMDA and GABA pathways, respectively, and are not known to cause changes in the lower frequency oscillations (Choi, 2017). However, benzodiazepines are used to treat seizures and, in high, sedative doses, benzodiazepines result in excessive activity in the beta band (Van Lier et al., 2004). While we did not observe any seizure-like spikes or discharges in DA exposed females, any seizure-like activity may have been suppressed under sedation. Still, all sedation effects were balanced between dosed and control animals; so, while sedation likely had some effects on the results reported here, the observed differences are notable and necessitate further investigation.

The results of the present study collectively suggest that chronic exposure to DA near the current human regulatory limit may result in subtle changes in EEG, possibly reflecting changes in pyramidal neurons. While the functional effects of these EEG changes are not evident from the current study, continued research efforts should focus on how chronic ingestion of real-world levels of DA may be related to neurophysiological and other neurological changes in human populations across the globe.

### 3.6 Acknowledgements

The authors would like to acknowledge the staff and volunteers of the Center on Human Development and Disability (CHDD), Infant Primate Research Laboratory and the University of Washington National Primate Research Center for their skilled assistance in this research.

### 3.7 References


Authier, S., Paquette, D., Gauvin, D., Sammut, V., Fournier, S., Chaurand, F., Troncy, E., 2009. Video-electroencephalography in conscious nonhuman primate using radiotelemetry and computerized analysis: Refinement of a safety pharmacology model. J. Pharmacol. Toxicol. Methods 60, 88–93. https://doi.org/10.1016/J.VASCN.2008.12.003

Backer, L.C., Miller, M., 2016. Sentinel animals in a one health approach to harmful cyanobacterial and algal blooms. Vet. Sci. 3, 8. https://doi.org/10.3390/vetsci3020008

Başar, E., Başar-Eroglu, C., Karakaş, S., Schürmann, M., 1999. Are cognitive processes manifested in event-related gamma, alpha, theta and delta oscillations in the EEG? Neurosci. Lett. 259, 165–168. https://doi.org/10.1016/S0304-3940(98)00934-3

Berdalet, E., Fleming, L.E., Gowen, R., Davidson, K., Hess, P., Backer, L.C., Moore, S.K., Hoagland, P., Enevoldsen, H., 2015. Marine harmful algal blooms, human health and wellbeing: Challenges and opportunities in the 21st century. J. Mar. Biol. Assoc. United Kingdom 96, 61–91. https://doi.org/10.1017/S0025315415001733

Bosboom, J.L.W., Stoffers, D., Wolters, E.C., Stam, C.J., Berendse, H.W., 2009. MEG resting state functional connectivity in Parkinson's disease related dementia. J. Neural Transm. 116, 193–202. https://doi.org/10.1007/s00702-008-0132-6

Burbacher, T., Grant, K., Petroff, R., Crouthamel, B., Stanley, C., McKain, N., Shum, S., Jing, J., Isoherranen, N., 2019. Effects of chronic, oral domoic acid exposure on maternal reproduction and infant birth characteristics in a preclinical primate model. Neurotoxicol. Teratol. 440354. https://doi.org/10.1101/440354

Carpenter, S., 1990. The human neuropathology of encephalopathic mussel toxin poisoning. Symp. Domoic Acid Toxic. 73–34.

Cendes, F., Andermann, F., Carpenter, S., Zatorre, R.J., Cashman, N.R., 1995. Temporal lobe epilepsy caused by domoic acid intoxication: Evidence for glutamate receptor–mediated excitotoxicity in humans. Ann. Neurol. 37, 123–126. https://doi.org/10.1002/ana.410370125

Choi, B.-M., 2017. Characteristics of electroencephalogram signatures in sedated patients induced by various anesthetic agents. J. Dent. Anesth. Pain Med. 17, 241. https://doi.org/10.17245/jdapm.2017.17.4.241

Clemens, B., Szigeti, G., Barta, Z., 2000. EEG frequency profiles of idiopathic generalised epilepsy syndromes. Epilepsy Res. 42, 105–115. https://doi.org/10.1016/S0920-1211(00)00167-4

Dakshinamurti, K., Sharma, S.K., Sundaram, M., 1991. Domoic acid induced seizure activity in rats. Neurosci. Lett. 127, 193–197. https://doi.org/10.1016/0304-3940(91)90792-R

Debonnel, G., Beauchesne, L., Montigny, C. de, 1989. Domoic acid, the alleged mussel toxin, might produce its neurotoxic effect through kainate receptor activation: an electrophysiological study in the rat dorsal hippocampus. Can. J. Physiol. Pharmacol. 67, 29–33. https://doi.org/10.1139/y89-005

Finnigan, S., Robertson, I.H., 2011. Resting EEG theta power correlates with cognitive performance in healthy older adults. Psychophysiology 48, 1083–1087. https://doi.org/10.1111/j.1469-8986.2010.01173.x

Fujita, T., Tanaka, T., Yonemasu, Y., Cendes, F., Cashman, N.R., Andermann, F., 1996. Electroclinical and pathological studies after parenteral administration of domoic acid in freely moving nonanesthetized rats: An animal model of excitotoxicity. J. Epilepsy 9, 87–93. https://doi.org/10.1016/0896-6974(95)00075-5

Grattan, L.M., Boushey, C.J., Liang, Y., Lefebvre, K.A., Castellon, L.J., Roberts, K.A., Toben, A.C., Morris, J.G.J., 2018. Repeated dietary exposure to low levels of domoic acid and problems with everyday memory: Research to public health outreach. Toxins. 10, 103. https://doi.org/10.3390/toxins10030103

Grattan, L.M., Boushey, C.J., Tracy, K., Trainer, V.L., Roberts, S.M., Schluterman, N., Morris, J.G.J., 2016a. The association between razor clam consumption and memory in the CoASTAL cohort. Harmful Algae 57, 20–25. https://doi.org/10.1016/j.hal.2016.03.011

Grattan, L.M., Holobaugh, S., Morris, J.G.J., 2016b. Harmful algal blooms and public health. Harmful Algae. https://doi.org/10.1016/j.hal.2016.05.003

Gulland, F.M.D., Haulena, M., Fauquier, D., Langlois, G., Lander, M.E., Zabka, T.S., Duerr, R., 2002. Domoic acid toxicity in Californian sea lions (Zalophus californianus): clinical signs. Vet. Rec. 150, 475–480. https://doi.org/doi:10.1136/vr.150.15.475

Harmony, T., 2013. The functional significance of delta oscillations in cognitive processing. Front. Integr. Neurosci. https://doi.org/10.3389/fnint.2013.00083

Herrmann, C.S., Strüber, D., Helfrich, R.F., Engel, A.K., 2016. EEG oscillations: From correlation to causality. Int. J. Psychophysiol. https://doi.org/10.1016/j.ijpsycho.2015.02.003

Hinrikus, H., Suhhova, A., Bachmann, M., Aadamsoo, K., Võhma, Ü., Lass, J., Tuulik, V., 2009. Electroencephalographic spectral asymmetry index for detection of depression. Med. Biol. Eng. Comput. 47, 1291–1299. https://doi.org/10.1007/s11517-009-0554-9

Hooper, G.S., 2005. Comparison of the distributions of classical and adaptively aligned EEG power spectra. Int. J. Psychophysiol. 55, 179–189. https://doi.org/10.1016/j.ijpsycho.2004.07.008

Iverson, F., Truelove, J., Nera, E., Tryphonas, L., Campbell, J., Lok, E., 1989. Domoic acid poisoning and mussel-associated intoxication: Preliminary investigations into the response of mice and rats to toxic mussel extract. Food Chem. Toxicol. 27, 377–384. https://doi.org/10.1016/0278-6915(89)90143-9

Kirschstein, T., Köhling, R., 2009. What is the source of the EEG? Clin. EEG Neurosci. 40, 146–149. https://doi.org/10.1177/155005940904000305

Klimesch, W., 1999. EEG alpha and theta oscillations reflect cognitive and memory performance: A review and analysis. Brain Res. Rev. https://doi.org/10.1016/S0165-0173(98)00056-3

Knyazev, G.G., 2012. EEG delta oscillations as a correlate of basic homeostatic and motivational processes. Neurosci. Biobehav. Rev. https://doi.org/10.1016/j.neubiorev.2011.10.002

Lefebvre, K.A., Kendrick, P.S., Ladiges, W., Hiolski, E.M., Ferriss, B.E., Smith, D.R., Marcinek, D.J., 2017. Chronic low-level exposure to the common seafood toxin domoic acid causes cognitive deficits in mice. Harmful Algae 64, 20–29. https://doi.org/10.1016/j.hal.2017.03.003

Mariën, K., 1996. Establishing tolerable Dungeness crab (Cancer magister) and razor clam (Siliqua patula) domoic acid contaminant levels. Environ. Health Perspect. 104, 1230–6. https://doi.org/10.1289/ehp.961041230

McKibben, S.M., Peterson, W., Wood, A.M., Trainer, V.L., Hunter, M., White, A.E., 2017. Climatic regulation of the neurotoxin domoic acid. Proc. Natl. Acad. Sci. 114, 239–244. https://doi.org/10.1073/pnas.1606798114

Muha, N., Ramsdell, J.S., 2011. Domoic acid induced seizures progress to a chronic state of epilepsy in rats. Toxicon 57, 168–171. https://doi.org/10.1016/j.toxicon.2010.07.018

Newson, J.J., Thiagarajan, T.C., 2019. EEG Frequency Bands in Psychiatric Disorders: A Review of Resting State Studies. Front. Hum. Neurosci. 12. https://doi.org/10.3389/fnhum.2018.00521

Perl, T.M., Bedard, L., Kosatsky, T., Hockin, J.C., Todd, E.C., McNutt, L.A., Remis, R.S., 1990a. Amnesic shellfish poisoning: a new clinical syndrome due to domoic acid. Canada Dis. Wkly. Rep. 16 Suppl 1, 7–8.

Perl, T.M., Bedard, L., Kosatsky, T., Hockin, J.C., Todd, E.C.D., 1990b. An outbreak of toxic encephalopathy caused by eating mussels contaminated with domoic acid. N. Engl. J. Med. 322, 1775–1780. https://doi.org/10.1056/NEJM199006213222504

Poza, J., Hornero, R., Abásolo, D., Fernández, A., García, M., 2007. Extraction of spectral based measures from MEG background oscillations in Alzheimer's disease. Med. Eng. Phys. 29, 1073–1083. https://doi.org/10.1016/j.medengphy.2006.11.006

Ramsdell, J.S., Gulland, F.M.D., 2014. Domoic acid epileptic disease. Mar. Drugs 12, 1185–1207. https://doi.org/10.3390/md12031185

Stewart, G.R., Zorumski, C.F., Price, M.T., Olney, J.W., 1990. Domoic acid: A dementia-inducing excitotoxic food poison with kainic acid receptor specificity. Exp. Neurol. 110, 127–138. https://doi.org/10.1016/0014-4886(90)90057-Y

Teitelbaum, J., Zatorre, R.J., Carpenter, S., Gendron, D., Cashman, N.R., 1990. Neurological sequelae of domoic acid intoxication. Symp. Domoic Acid Toxic. 16, 9–12. https://doi.org/10.2174/1381612823666170124l

Tiedeken, J.A., Ramsdell, J.S., 2013. Persistent neurological damage associated with spontaneous recurrent seizures and atypical aggressive behavior of domoic acid epileptic disease. Toxicol. Sci. 133, 133–143. https://doi.org/10.1093/toxsci/kft037

Toyofuku, H., 2006. Joint FAO/WHO/IOC activities to provide scientific advice on marine biotoxins (research report). Mar. Pollut. Bull. 52, 1735–1745. https://doi.org/10.1016/j.marpolbul.2006.07.007

Tryphonas, L., Truelove, J., Iverson, F., Todd, E.C.D., Nera, E., 1990. Neuropathology of Experimental Domoic Acid Poisoning in Nonhuman Primates and Rats. Symp. Domoic Acid Toxic. 78–81.

Van Lier, H., Drinkenburg, W.H.I.M., Van Eeten, Y.J.W., Coenen, A.M.L., 2004. Effects of diazepam and zolpidem on EEG beta frequencies are behavior-specific in rats. Neuropharmacology 47, 163–174. https://doi.org/10.1016/j.neuropharm.2004.03.017

Wekell, J.C., Jurst, J., Lefebvre, K. a, 2004. The origin of the regulatory limits for PSP and ASP toxins in shellfish. J. Shellfish Res. 23, 927–930.

Wells, M.L., Karlson, B., Wulff, A., Kudela, R., Trick, C., Asnaghi, V., Berdalet, E., Cochlan, W., Davidson, K., De Rijcke, M., Dutkiewicz, S., Hallegraeff, G., Flynn, K.J., Legrand, C., Paerl, H., Silke, J., Suikkanen, S., Thompson, P., Trainer, V.L., 2020. Future HAB science: Directions and challenges in a changing climate. Harmful Algae 91, 101632. https://doi.org/10.1016/j.hal.2019.101632

Wells, M.L., Trainer, V.L., Smayda, T.J., Karlson, B.S.O., Trick, C.G., Kudela, R.M., Ishikawa, A., Bernard, S., Wulff, A., Anderson, D.M., Cochlan, W.P., 2015. Harmful algal blooms and climate change: Learning from the past and present to forecast the future. Harmful Algae 49, 68–93. https://doi.org/10.1016/j.hal.2015.07.009

## 3.8 Figures

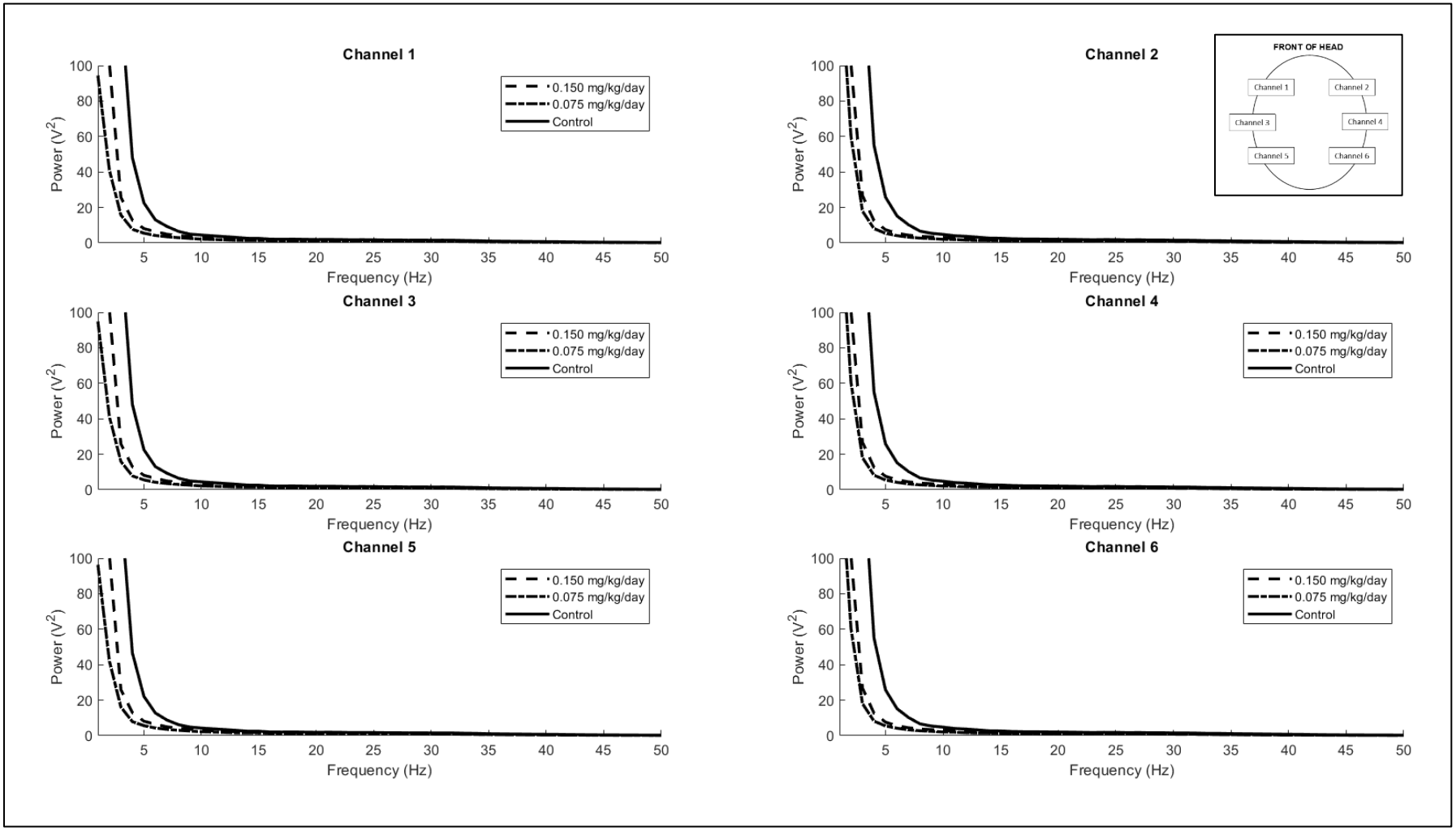


*Figure 3.4: Mean distributions of power spectral densities. Shows the group mean power spectral density across all frequencies for each channel on the EEG recording. Inset shows the position of each channel on the head.*

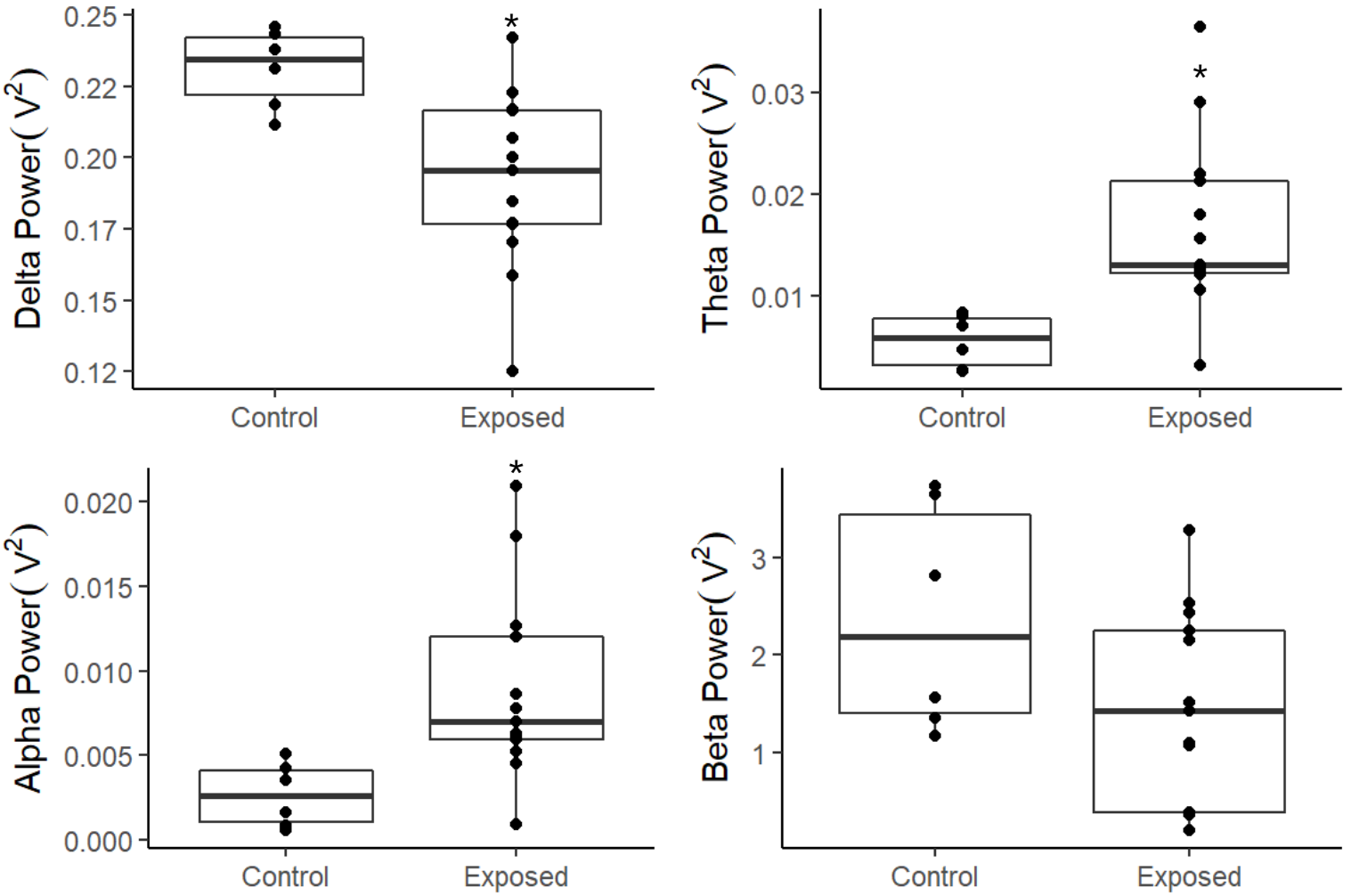


*Figure 3.5: Power comparisons by exposure. Shows the comparison of the mean total absolute power spectral density over the given frequency band among exposure groups. Each point overlay represents a single individual in the group (* denotes adjusted p-value<0.05).*

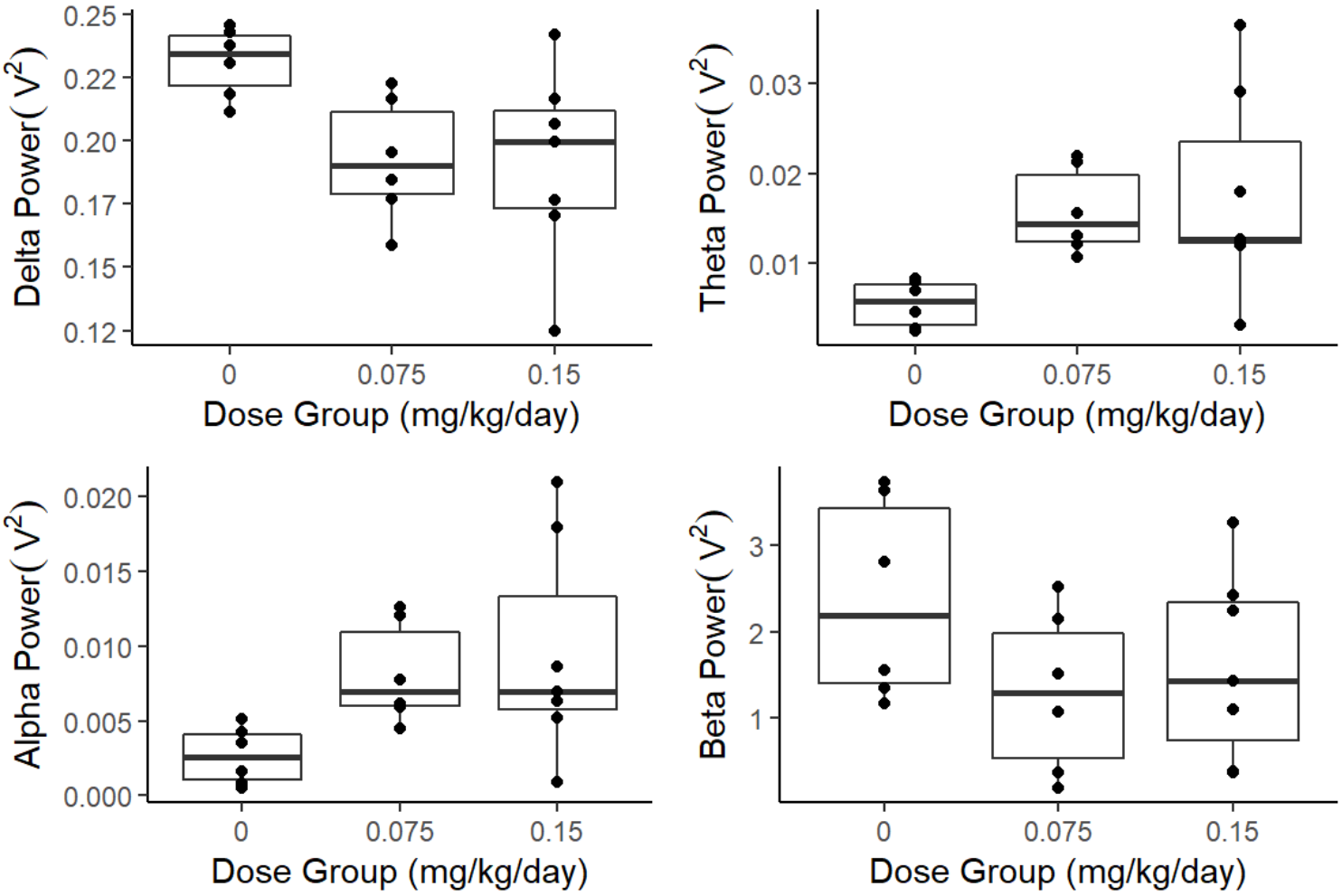


*Figure 3.6: Power comparisons by dose group. Shows the comparison of the mean total absolute power spectral density over the given frequency band among dose groups. Each point overlay represents a single individual in the group.*

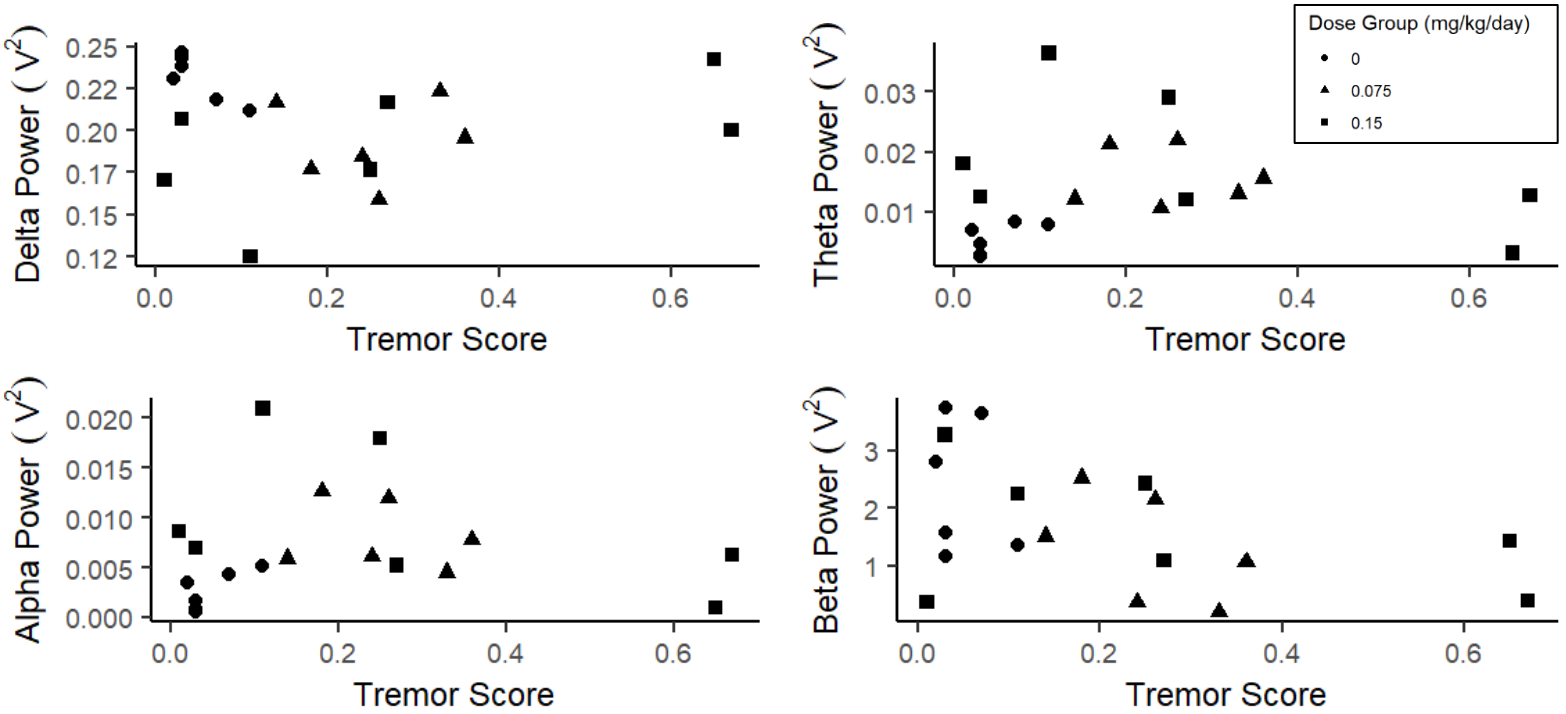


*Figure 3.7: Power associations with tremor. Shows plots of the tremor scores against the total power density in each frequency band of interest, by dose group. No significant relationships were observed between tremor scores and power in any band.*

## 3.9 Supplemental Data

***Supplement 3.1: Individual Animal Characteristics and Outcomes***

| Subject | Dose (mg/kg/day) | Weight (kg) | Age (years) | Days Exposed Pre-Pregnancy | Days Exposed in Pregnancy | Days Exposed Post Pregnancy | Total Days Exposed |
|---|---|---|---|---|---|---|---|
| 1 | 0 | 3.24 | 6.36 | 194 | 168 | 213 | 575 |
| 2 | 0 | 3.58 | 6.35 | 118 | 162 | 255 | 535 |
| 3 | 0 | 3.62 | 5.87 | N/A | N/A | 252 | 596 |
| 4 | 0 | 3.38 | 7.23 | 109 | 172 | 95 | 376 |
| 5 | 0 | 2.84 | 7.02 | 85 | 151 | 127 | 363 |
| 6 | 0 | 3.58 | 6.96 | 82 | 151 | 167 | 400 |
| 7 | 0 | 3.12 | 6.21 | 93 | 163 | 163 | 419 |
| 8 | 0.075 | 3.80 | 11.12 | 99 | 161 | 95 | 355 |
| 9 | 0.075 | 4.83 | 6.37 | 214 | 159 | 207 | 580 |
| 10 | 0.075 | 3.19 | 7.06 | 233 | 170 | 10 | 413 |
| 11 | 0.075 | 3.41 | 6.69 | 108 | 167 | 124 | 399 |
| 12 | 0.075 | 3.11 | 6.32 | 84 | 155 | 112 | 351 |
| 13 | 0.075 | 3.08 | 5.94 | 103 | 155 | 48 | 306 |
| 14 | 0.15 | 4.00 | 10.35 | 79 | 155 | 87 | 321 |
| 15 | 0.15 | 3.46 | 6.52 | 197 | 170 | 203 | 570 |
| 16 | 0.15 | 3.77 | 6.40 | 232 | 156 | 197 | 585 |
| 17 | 0.15 | 3.26 | 7.12 | 87 | 160 | 105 | 352 |
| 18 | 0.15 | 2.96 | 7.09 | 135 | 163 | 71 | 369 |
| 19 | 0.15 | 3.06 | 7.03 | 99 | 159 | 72 | 330 |
| 20 | 0.15 | 3.72 | 6.53 | 217 | 162 | 19 | 398 |

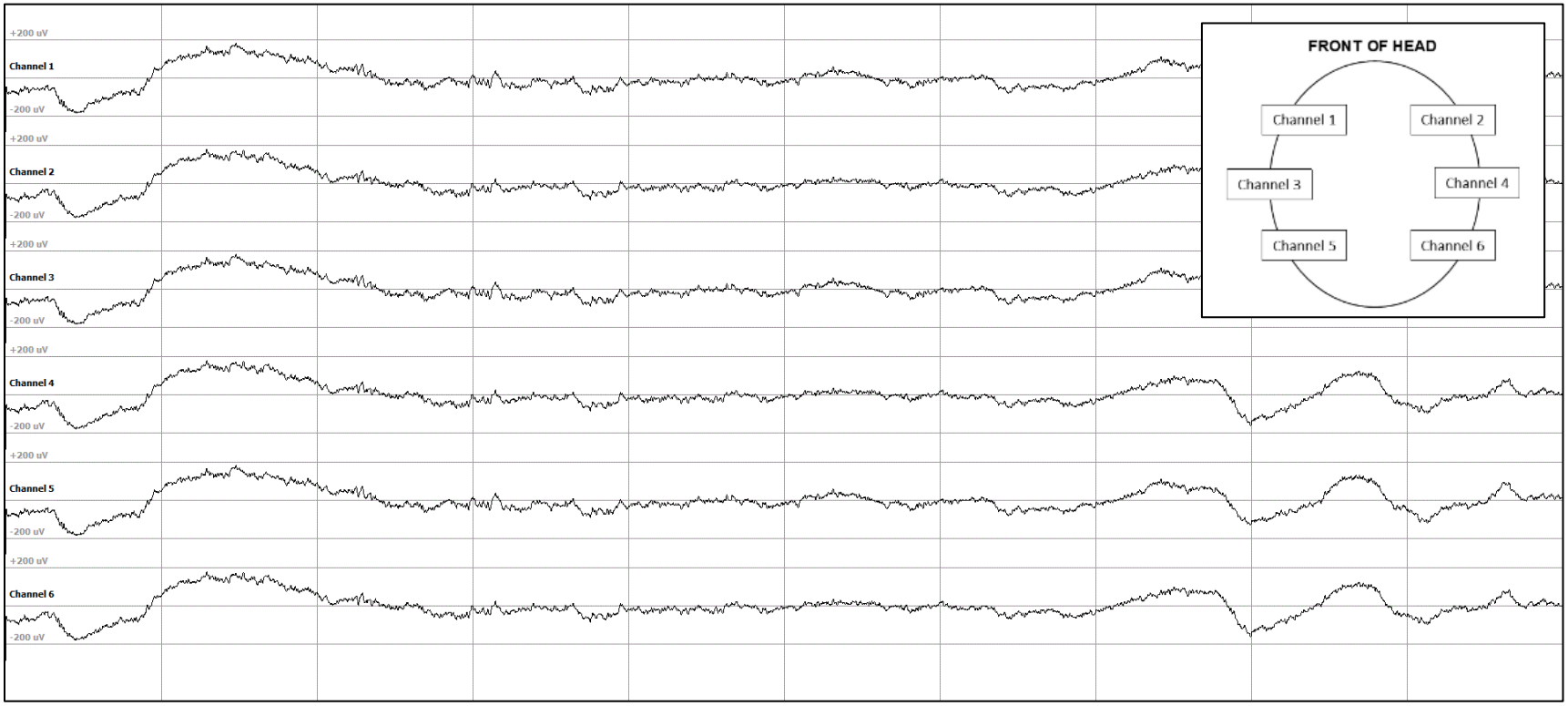


*Supplement 3.2: Raw EEG recording sample. Ten second sample of raw EEG recording from one control animal, midway through the session.*

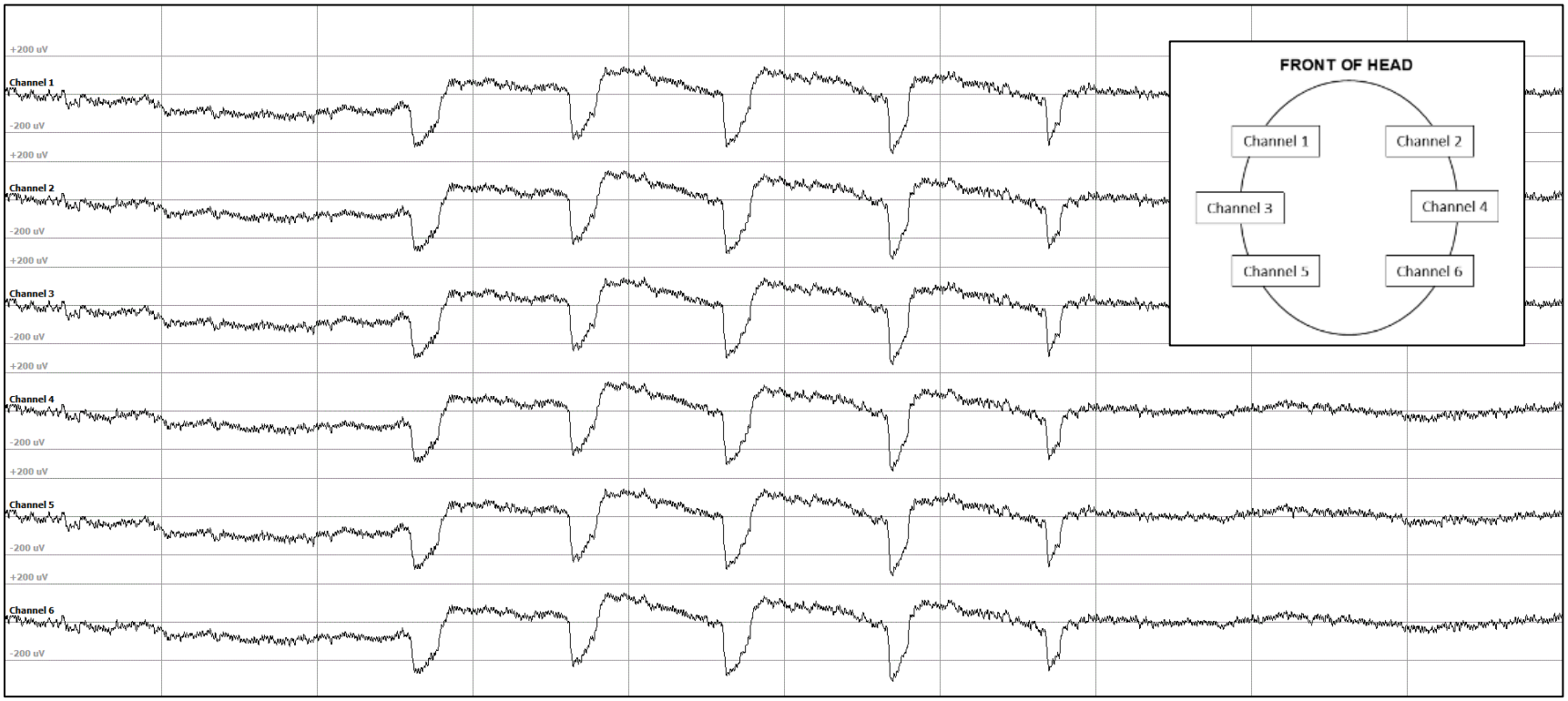


*Supplement 3.3: EOG sample. Displays the distinct electrooculographic (EOG) artifacts from one animal. Each vertical line represents a 1-second interval.*

**Chapter 4: White Matter Tractography and Neurohistopathology after Chronic, Low-Level Exposure to Domoic Acid in a Nonhuman Primate Model**

*This chapter will be submitted for publication in Toxicological Sciences. The authors are:*

Petroff, R.,[1] Harry, G.J.,[2] Richards, T.,[3] Baldessari, A.,[4] Grant, K.S.,[1,4] Crouthamel, B.,[1] McKain, N.,[1] Shum, S.,[5] Jing, J.,[5] Isoherranen, N.,[5,6] Burbacher, T.M.[1,4,6]

[1] Department of Environmental and Occupational Health Sciences, University of Washington, Seattle, Washington, USA

[2] Neurotoxicology Group, National Toxicology Program Laboratory, National Institute of Environmental Health Sciences, Research Triangle Park, North Carolina

[3] Department of Radiology, University of Washington, Seattle, Washington, USA

[4] Washington National Primate Research Center, Seattle, Washington, USA

[5] Department of Pharmaceutics, University of Washington, Seattle, Washington, USA

[6] Center on Human Development and Disability, Seattle, Washington, USA

Corresponding Author:

Dr. Thomas Burbacher

Department of Environmental and Occupational Health Sciences

School of Public Health, 357234

1959 NE Pacific Street

University of Washington

Seattle, WA 98195

tmb@uw.edu

**4.1 Abstract**

Domoic acid (DA), a potent glutamate agonist, is produced by marine algae and can bioconcentrate in finfish and shellfish. Current regulatory limits constrain environmental exposures to this toxin to 20 ppm in shellfish tissue (~0.075-0.1 mg/kg), but changing environmental conditions are leading to more frequent and longer lasting DA algal blooms. Further, recent studies suggest that chronic DA exposure, at levels below this limit, is associated with deficits in memory in adults. To understand how low-level, chronic exposure to this toxin impacts the limbic system of the brain, the present study used magnetic resonance imaging (MRI) and histopathology to assess changes in the hippocampus, thalamus, fornix, fimbria, and internal capsule in a nonhuman primate model. Twenty-eight adult, female *Macaca fascicularis* were orally exposed to 0.075 and 0.15 mg/kg/day for up to two years. A subset of these females (n=12) underwent a single, sedated MRI scan *in vivo*, to assess volumetric and tractography changes in the hippocampus, thalamus, and connecting white matter tracts, and all animals were necropsied to evaluate the cellularity and morphology of the neurons, astrocytes, and microglia in these regions. MRI and histopathology evaluations did not suggest signs of overt neuropathology, but revealed that some animals, especially in the 0.15 mg/kg/day DA exposure group, expressed focal microglia reactions within both white and gray matter structures of the limbic system. These results suggest that chronic exposure to levels of DA near the human regulatory limit does not lead to acute neuropathic effects but may induce microglial responses and promote neuroinflammatory pathways in a nonhuman primate model of contemporary human exposure to DA.

**Keywords:** domoic acid, microglia, histopathology, volumetric analysis, tractography, chronic exposure,

## 4.2 Introduction

Domoic acid (DA), a marine algal neurotoxin found in shellfish and finfish, is an agonist of α-amino-3-hydroxy-5-methyl-4-isoxazolepropionic acid (AMPA) and kainic acid (KA) type glutamate receptors (Debonnel et al., 1990; Hampson and Manalo, 1998). At high doses (>50 mg), glutamate excitotoxicity occurs primarily in the hippocampus and surrounding temporal lobe structures (Carpenter, 1990; Novelli et al., 1992; Tryphonas et al., 1990a). In human poisoning cases, these regions exhibit neuronal death, widespread neuronal atrophy, neuropil vacuolization, and injury associated astrogliosis (Carpenter, 1990; Cendes et al., 1995). This pattern of acute neurotoxicity is similarly observed in native sea mammals as well as experimental rodent and primate animal models (oral exposures: >60 mg/kg in rodents, >0.75 in monkeys) (Iverson et al., 1989; Silvagni et al., 2005; Tiedeken et al., 2013; Tryphonas et al., 1990b, 1990a, 1990c). Humans are exposed to DA through the consumption of contaminated shellfish and finfish, and regulatory limits of 0.075-0.1 mg/kg/day DA were established in the early 1990s to protect people from acute toxic exposures (>0.5 mg/kg) (Toyofuku, 2006; Wekell et al., 2004).

Since these regulations were put in place, high dose exposures have been largely mitigated. Yet today, people are at heightened risk of lower DA exposures because of increases in the severity, duration, and extent of toxin laden algal blooms worldwide (Berdalet et al., 2015; Trainer et al., 2020). Recent compelling evidence has suggested that repeated exposure to DA near the current regulatory limit results in clinical neurotoxic effects in humans and animal models (Burbacher et al., 2019; Grattan et al., 2018, 2016a; Lefebvre et al., 2017). While the neuropathology associated with high-dose exposure has been well-described, very little is known about neurotoxic injury at lower levels of exposure. In an early study examining the effect of low-level DA oral exposure (0.5-0.75 mg/kg DA for up to 30 days), no signs of neurotoxic injury were observed in 3 adult, female cynomolgus macaques (Truelove et al., 1997). Results

from a larger study, in which a cohort of female cynomolgus monkeys (n=32) were exposed to 0.075-0.15 mg/kg/day throughout a breeding, pregnancy, and postpartum period, identified increases in intention tremors when animals were performing a reaching task (Burbacher et al., 2019). *In vivo* diffusion tensor imaging (DTI), a type of magnetic resonance imaging (MRI), in a subset of animals from this primate cohort showed that DA-tremors were related to decreased white matter integrity in the fornix and internal capsule (Petroff et al., 2019). These two white matter tracts are part of key circuits in the limbic system. The fornix originates in the hippocampus, where it stems from a collection of white matter fibers (the fimbria), and terminates in several areas, including the thalamus (Lövblad et al., 2014; Meng et al., 2014). The internal capsule carries a multitude of white matter tracts, with the majority being sensorimotor inputs that connect to the thalamus (Schmahmann et al., 2004). DTI measurements capture the movement of water in tissue and is used to model the major white matter tracts in the brain (Beaulieu, 2002). Alterations in DTI, thus, can indicate direct changes in myelin or alternatively represent a neuroinflammatory response in the white matter (Werring et al., 2000), but DTI cannot pinpoint the underlying histopathology contributing to the alterations.

The present manuscript expands on our previous MRI findings from this primate cohort with assessments of volume, tractography modeling of white matter connectivity, and histopathological changes in key gray (hippocampus and thalamus) and white (fornix/fimbria and internal capsule) matter regions associated with DA toxicity. The goal of these studies was to identify the underlying morphological changes associated with the DTI findings reported from earlier studies of adult nonhuman primates chronically exposed to levels of DA near the human regulatory limit (Burbacher et al., 2019; Petroff et al., 2019).

## 4.3. Methods

*Animals*

Adult female fascicularis macaque monkeys between 5.5-11 years of age (mean: 7 years) and 2.8-4.2 kg in body weight (mean: 3.5 kg) were enrolled in the original study designed to assess the reproductive and neurodevelopmental effects of exposure to low-level DA (Burbacher et al., 2019). Animals were singly housed in stainless steel caging equipped with metabolic pans and a wide mesh that provided daily contact with an adjacent social partner in the Infant Primate Research Laboratory at the Washington National Primate Research Center (WaNPRC) in Seattle, WA, USA. The room was maintained 24 ± 4°C on a 12-hr light/dark schedule. Animals were given Lab Diet High Protein Monkey Diet (St. Louis, MO, USA) biscuits 2x/day, regular environmental enrichment (fresh and frozen fruit, vegetables, cereals, toys, puzzle balls etc.) daily, and provided filtered water ad libitum. All research protocols strictly adhered to the guidance of the Animal Welfare Act and the Guide for Care and Use of Laboratory Animals of the National Research Council and were approved by the University of Washington Institutional Animal Care and Use Committee.

Observers were experimentally blinded to the exposure conditions of the macaques and employed positive reinforcement techniques to train animals to drink out of a syringe to allow for controlled dosing of DA or vehicle control. Following training, animals underwent a baseline period of assessment designed to asses clinical signs of toxicity prior to starting daily oral exposure of 0 (n=10), 0.075 (n=11), or 0.15 (n=11) mg/kg of DA (BioVectra, Charlottetown, PE, Canada) in 5% sucrose water. Animals continued to be assessed 3-5x per week throughout a 2-month pre-breedingperiod, a 1-8-month breeding period, a 6-month pregnancy, and a 2-12-month postpartum period. Exposure ceased postpartum for 8 animals, and for 24 animals dosing continued until necropsy (Table 4.1). In all animals, behavioral assessment continued at least 3x/week until necropsy.

*MRI Acquisition*

Twelve animals representing the 6 highest tremoring, DA-dosed animals and 6 non-tremoring control animals were selected for the MRI study. Animals were sedated with ketamine (5-10 mg/kg im) and atropine (0.04 mg/kg im) and then intubated and maintained on inhaled sevoflurane (0.8 - 2.5%) and 100% oxygen. Vitals (including heart rate and saturated oxygen) were closely monitored throughout the scan. MRI scans were acquired during a single, ~1 hr long scan using a T3 Philips Scanner (version 5.17) with a custom made 8-channel rf head coil that was developed and optimized for the nonhuman primate head by Dr. Cecil Hayes at the University of Washington Department of Radiology.

The 3-D, high-resolution, T1-weighted MPRAGE images were acquired using a multishot turbo field echo (TFE) pulse sequence and an inversion prepulse (1,151 ms delay); repetition time (TR)/echo time (TE) = 14 s/7.1 ms; 130 axial slices; acquisition matrix 208 x 141 x 130; acquisition voxel size 0.48 x0.53 X1.0 mm; reconstructed voxel size 0.39 x 0.39 x 0.5 mm; slice over sample factor = 2; sense factor = 2 in the foot-head direction; turbo factor = 139; number of signaling averages = 1; TFE shots = 65, and acquisition time = 3 min 14 s. Diffusion weighted images were acquired with the following parameters: spin-echo echo-planar pulse sequence with diffusion gradients, repetition time 5500 ms, echo time 77.98 ms, reconstructed matrix 128x128, number of slices 44, resolution/voxel size 0.78x0.78x1.5mm, 64 different diffusion weighted directions and one non-diffusion volume at Blip right, b value 1500, 5 different diffusion weighted directions and one non-diffusion volume at Blip left, which where compatible with *FSL*'s (FMRIB Software Library v6.0) *topup* and *eddy* software (Andersson and Sotiropoulos, 2016).

*MR Image Processing and Analysis*

***T1 Image Processing:*** In *FSL*, *FLIRT* (FMBIR's Linear Image Registration Tool, https://fsl.fmrib.ox.ac.uk/fsl/fslwiki/FLIRT) was used to co-register all T1 images from the

animals and atlas to a single target brain (Jenkinson et al., 2012). The *buildtemplate* and *WarpImageMultiTransform* command from *ANTs* (Advanced Normalization Tools), were used to co-register all T1 images in common space (Avants et al., 2011), along with a labeled *Macaca mulatta* T1 atlas (Rohlfing et al., 2012). Labeled atlases were then inverse transformed into the original space of the 12 individual animals, using nearest-neighbor options. In individual space, *FSLmaths* was used to extract each region of interest (ROI) from the induvial atlases. ROIs included the left and right hippocampus (HIP) and thalamus (THA) (Fig. 4.1). ROI volumes were extracted using *FSLstats* and exported for statistical analysis in R (R Core Team, 2020).

***Diffusion Tensor Image Processing:*** Diffusion images were processed using *FSL'*s *topup* software and *FSL'*s *eddy* software to minimize distortion from eddy currents and head motion (Andersson et al., 2003; Smith et al., 2004). The *FSL* program, *dtifit* (https://fsl.fmrib.ox.ac.uk/fsl/fslwiki/FDT), was used to reconstruct the diffusion tensor for each voxel, and the matrix was diagonalized to obtain tensor eigenvalues, L1, L2, L3. *ANTs's buildtemplate* (Avants et al., 2011) was used to co-register individual FA maps to a target brain. Seed points were hand drawn in the HIP and THA in the viewing system, *FSLeyes*, and masks of the common space seed points were inverse transformed into original space. Using these seed points, *probtrackx* in *FSL* was used to generate probabilistic diffusion tractography, for assessing connectivity between the HIP and THA (Behrens et al., 2007).

***MRI Analysis and Statistics:*** Volumes from each brain ROI were exported to R. Comparisons of volume were conducted based on 1) control vs. DA-exposed, using a t-test, 2) DA dose, using a one-way ANOVA, and 3) tremor score, using linear regression. Because exposures were low, the first comparison was chosen to maximize statistical power to detect more subtle effects. For each comparison, a Bonferroni correction was applied to the p-values to account for the multiple comparisons made for the number of brain regions assessed. Differences were considered significant if corrected p-value was $<0.05$.

Connectivity between the HIP and THA was compared using *FSL* software *randomise*, a method that uses 500 random permutations and threshold-free cluster enhancement (TFCE) to correct for multiple voxel comparisons (Smith and Nichols, 2009; Winkler et al., 2014). Permutations were used to compare connectivity between groups based on: 1) control vs. DA-exposed animals, 2) DA-dose, and 3) tremor scores. Any significant alterations in connectivity, as identified with a p-value of $<0.05$, were visually identified in the brain as a cluster in *FSLeyes*.

*Tissue Collection*

The 12 animals selected for MRI, plus 16 additional macaques, for a total of 28 animals were used for histopathology (control: n=8; 0.075 mg/kg/day: n=11; 0.15 mg/kg/day: n=9). Animals were fasted for 12 hrs and sedated under 20 mg/kg ketamine, before transportation to the necropsy room at the WaNRPC. Sedated animals were euthanized with an intravenous overdose of sodium pentobarbital, as per the AMVA Panel on Euthanasia recommendations (Leary et al., 2020). Euthanasia was confirmed and the brain quickly excised from the skull. The brain was bisected along the midsagittal plane. ROIs, including the HIP and THA, were identified by a certified veterinary pathologist. From the left hemisphere, dissected tissue was sliced into small, approximately 3 cm sections (representing 1-3 sections/ROI), placed in a 2 ml cryostat tube, immediately frozen in liquid nitrogen, and stored at -80°C. Matching sections from the contralateral hemisphere were immersion fixed in 10% formalin. Sections were processed through a graded series of ethanol and embedded in paraffin.

*Tissue Preparation, Histology, and Immunohistochemistry*

Formalin-fixed, paraffin-embedded sections, including the HIP, THA, fornix/fimbria, and internal capsule from 28 animals, were serial sectioned at 10 µm. Two control animals and 2

high dose animals were excluded due to differences in tissue collection. Sections were deparaffinized in xylene and rehydrated in distilled water.

For histology, sections were stained for general cellularity with Hematoxylin and Eosin (H&E), for neurons with the Nissl stain and cresyl violet (CV), and for myelin with Luxol Fast Blue (LFB). For LFB, sections were incubated overnight at 57°C with 0.1% LFB solution (Rowley Biochemical Inc., Danvers, MA, USA) followed by a rinse with 95% alcohol, then distilled water, and differentiated with 0.05% lithium carbonate (Poly Scientific, Bay Shore, NY, USA) and 70% alcohol. Sections were counterstained with CV (Poly Scientific, Bay Shore, NY, USA) to detect neurons. All sections were dehydrated through graded ethanol, cleared in xylene, and coverslipped.

For immunohistochemistry, endogenous peroxidase was blocked using 3% $H_2O_2$ followed by heat-induced epitope retrieval using a 10mM citrate buffer solution, pH 6.0, in a Decloaker® pressure chamber (Biocare Medical, Concord, CA, USA) for 15 min at 110°C. In cleared sections, non-specific sites were blocked using 10% normal goat serum (Jackson Immunoresearch, West Grove, PA, USA) for 20 min at ~23°C (RT) and an avidin/biotin blocking kit (Vector Laboratories, Burlingame, CA, USA). To identify microglia, sections were incubated with rabbit monoclonal anti-ionized calcium binding adaptor molecule 1 (Iba-1) (1:2000; (Cat# 019-19741, Lot# CAL0291, Wako Chemicals USA, Inc., Richmond, VA, USA) for 60 min at RT followed by incubation with biotinylated goat anti-rabbit IgG antibody (1:300; Vector Laboratories, Burlingame, CA, USA) 30 min at RT. To identify astrocytes, sections were incubated with an antibody to the structural protein, glial fibrillary acidic protein (GFAP), rabbit anti-GFAP (1:7000, Cat# X0936, Lot# 200256262, Dakocytomation Corporation, Carpinteria, CA, USA), for 30 min at RT then incubated with biotinylated Goat anti-rabbit IgG (Vector-Laboratories) at a 1:500 dilution. Antigen-antibody complexes were visualized with a Vectastain Elite ABC R.T.U. label, (Vector Laboratories, Burlingame, CA, USA) and 3,3-diaminobenzidine

(Dako, Carpinteria, CA, USA). Iba-1 negative controls were stained with normal rabbit IgG (1:400; Calbiochem/EMD Millipore, Billerica, MA, USA), and GFAP negative controls were stained with rabbit immunoglobulin fraction (solid phase adsorbed) control (Dakocytomation Corporation, Carpinteria, CA, USA). All immunohistochemistry sections were counterstained with hematoxylin.

*Microscopy*

Sections were scanned under 40x magnification using an Aperio ScanScope AT2 DX System (Leica Biosystems Imaging Inc., Buffalo Grove, IL, USA) and viewed using Aperio ImageScope v.6.25.0.1117. The HIP (including CA1-4 and dentate gyrus), THA, fornix, fimbria, and internal capsule were identified using the *Macaca mulatta* BrainMaps labeled atlas ("BrainMaps: An Interactive Multiresolution Brain Atlas"; Mikula et al., 2007). These regions were selected to include the white matter tracts previously found by MRI to have decreased structural integrity. In this atlas, the hippocampus coordinates were identified on coronal sections as A0.4-A15.0, at 27.5-36.5 mm deep, and 8.5-21.5 mm from the midsagittal plane. The fornix coordinates were P1.7-A16.1, at 16-30 mm deep and 0-16.5 mm from the midsagittal plane. The internal capsule coordinates were A1.3-A20.6, at 15-26.5 mm deep and 3.5-20 mm from the midsagittal plane. Additionally, white matter of the fornix or hippocampal fimbria was evaluated for myelin tract connection to the HIP. Atlas coordinates for fornix connections to the hippocampus were A0.4-A0.6 and for fimbria connections were A0.9-A12.0 on stained slides. The fornix and fimbria were visually differentiated by the corresponding shape of the dentate gyrus and surrounding CA1-4 regions.

Sequential slides were examined for signs cellular changes using an approach progressing from the 4x, 10x, to the higher 40x magnification. Morphological indications of neuronal death were noted with changes in H&E and CV. Disruptions in myelin tracts were

assessed with LFB. Microglia and astrocyte responses to perturbations were assessed with Iba-1 and GFAP immunostaining. These stains were used to corroborate any signs of neuronal death or changes in myelin, as well as to identify unique foci of reactive glia. Histopathology was examined using non-tremoring controls as the standard for the species. A summary of histopathological outcomes is detailed in Table 4.2.

## 4.4 Results

*MR Volume and Tractography*

MR T1-weighted images from 6 controls and 6 DA-exposed animals (0.075 mg/kg/day: n=2; 0.15 mg/kg/day: n=4) were used to calculate volume of key gray matter structures associated with DA toxicity, including the hippocampus and thalamus. Probabilistic DTI tractography was used to model dense white matter tracts between the thalamus and hippocampus and associated histological changes (Fig. 4.1). Mean right hippocampal volumes for the control group was 393.4 mm ±14.3, 385.8 mm ±12.5 for exposed animals; left hippocampal volume was 402.6 mm ±15.8 for the controls and 381.0 mm ±15.6; right thalamic volume was 496.1 mm ±14.8 for the controls and 513.8 mm ±17.9 for the exposed; and left thalamic volume was 501.2 mm ±18.3 for the control and 515.8 mm ± 20.2 for the exposed animals. Results from the volumetric analyses did not indicate significant differences in total cellular volume in either the left or right hemisphere of these gray matter structures comparing DA-exposed and control animals (adj. t-test, $p>0.05$). In addition, no significant differences were observed comparing the different DA dose groups and controls (ANOVA, adj. $p>0.05$). Finally, the results of the linear regression examining the association between volumetric outcomes and tremor scores did not indicate a significant association between the two outcomes (adj. $p>0.05$) (Table 4.3). DTI tractography, a measure of the strength and direction of the white matter fibers between the hippocampus and thalamus was assessed using a threshold clustering permutation

to compare differences between exposures, dosed animals, and tremor scores. Comparisons suggested that the strength and direction of the white matter fiber tracts between these structures were similar across dose groups and when comparing tremoring and non-tremoring animals ($p>0.05$).

*White Matter Histology and Immunohistochemistry*

Histological examination of the fornix/fimbria and internal capsule was conducted on 28 animals, including the 12 MRI animals, plus 16 additional monkeys (control: n=8; 0.075 mg/kg/day: n=11; 0.15 mg/kg/day: n=9). None of the animals showed evidence of cell death, alterations in staining for myelin, or reactive responses of astrocytes or microglia. H&E staining showed a normal pattern of staining with no evidence of eosin+ cells indicative of cell death within the myelin tracts. LFB staining of distinct myelin tracts indicated no overt disruption indicative of de- or dys-myelination. Staining density was similar across all animals for each region. Staining of the smaller processes projecting from the tract showed no evidence of reduced myelin or disorganization. Astrocytes within the white matter showed a normal morphological pattern characterized by small cell bodies with processes aligned with the myelinated fibers (Oberheim et al., 2009, 2006). No evidence of astrocytic hypertrophy was observed suggesting the absence on an underlying cell injury response.

In 2 DA-exposed animals (1 in the 0.075 and 1 in the 0.15 mg/kg/day group) and 1 control, there were focal Iba-1+ microglia reactions in the white matter tracts of the internal capsule, fornix, and fimbria (Fig. 4.2). The reactions in these three animals spanned an area of approximately 200 µm. The clusters of glia cells were characterized by increased branching and thickening of processes, with evidence of individual cells shifting to an ameboid morphology. Another DA exposed animal in the 0.15 mg/kg/day group displayed a more expanded reaction area of microglia in the fornix, fimbria, and internal capsule which was characterized by an

increase in the number of cells that showed enhanced process density and fragmentation (Fig. 4.3). Within the sections examined, there was no indication of localized cell death as observed by H&E and Nissl stains. In addition, the focal areas of microglia activation were not accompanied by changes in astrocytes.

*Histological Examination of Gray Matter Regions*

Histological examination of the hippocampus and thalamus showed no evidence of cell death in most animals (control: 8/8 animals; 0.075 mg/kg/day: 11/11; 0.15 mg/kg/day:7/9). For these animals, the staining pattern and cellular distribution observed with Nissl staining and H&E was similar across animals, with no indication of eosin+ cells (Fig. 4.4). GFAP+ astrocytes within the grey matter regions showed anatomical differences as compared to white matter. The cell morphology was characterized by larger cells with a more sheath-like morphology as compared to those observed in the white matter, consistent with what has been observed in human tissue (Oberheim et al., 2006; 2009). Within each region, the overall astrocyte morphology was similar across animals (Table 4.1).

Two high dose DA animals, who both had some of the highest tremor scores, demonstrated signs of more extensive neuropathological responses with evidence of an active glial reaction accompanied by infiltration of small perivascular mononuclear cells (Fig. 4.5). The observed injuries did not appear to rely on continued DA exposure, as one animal was removed from DA exposure for 221 days prior to necropsy, while the other animal continued on DA until necropsy. The characteristics of the glia responses, however, were slightly different between the two animals. With cessation of DA exposure, astrocyte hypertrophy and increased process density of microglia were observed. Further examination of this animal suggested that the lesion observed was likely not due to DA exposure but rather represented a tumor. In the animal with continued DA exposure, the prominent response was in the microglia with evidence of an

amoeboid morphology suggestive of active phagocytosis and the possibility of an underlying cell death.

Disperse morphological responses of Iba-1+ microglia were noted in five other DA-exposed animals, including 2 monkeys in the 0.075 mg/kg/day group and 3 in the 0.15 mg/kg/day group. In one low-dose DA animal, a focal response was observed in the thalamus. In a second low-dose DA animal, a focal response was observed in an area adjacent to the thalamus, the nucleus accumbens. In the high dose DA group, morphological responses of microglia were observed in one animal in the subgranular zone of the dentate gyrus and in the thalamus of two additional animals (Fig. 4.6). The responses followed two morphological patterns: focal reactions (<200 µm large, with increased branching, thickening processes) or reactions >200 µm suggestive of a more dispersed response. In all cases, there were no indications of cell death as detected by H&E or CV nor associated histological changes in GFAP+ astrocytes.

**4.5 Discussion**

Acute neurotoxicity associated with high dose DA exposure is typically characterized by neuronal death in the hippocampus (Carpenter, 1990; Chandrasekaran et al., 2004; Colman et al., 2005) that is accompanied by seizure activity and disrupted memory processing (Cook et al., 2015; Grant et al., 2010; Perl et al., 1990b; Ramsdell and Gulland, 2014). Initial studies after the 1987 poisoning demonstrated that these effects are replicated across naturally exposed sea lions and laboratory models (rodents and nonhuman primates), with gross histopathological damage in much of limbic lobe, including the hippocampus, and a wealth of behavioral symptoms, such as hind-limb scratching, confusion, and seizures (Iverson et al., 1989; Scholin et al., 2000; Tryphonas et al., 1990b). Acute exposures with *in vitro* neuronal cultures and mammalian models suggest that high levels of DA cause glutamate toxicity and overexcitation,

resulting in necrotic cell death and astrogliosis (Iverson and Truelove, 1994; Stewart et al., 1990; Vieira et al., 2015). *In vivo* toxicity is paired with a persistent activation of microglia for up to three months post-exposure following a single iv dose of DA (0.75 mg/kg in rats) (Ananth et al., 2003). In feral sea lions exposed to high levels of DA, clinical symptoms (e.g. seizures, epilepsy, memory loss) have also been associated with decreased white matter integrity of the fornix and increased structural white matter connectivity between the thalamus and hippocampus (Cook et al., 2018, 2015). These types of structural integrity changes in MRI can be related to direct effects on the myelin sheath, underlying axons, or reflect ongoing neuroinflammation (Werring et al., 2000).

While high dose studies are essential for understanding the basic mechanism of toxicity, experimental work with lower levels of DA are more representative of contemporary human exposures. The current regulatory limit caps human exposures at 20 ppm in shellfish, or 0.075-0.1 mg/kg. DA administered at these low levels does not cause necrotic death in cerebral neuronal cultures, but instead induces the production of reactive oxygen species, leading to lipid peroxidation and apoptosis (Giordano et al., 2013, 2006). In a long-term study with mice exposed to lower levels of DA for at least 22 weeks (0.75 mg/kg ip 1x/wk), researchers did not observe overt pathology in the neurons or astrocytes of the hippocampus, but microglia were not assessed (Lefebvre et al., 2017; Moyer et al., 2018). These mice also expressed deficits in learning and memory (Lefebvre et al., 2017), similar to results from human studies. In a cohort of adults in tribes on the coast of Washington state, deficits in memory were linked with higher consumption of DA contaminated shellfish (>15 clams/month) (Grattan et al., 2016a). Continued investigation demonstrated that even adults consuming higher amounts of clams in the previous 10 days had more reported problems with everyday memory, suggesting that repeat exposure to DA levels below the current regulatory limit may be linked to functional neurotoxicity in adults (Grattan et al., 2018).

Recent work from the present authors used a nonhuman primate model designed to assess the reproductive and offspring neurodevelopmental effects of daily exposure near the current regulatory limit of DA (0.075 and 0.15 mg DA/kg/day). A previous study using nonhuman primates orally exposed to 0.5-0.75 mg/kg/day DA for up to 30 days did not report signs of overt toxicology in macaque monkeys (Truelove et al., 1997). However, reports from the study that provided the animals for the current research indicated that daily oral exposure to 0.075-0.15 mg/kg/day DA for over a year resulted in subtle behavioral signs of neurotoxicity: intention tremors when preforming a reaching task (Burbacher et al., 2019). To better understand the neurological underpinnings of these tremors, additional studies using MRI were conducted on a subset of these animals. Results from these MRI studies found that intention tremor severity was associated with decreases in the integrity of internal capsule and fornix major white matter tracts, thus mirroring some of the sea lion MRI findings (Petroff et al., 2019).

In the present study, additional MRI analyses and histopathological examinations of these animals were used to assess the macro and microscopic changes in these white matter tracts and the major gray matter structures associated with DA toxicity. Exposure to 0.075 and 0.15 mg DA/kg/day for nearly two years in the nonhuman primate model did not result in overt MRI or histological evidence of demyelination or atrophy in the hippocampus and thalamus, confirming that chronic, lower level exposure to DA does not give rise to acute neuronal damage. In the absence of overt demyelination or cell death, the previously reported decreased structural integrity in the fornix and internal capsule may be linked to a neuroinflammatory response. Within the nonhuman primate model, neuroinflammatory responses associated with structural changes are likely to be evident in morphological responses of glia. Microglia, the primary immune cell of the brain, may manifest changes in morphology that are reactive to changes in the surrounding environment and cell damage (Colonna and Butovsky, 2017; Kono and Rock, 2008).

The majority of the control and low DA dose macaques in the present study had normal myelin and neuronal cells in the regions examined (controls: 8/8 animals, 0.075 mg/kg: 10/10, and 0.15 mg/kg: 7/9), in agreement with previous literature examining chronically exposed rodents (Lefebvre et al., 2017; Moyer et al., 2018), and further indicating that previously observed structural integrity differences are suggestive of a neuroinflammatory response. Indeed, of the animals showing evidence of morphological alterations that were not overt, the predominant histological change was a focal response of microglia (controls: 7/8 animals, 0.075 mg/kg: 7/10, and 0.15 mg/kg: 4/9). This observation was noted more frequently in high dosed animals and in animals showing clinical tremors, including those high tremoring animals that had a recovery period after DA exposure for nearly 1 year. Additionally, focal microglia responses were observed most frequently in the highest tremoring animals, regardless of dose or length of time of exposure. The focal responses observed in some of the DA-exposed animals likely reflect microglia activation due to responses to the presence of proinflammatory cytokines, in the absence of robust neuropathology (Harry and Kraft, 2008).

The present research has identified increased microglia responses in a major neuronal circuit that is frequently impaired in memory disorders and is comprised of many white matter fibers that conduct both cognitive and motor processes (Aggleton et al., 2010; Aggleton and Brown, 1999, Morecraft et al., 2002). The authors were unable to determine if focal glia reactions are indicative of a protective effect or a neurotoxic response to DA, thus, the underlying implication of this finding bears further investigation (Biber et al., 2014). No other study has assessed oral exposures to this toxin at levels near to the human regulatory limit, so translating these results to contemporary human health scenarios may be difficult. Despite these limitations, even subtle effects observed in this nonhuman primate model may have profound importance for human health, given the high degree of translation and the similarity of exposure levels. Overall, the data suggest that exposure of nonhuman primates to levels of DA

near the current human regulatory limit may cause alterations in neural circuity and that additional research is needed to more fully explore the long-term effects of such dietary exposure.

*Conclusion*

Today, people are at heightened risk from DA exposure due to shifting climatic patterns that are triggering record breaking, long-lasting DA-algal blooms (McCabe et al., 2016; Zhu et al., 2017). In the present nonhuman primate model, chronic, oral exposure to DA near the current regulatory limit produced clinical signs of neurotoxicity (tremors) and altered the integrity of specific white matter tracts in the brain (Burbacher et al., 2019; Petroff et al., 2019). Results from the current study demonstrate that these exposure-related effects occurred in the absence of overt neuropathology in the hippocampus and thalamus. Changes in microglia responses, however, highlight the possible role of neuroinflammation in DA exposure effects. These data reveal the complex nature of DA neurotoxicity at environmentally relevant levels of exposure and support the need for continued research on this emerging neurotoxin and its effects on the mammalian brain.

*Additional Research Opportunities*

Additional frozen and formalin preserved samples from the brain and most major organs are available for future collaborative research opportunities for interested parties. Please contact the corresponding author if you are interested in receiving samples.

**4.6 Acknowledgements**

The authors would like to acknowledge and thank the dedicated staff and volunteers of the Infant Primate Research Laboratory and the University of Washington National Primate

Research Center for their skilled assistance in this research; Mr. Tim Wilbur for this help with the RF coil and MR scanning; staff at the University of Washington Diagnostics Imaging Sciences Center for their technical aid; and the NIEHS histology core for their support in the histopathology processing.

### 4.7 References

Ananth, C., Gopalakrishnakone, P., Kaur, C., 2003. Induction of inducible nitric oxide synthase expression in activated microglia following domoic acid (DA)-induced neurotoxicity in the rat hippocampus. Neurosci. Lett. 338, 49–52. https://doi.org/10.1016/S0304-3940(02)01351-4

Andersson, J.L.R., Sotiropoulos, S.N., 2016. An integrated approach to correction for off-resonance effects and subject movement in diffusion MR imaging. Neuroimage 125, 1063–1078. https://doi.org/10.1016/j.neuroimage.2015.10.019

Avants, B.B., Tustison, N.J., Song, G., Cook, P.A., Klein, A., Gee, J.C., 2011. A reproducible evaluation of ANTs similarity metric performance in brain image registration. Neuroimage 54, 2033–44. https://doi.org/10.1016/j.neuroimage.2010.09.025

Beaulieu, C., 2002. The basis of anisotropic water diffusion in the nervous system - A technical review. NMR Biomed. https://doi.org/10.1002/nbm.782

Behrens, T.E.J., Johansen Berg, H., Jbabdi, S., Rushworth, M.F.S., Woolrich, M.W., 2007. Probabilistic diffusion tractography with multiple fibre orientations: What can we gain? NeuroImage 34, 144-155. https://doi.org/10.1016/j.neuroimage.2006.09.018

Berdalet, E., Fleming, L.E., Gowen, R., Davidson, K., Hess, P., Backer, L.C., Moore, S.K., Hoagland, P., Enevoldsen, H., 2015. Marine harmful algal blooms, human health and wellbeing: Challenges and opportunities in the 21st century. J. Mar. Biol. Assoc. United Kingdom 96, 61–91. https://doi.org/10.1017/S0025315415001733

Biber, K., Owens, T., Boddeke, E., 2014. What is microglia neurotoxicity (Not)? Glia 62, 841–854. https://doi.org/10.1002/glia.22654

Burbacher, T., Grant, K., Petroff, R., Crouthamel, B., Stanley, C., McKain, N., Shum, S., Jing, J., Isoherranen, N., 2019. Effects of chronic, oral domoic acid exposure on maternal reproduction and infant birth characteristics in a preclinical primate model. Neurotoxicol. Teratol. 440354. https://doi.org/10.1101/440354

Carpenter, S., 1990. The human neuropathology of encephalopathic mussel toxin poisoning. Symp. Domoic Acid Toxic. 73–34.

Cendes, F., Andermann, F., Carpenter, S., Zatorre, R.J., Cashman, N.R., 1995. Temporal lobe epilepsy caused by domoic acid intoxication: Evidence for glutamate receptor–mediated excitotoxicity in humans. Ann. Neurol. 37, 123–126. https://doi.org/10.1002/ana.410370125

Chandrasekaran, A., Ponnambalam, G., Kaur, C., 2004. Domoic acid-induced neurotoxicity in the hippocampus of adult rats. Neurotox. Res. 6, 105–117. https://doi.org/10.1007/BF03033213

Colman, J.R., Nowocin, K.J., Switzer, R.C., Trusk, T.C., Ramsdell, J.S., 2005. Mapping and reconstruction of domoic acid-induced neurodegeneration in the mouse brain, in: Neurotoxicology and Teratology. Pergamon, pp. 753–767. https://doi.org/10.1016/j.ntt.2005.06.009

Colonna, M., Butovsky, O., 2017. Microglia function in the central nervous system during health and neurodegeneration. Annu. Rev. Immunol. 35, 441–468. https://doi.org/10.1146/annurev-immunol-051116-052358

Cook, P.F., Berns, G.S., Colegrove, K., Johnson, S., Gulland, F.M.D., 2018. Postmortem DTI reveals altered hippocampal connectivity in wild sea lions diagnosed with chronic toxicosis from algal exposure. J. Comp. Neurol. 526, 216–228. https://doi.org/10.1002/cne.24317

Cook, P.F., Reichmuth, C., Rouse, A.A., Libby, L.A., Dennison, S.E., Carmichael, O.T., Kruse-Elliott, K.T., Bloom, J., Singh, B., Fravel, V.A., Barbosa, L., Stuppino, J.J., Van Bonn, W.G., Gulland, F.M.D., Ranganath, C., 2015. Algal toxin impairs sea lion memory and hippocampal connectivity, with implications for strandings. Science. 350, 1545–1547. https://doi.org/10.1126/science.aac5675

Debonnel, G., Weiss, M., de Montigny, C., 1990. Neurotoxic effect of domoic acid: mediation by kainate receptor electrophysiological studies in the rat. 16 Suppl 1, 59–68.

Giordano, G., Kavanagh, T.J., Faustman, E.M., White, C.C., Costa, L.G., 2013. Low-level domoic acid protects mouse cerebellar granule neurons from acute neurotoxicity: Role of glutathione. Toxicol. Sci. 132, 399–408. https://doi.org/10.1093/toxsci/kft002

Giordano, G., White, C.C., McConnachie, L.A., Fernandez, C., Kavanagh, T.J., Costa, L.G., 2006. Neurotoxicity of domoic acid in cerebellar granule neurons in a genetic model of glutathione deficiency. Mol. Pharmacol. 70, 2116–2126. https://doi.org/10.1124/mol.106.027748

Grant, K.S., Burbacher, T.M., Faustman, E.M., Grattan, L.M., 2010. Domoic acid: Neurobehavioral consequences of exposure to a prevalent marine biotoxin. Neurotoxicol. Teratol. 32, 132–141. https://doi.org/10.1016/j.ntt.2009.09.005

Grattan, L.M., Boushey, C.J., Liang, Y., Lefebvre, K.A., Castellon, L.J., Roberts, K.A., Toben, A.C., Morris, J.G.J., 2018. Repeated dietary exposure to Low Levels of Domoic Acid and Problems with Everyday Memory: Research to Public Health Outreach. Toxins (Basel). 10, 103. https://doi.org/10.3390/toxins10030103

Grattan, L.M., Boushey, C.J., Tracy, K., Trainer, V.L., Roberts, S.M., Schluterman, N., Morris, J.G.J., 2016. The association between razor clam consumption and memory in the CoASTAL cohort. Harmful Algae 57, 20–25. https://doi.org/10.1016/j.hal.2016.03.011

Hampson, D.R., Manalo, J.L., 1998. The activation of glutamate receptors by kainic acid and domoic acid. Nat. Toxins. https://doi.org/10.1002/(SICI)1522-7189(199805/08)6:3/4<153::AID-NT16>3.0.CO;2-1

Harry, G.J., Kraft, A.D., 2008. Neuroinflammation and microglia: Considerations and approaches for neurotoxicity assessment. Expert Opin. Drug Metab. Toxicol. 4, 1265–1277. https://doi.org/10.1517/17425255.4.10.1265

Iverson, F., Truelove, J., 1994. Toxicology and seafood toxins: Domoic acid. Nat. Toxins 2, 334–339. https://doi.org/10.1002/nt.2620020514

Iverson, F., Truelove, J., Nera, E., Tryphonas, L., Campbell, J., Lok, E., 1989. Domoic acid poisoning and mussel-associated intoxication: Preliminary investigations into the response of mice and rats to toxic mussel extract. Food Chem. Toxicol. 27, 377–384. https://doi.org/10.1016/0278-6915(89)90143-9

Jenkinson, M., Beckmann, C.F., Behrens, T.E.J., Woolrich, M.W., Smith, S.M., 2012. FSL. Neuroimage. https://doi.org/10.1016/j.neuroimage.2011.09.015

Kono, H., Rock, K.L., 2008. How dying cells alert the immune system to danger. Nat. Rev. Immunol. https://doi.org/10.1038/nri2215

Leary, S., Underwood, W., Anthony, R., Cartner, S., Grandin, T., Greenacre, C., Gwaltney-Brant, S., McCrackin, M.A., Meyer, R., Miller, D., Shearer, J., Turner, T., Yanong, R., Johnson, C.L., Patterson-Kane, E., 2020. AVMA Guidelines for the Euthanasia of Animals: 2020 Edition.

Lefebvre, K.A., Kendrick, P.S., Ladiges, W., Hiolski, E.M., Ferriss, B.E., Smith, D.R., Marcinek, D.J., 2017. Chronic low-level exposure to the common seafood toxin domoic acid causes cognitive deficits in mice. Harmful Algae 64, 20–29. https://doi.org/10.1016/j.hal.2017.03.003

Lövblad, K.O., Schaller, K., Isabel Vargas, M., 2014. The fornix and limbic system. Semin. Ultrasound, CT MRI 35, 459–473. https://doi.org/10.1053/j.sult.2014.06.005

McCabe, R.M., Hickey, B.M., Kudela, R.M., Lefebvre, K.A., Adams, N.G., Bill, B.D., Gulland, F.M.D., Thomson, R.E., Cochlan, W.P., Trainer, V.L., 2016. An unprecedented coastwide toxic algal bloom linked to anomalous ocean conditions. Geophys. Res. Lett. 43, 10,366-10,376. https://doi.org/10.1002/2016GL070023

Meng, Y., Payne, C., Li, L., Hu, X., Zhang, X., Bachevalier, J., 2014. Alterations of hippocampal projections in adult macaques with neonatal hippocampal lesions: A Diffusion Tensor Imaging study. Neuroimage 102, 828–837. https://doi.org/10.1016/j.neuroimage.2014.08.059

Mikula, S., Trotts, I., Stone, J.M., Jones, E.G., 2012. BrainMaps: An interactive multiresolution brain atlas; http://brainmaps.org [WWW Document]. URL http://brainmaps.org/index.php?p=citing-brainmaps (accessed 3.9.20).

Mikula, S., Trotts, I., Stone, J.M., Jones, E.G., 2007. Internet-enabled high-resolution brain mapping and virtual microscopy. Neuroimage 35, 9–15. https://doi.org/10.1016/j.neuroimage.2006.11.053

Morecraft, R. J., Herrick, J. L., Stilwell-Morecraft, K. S., Louie, J. L., Schroeder, C. M., Ottenbacher, J. G., & Schoolfield, M. W. (2002). Localization of arm representation in the corona radiata and internal capsule in the non-human primate. Brain, 125(1), 176–198. https://doi.org/10.1093/brain/awf011

Moyer, C.E., Hiolski, E.M., Marcinek, D.J., Lefebvre, K.A., Smith, D.R., Zuo, Y., 2018. Repeated low level domoic acid exposure increases CA1 VGluT1 levels, but not bouton density, VGluT2 or VGAT levels in the hippocampus of adult mice. Harmful Algae 79, 74–86. https://doi.org/10.1016/j.hal.2018.08.008

Novelli, A., Kispert, J., Fernandez-Sanchez, M.T., Torreblanca, A., Zitko, V., 1992. Domoic acid-containing toxic mussels produce neurotoxicity in neuronal cultures through a synergism between excitatory amino acids. Brain Res. 577, 41–48. https://doi.org/10.1016/0006-8993(92)90535-H

Oberheim, N.A., Takano, T., Han, X., He, W., Lin, J.H.C., Wang, F., Xu, Q., Wyatt, J.D., Pilcher, W., Ojemann, J.G., Ransom, B.R., Goldman, S.A., Nedergaard, M., 2009. Uniquely Hominid Features of Adult Human Astrocytes. J. Neurosci. 29, 3276–3287. https://doi.org/10.1523/JNEUROSCI.4707-08.2009

Oberheim, N.A., Wang, X., Goldman, S., Nedergaard, M., 2006. Astrocytic complexity distinguishes the human brain. Trends Neurosci. 29, 547–553. https://doi.org/10.1016/j.tins.2006.08.004

Perl, T.M., Bedard, L., Kosatsky, T., Hockin, J.C., Todd, E.C.D., 1990. An outbreak of toxic encephalopathy caused by eating mussels contaminated with domoic acid. N. Engl. J. Med. 322, 1775–1780. https://doi.org/10.1056/NEJM199006213222504

Petroff, R., Richards, T., Crouthamel, B., Mckain, N., Stanley, C., Grant, K.S., Shum, S., Jing, J., Isoherranen, N., Burbacher, T.M., 2019. Chronic, low-level oral exposure to marine toxin, domoic acid, alters whole brain morphometry in nonhuman primates. Neurotoxicology 72, 114–124. https://doi.org/10.1016/j.neuro.2019.02.016

R Core Team, 2020. R: A language and environment for statistical computing. https://doi.org/http://www.R-project.org/

Ramsdell, J.S., Gulland, F.M.D., 2014. Domoic acid epileptic disease. Mar. Drugs 12, 1185–1207. https://doi.org/10.3390/md12031185

Rohlfing, T., Kroenke, C.D., Sullivan, E. V., Dubach, M.F., Bowden, D.M., Grant, K.A., Pfefferbaum, A., 2012. The INIA19 template and NeuroMaps atlas for primate brain image parcellation and spatial normalization. Front. Neuroinform. 6, 27. https://doi.org/10.3389/fninf.2012.00027

Schmahmann, J.D., Rosene, D.L., Pandya, D.N., 2004. Motor projections to the basis pontis in rhesus monkey. J. Comp. Neurol. 478, 248–268. https://doi.org/10.1002/cne.20286

Scholin, C.A., Gulland, F., Doucette, G.J., Benson, S., Busman, M., Chavez, F.P., Cordaro, J., DeLong, R., De Vogelaere, A., Harvey, J., Haulena, M., Lefebvre, K., Lipscomb, T., Loscutoff, S., Lowenstine, L.J., Marin, R., Miller, P.E., McLellan, W.A., Moeller, P.D.R., Powell, C.L., Rowles, T., Silvagni, P., Silver, M., Spraker, T., Trainer, V., Van Dolah, F.M., 2000. Mortality of sea lions along the central California coast linked to a toxic diatom bloom. Nature 403, 80–84. https://doi.org/10.1038/47481

Silvagni, P.A., Lowenstine, L.J., Spraker, T., Lipscomb, T.P., Gulland, F.M.D., 2005. Pathology of domoic acid toxicity in California sea lions (Zalophus californianus). Vet. Pathol. 42, 184–191. https://doi.org/10.1354/vp.42-2-184

Stewart, G.R., Zorumski, C.F., Price, M.T., Olney, J.W., 1990. Domoic acid: A dementia-inducing excitotoxic food poison with kainic acid receptor specificity. Exp. Neurol. 110, 127–138. https://doi.org/10.1016/0014-4886(90)90057-Y

Tiedeken, J.A., Muha, N., Ramsdell, J.S., 2013. A cupric silver histochemical analysis of domoic acid damage to olfactory pathways following status epilepticus in a rat model for chronic recurrent spontaneous seizures and aggressive behavior. Toxicol. Pathol. 41, 454–469. https://doi.org/10.1177/0192623312453521

Toyofuku, H., 2006. Joint FAO/WHO/IOC activities to provide scientific advice on marine biotoxins (research report). Mar. Pollut. Bull. 52, 1735–1745. https://doi.org/10.1016/j.marpolbul.2006.07.007

Trainer, V.L., Moore, S.K., Hallegraeff, G., Kudela, R.M., Clement, A., Mardones, J.I., Cochlan, W.P., 2020. Pelagic harmful algal blooms and climate change: Lessons from nature's experiments with extremes. Harmful Algae 91, 101591. https://doi.org/10.1016/j.hal.2019.03.009

Truelove, J., Mueller, R., Pulido, O., Martin, L., Fernie, S., Iverson, F., 1998. 30-day oral toxicity study of domoic acid in cynomolgus monkeys: Lack of overt toxicity at doses approaching the acute toxic dose. Nat. Toxins 5, 111–114. https://doi.org/10.1002/1522-7189(1997)5:3<111::aid-nt5>3.0.co;2-6

Tryphonas, L., Truelove, J., Iverson, F., 1990a. Acute neurotoxicity of domoic acid in cynomolgus monkeys (M. fascicularis). Toxicol. Pathol. 18, 297–303. https://doi.org/10.1177/019262339001800101

Tryphonas, L., Truelove, J., Iverson, F., Todd, E.C.D., Nera, E., 1990b. Neuropathology of experimental domoic acid poisoning in nonhuman primates and rats. Symp. Domoic Acid Toxic. 78–81.

Tryphonas, L., Truelove, J., Todd, E.C.D., Nera, E., Iverson, F., 1990c. Experimental oral toxicity of domoic acid in cynomolgus monkeys (Macaca fascicularis) and rats. Food Chem. Toxicol. 28, 707–715. https://doi.org/10.1016/0278-6915(90)90147-F

Vieira, A.C., Alemañ, N., Cifuentes, J.M., Bermúdez, R., Peña, M.L., Botana, L.M., 2015. Brain pathology in adult rats treated with domoic acid. Vet. Pathol. 52, 1077–1086. https://doi.org/10.1177/0300985815584074

Wekell, J.C., Jurst, J., Lefebvre, K. a, 2004. The origin of the regulatory limits for PSP and ASP toxins in shellfish. J. Shellfish Res. 23, 927–930.

Werring, D.J., Toosy, A.T., Clark, C.A., Parker, G.J.M., Barker, G.J., Miller, D.H., Thompson, A.J., 2000. Diffusion tensor imaging can detect and quantify corticospinal tract degeneration after stroke. J. Neurol. Neurosurg. Psychiatry 69, 269–272. https://doi.org/10.1136/jnnp.69.2.269

Zhu, Z., Qu, P., Fu, F., Tennenbaum, N., Tatters, A.O., Hutchins, D.A., 2017. Understanding the blob bloom: Warming increases toxicity and abundance of the harmful bloom diatom Pseudo-nitzschia in California coastal waters. Harmful Algae 67, 36–43. https://doi.org/10.1016/j.hal.2017.06.004

## 4.8 Tables and Figures

***Table 4.1: Animal Characteristics and Pathology Outcomes***

| Animal Number | Dose (mg/kg/day) | Weight (kg) | Age (years) | Total Dosing Time (days) | n tremors observed /n sessions during dosing | Time Postdosing (days) | n tremors observed /n sessions postdosing | Pathology |
|---|---|---|---|---|---|---|---|---|
| **1** | **0** | **3.98** | **7.33** | **724** | **0.02** | **0** | | **None** |
| 2 | 0 | 3.62 | 5.87 | 717 | 0.11 | 0 | | 1 focal microglia reaction in internal capsule |
| **3** | **0** | **3.24** | **6.36** | **678** | **0.02** | **0** | | **None** |
| 4 | **0** | **3.58** | **6.35** | **653** | **0.03** | **0** | | **None** |
| **5** | **0** | **3.12** | **6.21** | **477** | **0.06** | **0** | | **None** |
| 6 | 0 | 2.84 | 7.02 | 469 | 0.64 | 0 | | None |
| **7** | **0** | **3.58** | **6.96** | **454** | **0.04** | **0** | | **None** |
| **8** | **0** | **3.38** | **7.23** | **448** | **0.06** | **0** | | **None** |
| 9 | 0.075 | 4.83 | 6.37 | 604 | 0.18 | 0 | | 1 focal microglia reaction in thalamus |
| 10 | 0.075 | 3.19 | 7.06 | 436 | 0.37 | 0 | | 1 microglia reaction in nucleus accumbens |
| **11** | **0.075** | **3.41** | **6.69** | **420** | **0.26** | **0** | | **None** |
| 12 | 0.075 | 3.33 | 7.07 | 392 | 0 | 0 | | 2 focal microglia reactions in fornix/fimbria |
| **13** | **0.075** | **3.11** | **6.32** | **385** | **0.4** | **0** | | **None** |
| 14 | 0.075 | 3.80 | 11.12 | 371 | 0.29 | 0 | | None |
| 15 | 0.075 | 3.03 | 5.98 | 322 | 0.36 | 176 | 0.37 | None |
| 16 | 0.075 | 3.08 | 5.94 | 321 | 0.18 | 0 | | None |
| 17 | 0.075 | 3.05 | 6.48 | 268 | 0.08 | 216 | 0.13 | None |
| 18 | 0.075 | 4.69 | 6.72 | 259 | 0.02 | 302 | 0.06 | None |
| 19 | 0.075 | 3.46 | 6.71 | 221 | 0 | 355 | 0 | None |
| **20** | **0.15** | **3.77** | **6.40** | **612** | **0.68** | **0** | | **2 microglia reactions in SGZ and fornix/fimbria** |
| **21** | **0.15** | **3.46** | **6.52** | **598** | **0.25** | **0** | | **None** |
| 22 | 0.15 | 3.72 | 6.53 | 428 | 0.11 | 0 | | 1 focal microglia reaction in thalamus |
| **23** | **0.15** | **4.00** | **10.35** | **413** | **0.3** | **0** | | **None** |
| **24** | **0.15** | **2.96** | **7.09** | **392** | **0.8** | **0** | | **Focal, active neuronal death in thalamus** |
| 25 | 0.15 | 3.26 | 7.12 | 371 | 0.01 | 0 | | None |
| 26 | 0.15 | 3.06 | 7.03 | 343 | 0.03 | 0 | | None |
| 27 | 0.15 | 4.22 | 5.53 | 294 | 0.59 | 231 | 0.66 | Widespread microglia reaction in fornix/fimbria, internal capsule, and thalamus |
| 28 | 0.15 | 3.56 | 7.72 | 268 | 0.76 | 221 | 0.6 | Extensive, older lesion in thalamus |

***Bolded** indicates animals selected for MRI.*

***Table 4.2: Outcomes of Interest***

| **Assessment** | **Brain Region** | **Signs of Neurotoxicity** |
|---|---|---|
| MRI: Brain Volume | Hippocampus and thalamus | Neuronal atrophy (decreased volume) |
| MRI: Tractography | White matter between hippocampus and thalamus (including fimbria, fornix, and internal capsule) | Structural connectivity changes (increased or decreased clusters in tractography model) |
| H&E | Hippocampus, thalamus, fimbria, fornix, and internal capsule | Dead cells (eosin+) |
| LFB | Fimbria, fornix, and internal capsule | Demyelination (decreased LFB) |
| CV | Hippocampus and thalamus | Fewer neurons (decreased CV) |
| GFAP | Hippocampus, thalamus, fimbria, fornix, and internal capsule | Astrocyte reactivity (increased processes number and density) |
| Iba-1 | Hippocampus, thalamus, fimbria, fornix, and internal capsule | Microglia reactivity (increased microglia density, ameboid cell body, blebbing, fragmentation, increased process number and density, increased irregulatities) |

***Table 4.3: ROI Volumes***

| Animal Number | Dose (mg/kg/day) | Right Hippocampus | Left Hippocampus | Right Thalamus | Left Thalamus |
|---|---|---|---|---|---|
| 1 | 0 | 413.1 | 419.7 | 478.2 | 477.4 |
| 3 | 0 | 355.4 | 359.4 | 482.6 | 483.6 |
| 4 | 0 | 378.8 | 382.8 | 491.0 | 503.1 |
| 5 | 0 | 346.9 | 358.1 | 440.5 | 432.3 |
| 7 | 0 | 436.2 | 434.8 | 540.0 | 538.7 |
| 8 | 0 | 429.8 | 460.7 | 544.4 | 572.2 |
| | **Mean** | **393.4** | **402.6** | **496.1** | **501.2** |
| | **SEM** | **14.3** | **15.8** | **14.8** | **18.3** |
| 11 | 0.075 | 399.2 | 394.1 | 511.7 | 517.6 |
| 13 | 0.075 | 413.5 | 401.2 | 595.2 | 605.3 |
| 20 | 0.15 | 340.2 | 325.6 | 478.5 | 477.3 |
| 21 | 0.15 | 404.4 | 404.3 | 498.7 | 502.0 |
| 23 | 0.15 | 411.8 | 428.0 | 538.2 | 542.4 |
| 24 | 0.15 | 345.7 | 332.6 | 460.2 | 450.2 |
| | **Mean** | **385.8** | **381.0** | **513.8** | **515.8** |
| | **SEM** | **12.5** | **15.6** | **17.9** | **20.2** |

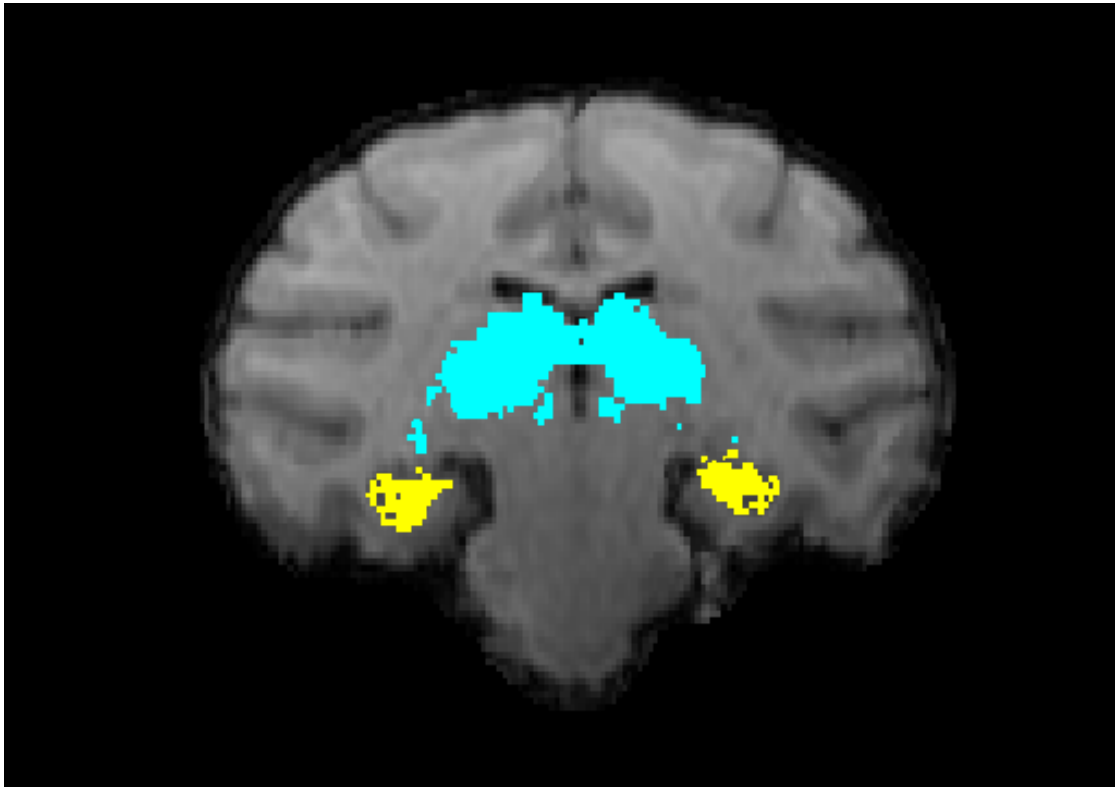

*Figure 4.1: MRI tracings of the hippocampus and thalamus. Shows the hippocampus (yellow) and thalamus (blue) regions masks used for volumetric analyses and tractography seed points.*

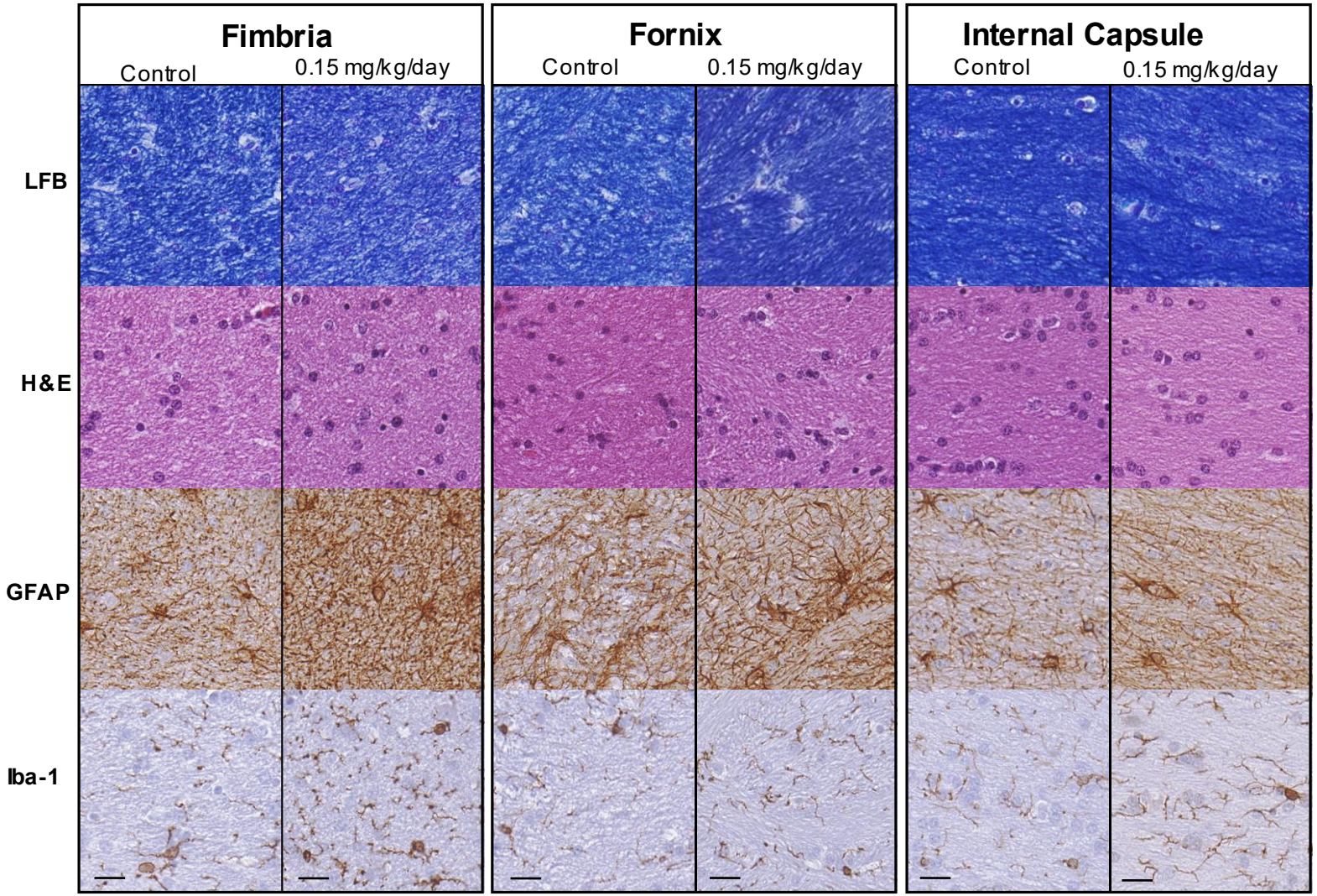


*Figure 4.2: Normal pathology in the white matter tracts. Shows the staining of Luxol Fast Blue (LFB), hematoxylin and eosin (H&E), anti-glial fibrillary acidic protein (GFAP), and anti-ionized calcium binding adaptor molecule 1 (Iba-1) in representative a control and high dose animal across the fimbria of the hippocampus, the fornix, and internal capsule. Images are represented at 40x magnification. Scale = 20 µm.*

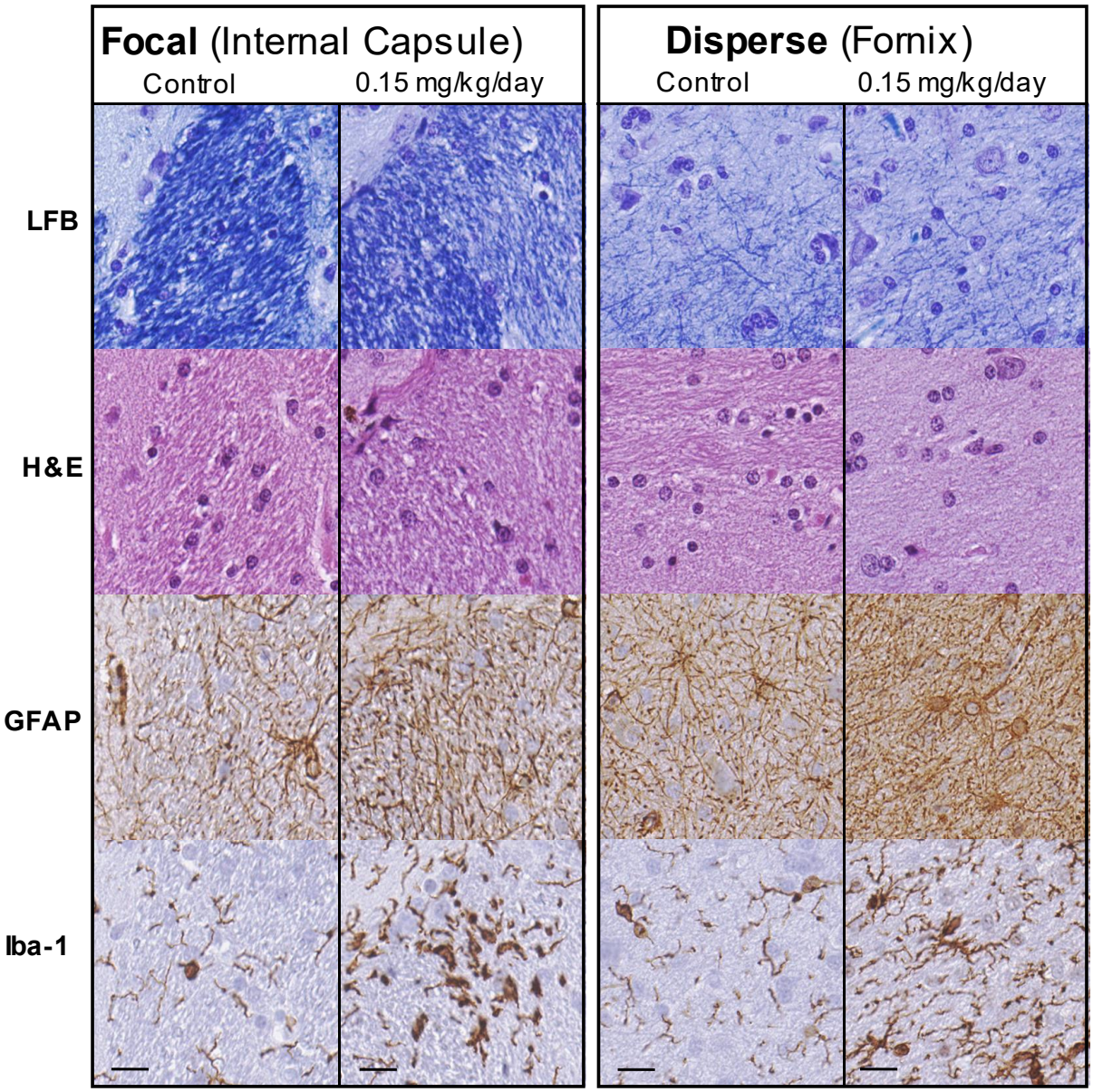


*Figure 4.3: White matter microglia reactions. Shows the staining of Luxol Fast Blue (LFB), hematoxylin and eosin (H&E), anti-glial fibrillary acidic protein (GFAP), and anti-ionized calcium binding adaptor molecule 1 (Iba-1) in a representative control and high dose animal demonstrating either focal microglia reactions (LEFT) or disperse microglia reactions (RIGHT). No signs of cell death were suggested by adjacent slides in the H&E images. Images are represented at 40x magnification. Scale = 20 μm.*

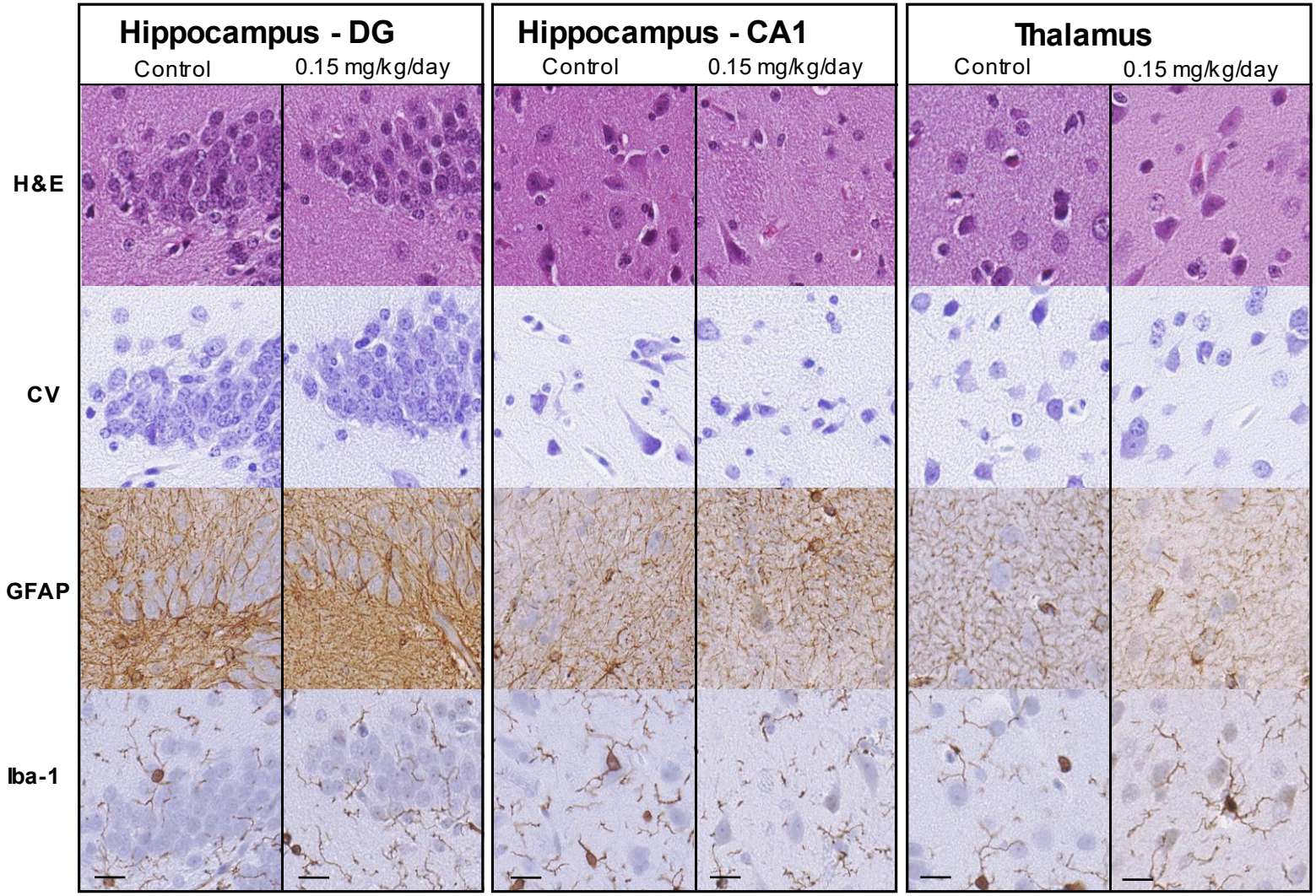


*Figure 4.4: Normal pathology in the gray matter. Shows the staining of hematoxylin and eosin (H&E), cresyl violet (CV), anti-glial fibrillary acidic protein (GFAP), and anti-ionized calcium binding adaptor molecule 1 (Iba-1) in representative control and high dose animals across the dentate gyrus of the hippocampus, the CA1 region of the hippocampus, and thalamus. Images are represented at 40x magnification. Scale = 20 µm.*

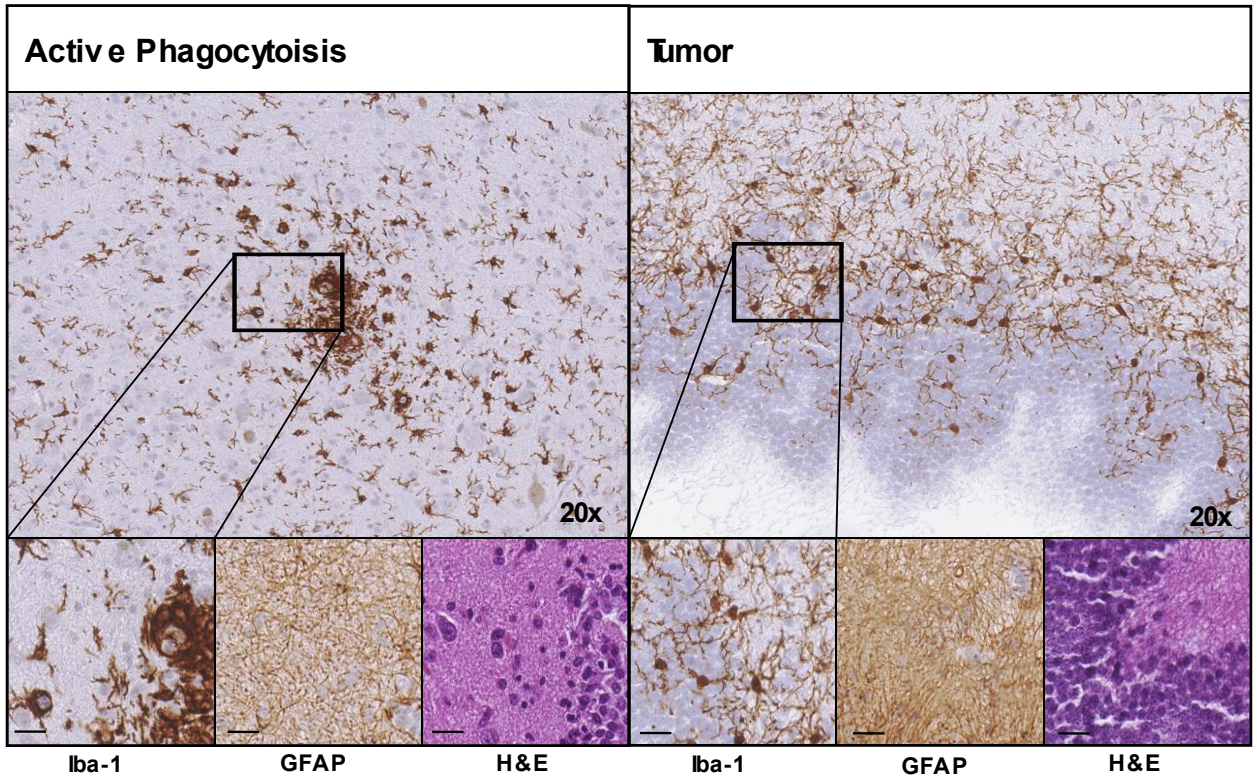


*Figure 4.5: Overt pathology in the gray matter. Shows the staining of anti-ionized calcium binding adaptor molecule 1 (Iba-1), anti-glial fibrillary acidic protein (GFAP), and hematoxylin and eosin (H&E) from two separate 0.15 mg/kg/day demonstrating cell death in the thalamus. LEFT: Active phagocytosis of dying cells occurring. RIGHT: Morphology representing a tumor and abnormal cell development. TOP: Images are represented at 20x magnification. BOTTOM: Images are represented at 40x magnification and scale = 20 μm.*

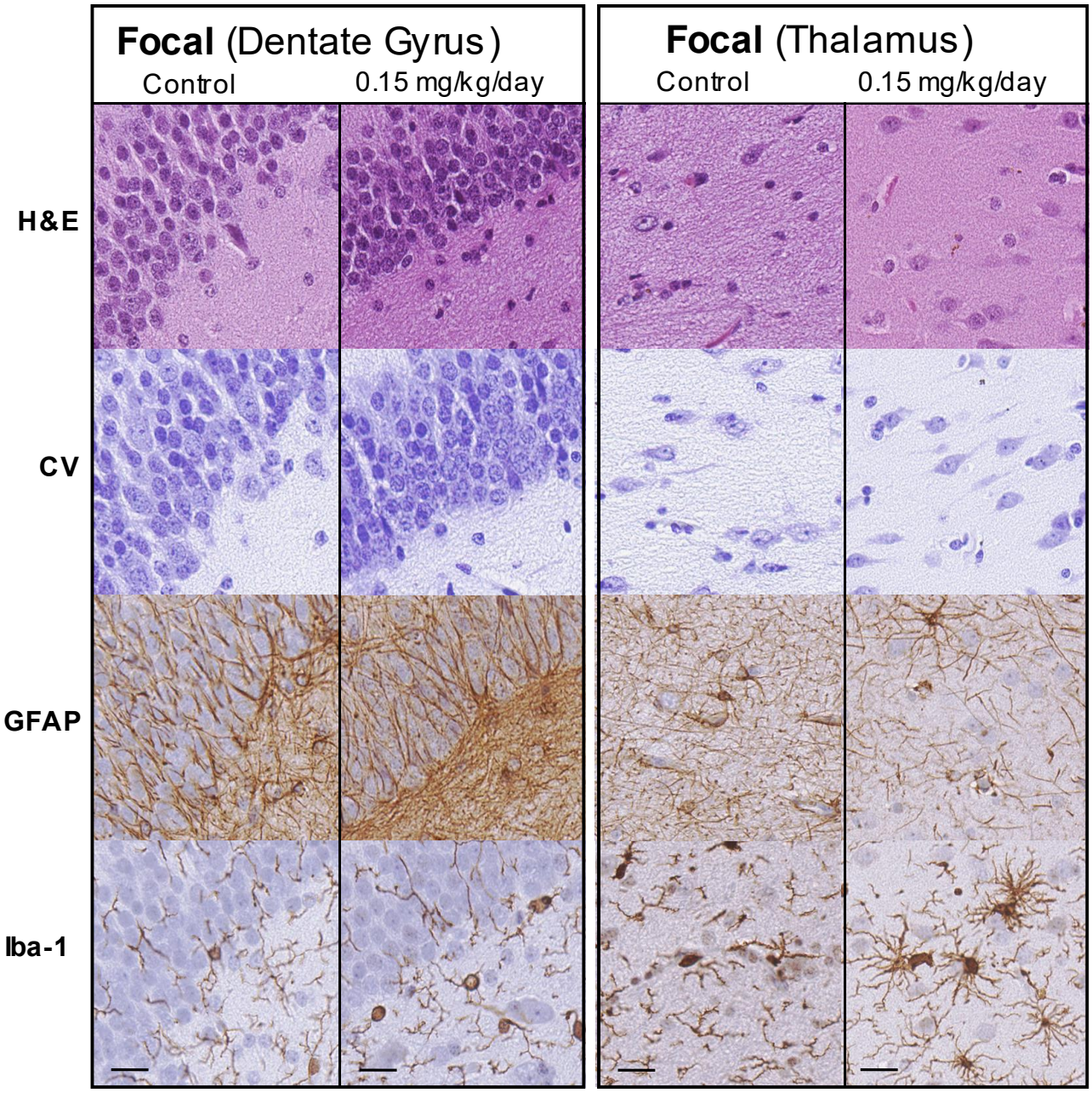


*Figure 4.6: Gray matter microglia reactions. Shows the staining of hematoxylin and eosin (H&E), cresyl violet (CV), anti-glial fibrillary acidic protein (GFAP), and anti-ionized calcium binding adaptor molecule 1 (Iba-1) in a representative control and high dose animal demonstrating two different morphology observed in focal microglia reactions. No signs of neuronal death were suggested by adjacent slides in the H&E and CV images. Images are represented at 40x magnification. Scale = 20 µm.*

## Chapter 5: Conclusions and Future Directions

### 5.1 Dissertation Summary

Domoic acid (DA) is a naturally occurring, marine algal toxin and a potent human neurotoxin. While there is presently a regulatory limit constraining human exposure to this toxin (20 ppm in shellfish or approximately 0.075-0.15 mg/kg) (Mariën, 1996; Toyofuku, 2006; Wekell et al., 2004), this limit may not be adequately protective. Studies of frequent shellfish consumers have reported deficits in memory that impact everyday life (Grattan et al., 2018, 2016). These effects are significant, but other neurological effects from chronic DA exposures near the regulatory limit are not well studied.

Previous research from our lab used a cohort of *Macaca fascicularis* monkeys to study the reproductive and offspring neurodevelopmental effects of chronic, oral exposure to 0.075 and 0.15 mg DA/kg/day (Burbacher et al., 2019). Exposure to DA at these low levels resulted in clinical symptoms of neurotoxicity in adult animals, with exposed monkeys demonstrating intention tremors when performing a reaching task. This dissertation describes studies using this cohort of monkeys to address the neurological effects of low-level, chronic exposure to DA, by using multimodal neurological tools, including magnetic resonance imaging (MRI), electroencephalography (EEG), and histopathology. MRI and EEG experiments were conducted concurrently, after monkeys had been exposed to DA daily for over a year, and histopathology was assessed postmortem, after approximately 2 years of exposure.

First, as detailed in Chapter 2, *in vivo*, global brain analyses were conducted using MRI to locate injury associated with DA exposure and tremors. DA causes atrophy and lesions at high doses in the hippocampus, amygdala and thalamus (Teitelbaum et al., 1990), and tremors have been linked to damage in the cerebellum, thalamus, frontal cortex, sensory cortex, and motor cortex (Brittain and Brown, 2013; Louis, 2014; Muthuraman et al., 2015). Initial MRI analyses in this dissertation were aimed at evaluating the association of DA exposure and

tremor severity by 1) locating any signs of brain lesions, 2) assessing global white matter structural changes, and 3) evaluating neurochemical changes that have been linked to global brain damage. These assessments showed that DA exposed, tremoring animals did not have gross brain lesions, and neurochemistry was indistinguishable when comparing control and DA-exposed animals. Tremor severity, however, was significantly related to clusters of decreased fractional anisotropy (FA), a measure of white matter integrity, primarily in the fornix and internal capsule. Additionally, there was small, but significant correlation between tremor severity and increased lactate in the thalamus.

The fornix is the primary white matter tract that connects fibers from the hippocampus and fimbria of the hippocampus to the thalamus and other structures in the brain (Christiansen et al., 2016). The internal capsule is the key white matter tract that carries fiber bundles from the spinal cord to the thalamus and motor cortex (Morecraft et al., 2002). These two key white matter structures are connected to areas of the brain previously associated with both DA exposure effects as well as cases of human tremors; but this MRI measure for white matter integrity can be indicative of several different biological responses to injury. Specifically, decreases in integrity have been associated with decreases in the axons or myelin or an increase in glia cells as in injury responses (Werring et al., 2000). Further, the increase in lactate observed with increasing tremor scores has also been linked to changes in glia in the brain. We hypothesized that because there were no other alterations in global MRI measures, the observed changes were most likely linked to changes in glia cells. Alteration in glia could be due to an underlying response to toxic assault, but further investigation was needed to assess glia responses and other cellular impacts within the affected regions found in these global assessments (see Chapter 4).

Chapter 3 outlines studies designed to assess functional neuroelectric changes after DA exposure. DA is a known epileptogen and can lead to seizures and gross neuronal damage

(Teitelbaum et al., 1990), and tremors can be an inidcator of early signs of seizures or epilepsy (Authier et al., 2019). Previous research has identified spectral changes in neurophysiology in cases of DA-induced epilepsy (Sawant et al., 2010). These changes can be observed with power, a quantitatve measure from EEGs that reflects the degree of signal generated across the brain. Sedated EEG power was compared between DA exposed animals and controls as well as based on observed tremors. Results suggested that power was differentially altered due to DA exposure, but alterations were not dose-dependent or related to tremor scores. Exposure to DA was associated with increased power in the lowest power band (delta, 1-4 Hz), but increased power in other bands (alpha, 5-8 Hz; theta, 9-12 Hz). While these alterations in power were not related to our clinical outcome (intention tremors), observed changes may still have broad implications, considering animals were sedated during EEG. Even small alterations in power have been associated with a variety of different emotional activities (Knyazev, 2007), memory functions, and other cognitive processes (Cavanagh and Frank, 2014; Harmony, 2013), as well as neurological disease states (Newson and Thiagarajan, 2019). The difference observed may be suggestive of subtle changes in neurosynaptic function after chronic DA exposure *in vivo*.

In Chapter 4, follow-up MRI techniques and postmortem histopathological assessments were used to better understand the underlying pathology and cellular changes from the global results presented in Chapter 2. Altered white matter integrity in the fornix and internal capsule may also affect associated gray matter regions, including the hippocampus and thalamus. Tractography was used to assess the white matter connectivity (i.e. axons and myelin) between these two gray matter structures, and volumetric analyses were used to assess any neuronal cell-body death that could result in decreased axons. All additional MRI analyses did not suggest that axons, myelin, or neurons were structurally disturbed after long-term exposure to DA. Histopathological examination of the neurons, myelin, and glial cells in these regions further

supported this finding and did not suggest that the white matter structural integrity alterations associated with DA were due to changes in neurons, axons, or myelin. Interestingly, small focal reactions of microglia, the primary immune cell of the brain, were found to be more prevalent in DA exposed animals than in control animals. Previous work has shown that low levels of DA can lead to the production of reactive oxygen species (Giordano et al., 2013), which can promote neuroinflammatory pathways and recruit microglia (Kono and Rock, 2008). Other glia, including astrocytes, did not appear to be affected by low-level exposure to DA. These findings suggest that the decreased integrity in white matter macrostructure may be connected primarily with changes in glia, which could be linked with neuroinflammation, but not neuronal cell death or changes in axons/myelin structure (Fig. 5.1).

**5.2 Conclusions**

The collective work from this dissertation indicate that levels of DA near the current human regulatory limit do not cause overt neuroinjury in a nonhuman primate model, but do cause subtle, neurotoxic effects that can impact the structure, physiology, and cellular response in the brain. These aberrations were observed in white and gray matter structures within circuits that include fibers that connect to key DA targets in the brain, including the hippocampus and thalamus, and damage in these tracts has been associated with anterograde amnesia, the key symptom from acute DA exposure (Aggleton and Brown, 1999). The underlying link to changes in brain regions associated with memory function is concerning, given that recent human evidence suggests that chronic exposure to DA in adults is connected with clinically meaningful decreases in everyday memory function (Grattan et al., 2018). Altogether, findings from this dissertation suggest that DA exposure in the nonhuman primate model, even at levels that are currently safe for human consumption, is linked to neurotoxic effects in key regions of the brain associated with memory and motor function.

## 5.2 Future Research

Additional studies are necessary to understand the underlying mechanism of low-level chronic exposure to DA and how the present findings translate to vulnerable populations (i.e. young children or aged adults). While there are some *in vitro* studies assessing the mechanism of neurotoxicity of low-level DA exposure, there is presently a highly limited body of evidence from *in vivo* laboratory models and human epidemiological cohorts linking contemporary DA exposures to health effects. Some models suggest that there are significant neurological effects, but the mechanism associated with the functional effects reported is presently unknown (Grattan et al., 2018, 2016; Lefebvre et al., 2017; Moyer et al., 2018). This is of particular concern to communities that are chronically exposed to DA, such as those in coastal Native Nations in Washington state (Boushey et al., 2016). Continued research is needed to further protect vulnerable population from toxic effects associated with DA exposure. Finally, current regulatory limits should be re-examined with all of this information at hand, to best protect the health of vulnerable populations exposed to this common marine contaminant.

## 5.3 References

Aggleton, J.P., Brown, M.W., 1999. Episodic memory, amnesia, and the hippocampal-anterior thalamic axis. Behav. Brain Sci. 22, 425–444. https://doi.org/10.1017/S0140525X99002034

Authier, S., Arezzo, J., Pouliot, M., Accardi, M. V., Boulay, E., Troncy, E., Dubuc Mageau, M., Tan, W., Sanfacon, A., Mignault Goulet, S., Paquette, D., 2019. EEG: Characteristics of drug-induced seizures in rats, dogs and non-human primates. J. Pharmacol. Toxicol. Methods 97, 52–58. https://doi.org/10.1016/j.vascn.2019.03.004

Boushey, C.J., Delp, E.J., Ahmad, Z., Wang, Y., Roberts, S.M., Grattan, L.M., 2016. Dietary assessment of domoic acid exposure: What can be learned from traditional methods and new applications for a technology assisted device. Harmful Algae 57, 51–55. https://doi.org/10.1016/j.hal.2016.03.013

Brittain, J.S., Brown, P., 2013. The many roads to tremor. Exp. Neurol. 250, 104–107. https://doi.org/10.1016/j.expneurol.2013.09.012

Burbacher, T., Grant, K., Petroff, R., Crouthamel, B., Stanley, C., McKain, N., Shum, S., Jing, J., Isoherranen, N., 2019. Effects of chronic, oral domoic acid exposure on maternal

reproduction and infant birth characteristics in a preclinical primate model. Neurotoxicol. Teratol. 440354. https://doi.org/10.1101/440354

Cavanagh, J.F., Frank, M.J., 2014. Frontal theta as a mechanism for cognitive control. Trends Cogn. Sci. https://doi.org/10.1016/j.tics.2014.04.012

Christiansen, K., Dillingham, C.M., Wright, N.F., Saunders, R.C., Vann, S.D., Aggleton, J.P., 2016. Complementary subicular pathways to the anterior thalamic nuclei and mammillary bodies in the rat and macaque monkey brain. Eur. J. Neurosci. 43, 1044–1061. https://doi.org/10.1111/ejn.13208

Giordano, G., Kavanagh, T.J., Faustman, E.M., White, C.C., Costa, L.G., 2013. Low-level domoic acid protects mouse cerebellar granule neurons from acute neurotoxicity: Role of glutathione. Toxicol. Sci. 132, 399–408. https://doi.org/10.1093/toxsci/kft002

Grattan, L.M., Boushey, C.J., Liang, Y., Lefebvre, K.A., Castellon, L.J., Roberts, K.A., Toben, A.C., Morris, J.G.J., 2018. Repeated dietary exposure to low levels of domoic acid and problems with everyday memory: Research to public health outreach. Toxins (Basel). 10, 103. https://doi.org/10.3390/toxins10030103

Grattan, L.M., Boushey, C.J., Tracy, K., Trainer, V.L., Roberts, S.M., Schluterman, N., Morris, J.G.J., 2016. The association between razor clam consumption and memory in the CoASTAL cohort. Harmful Algae 57, 20–25. https://doi.org/10.1016/j.hal.2016.03.011

Harmony, T., 2013. The functional significance of delta oscillations in cognitive processing. Front. Integr. Neurosci. https://doi.org/10.3389/fnint.2013.00083

Knyazev, G.G., 2007. Motivation, emotion, and their inhibitory control mirrored in brain oscillations. Neurosci. Biobehav. Rev. https://doi.org/10.1016/j.neubiorev.2006.10.004

Kono, H., Rock, K.L., 2008. How dying cells alert the immune system to danger. Nat. Rev. Immunol. https://doi.org/10.1038/nri2215

Lefebvre, K.A., Kendrick, P.S., Ladiges, W., Hiolski, E.M., Ferriss, B.E., Smith, D.R., Marcinek, D.J., 2017. Chronic low-level exposure to the common seafood toxin domoic acid causes cognitive deficits in mice. Harmful Algae 64, 20–29. https://doi.org/10.1016/j.hal.2017.03.003

Louis, E.D., 2014. Understanding Essential Tremor: Progress on the Biological Front. Neurol Neurosci. Rep 14, 450. https://doi.org/10.1080/10810730902873927.Testing

Mariën, K., 1996. Establishing tolerable dungeness crab (Cancer magister) and razor clam (Siliqua patula) domoic acid contaminant levels. Environ. Health Perspect. 104, 1230–6. https://doi.org/10.1289/ehp.961041230

Morecraft, R.J., Herrick, J.L., Stilwell-Morecraft, K.S., Louie, J.L., Schroeder, C.M., Ottenbacher, J.G., Schoolfield, M.W., 2002. Localization of arm representation in the corona radiata and internal capsule in the non-human primate. Brain 125, 176–198. https://doi.org/10.1093/brain/awf011

Moyer, C.E., Hiolski, E.M., Marcinek, D.J., Lefebvre, K.A., Smith, D.R., Zuo, Y., 2018. Repeated low level domoic acid exposure increases CA1 VGluT1 levels, but not bouton density, VGluT2 or VGAT levels in the hippocampus of adult mice. Harmful Algae 79, 74–86. https://doi.org/10.1016/j.hal.2018.08.008

Muthuraman, M., Deuschl, G., Anwar, A.R., Mideksa, K.G., Von Helmolt, F., Schneider, S.A., 2015. Essential and aging-related tremor: Differences of central control. Mov. Disord. 30, 1673–1680. https://doi.org/10.1002/mds.26410

Newson, J.J., Thiagarajan, T.C., 2019. EEG Frequency Bands in Psychiatric Disorders: A Review of Resting State Studies. Front. Hum. Neurosci. 12. https://doi.org/10.3389/fnhum.2018.00521

Sawant, P.M., Mountfort, D.O., Kerr, D.S., 2010. Spectral analysis of electrocorticographic activity during pharmacological preconditioning and seizure induction by intrahippocampal domoic acid. Hippocampus 20, 994–1002. https://doi.org/10.1002/hipo.20698

Teitelbaum, J., Zatorre, R.J., Carpenter, S., Gendron, D., Cashman, N.R., 1990. Neurological Sequelae of Domoic Acid Intoxication. Symp. Domoic Acid Toxic. 16, 9–12. https://doi.org/10.2174/13816128236661701241

Toyofuku, H., 2006. Joint FAO/WHO/IOC activities to provide scientific advice on marine biotoxins (research report). Mar. Pollut. Bull. 52, 1735–1745. https://doi.org/10.1016/j.marpolbul.2006.07.007

Wekell, J.C., Jurst, J., Lefebvre, K. a, 2004. The origin of the regulatory limits for PSP and ASP toxins in shellfish. J. Shellfish Res. 23, 927–930.

Werring, D.J., Toosy, A.T., Clark, C.A., Parker, G.J.M., Barker, G.J., Miller, D.H., Thompson, A.J., 2000. Diffusion tensor imaging can detect and quantify corticospinal tract degeneration after stroke. J. Neurol. Neurosurg. Psychiatry 69, 269–272. https://doi.org/10.1136/jnnp.69.2.269

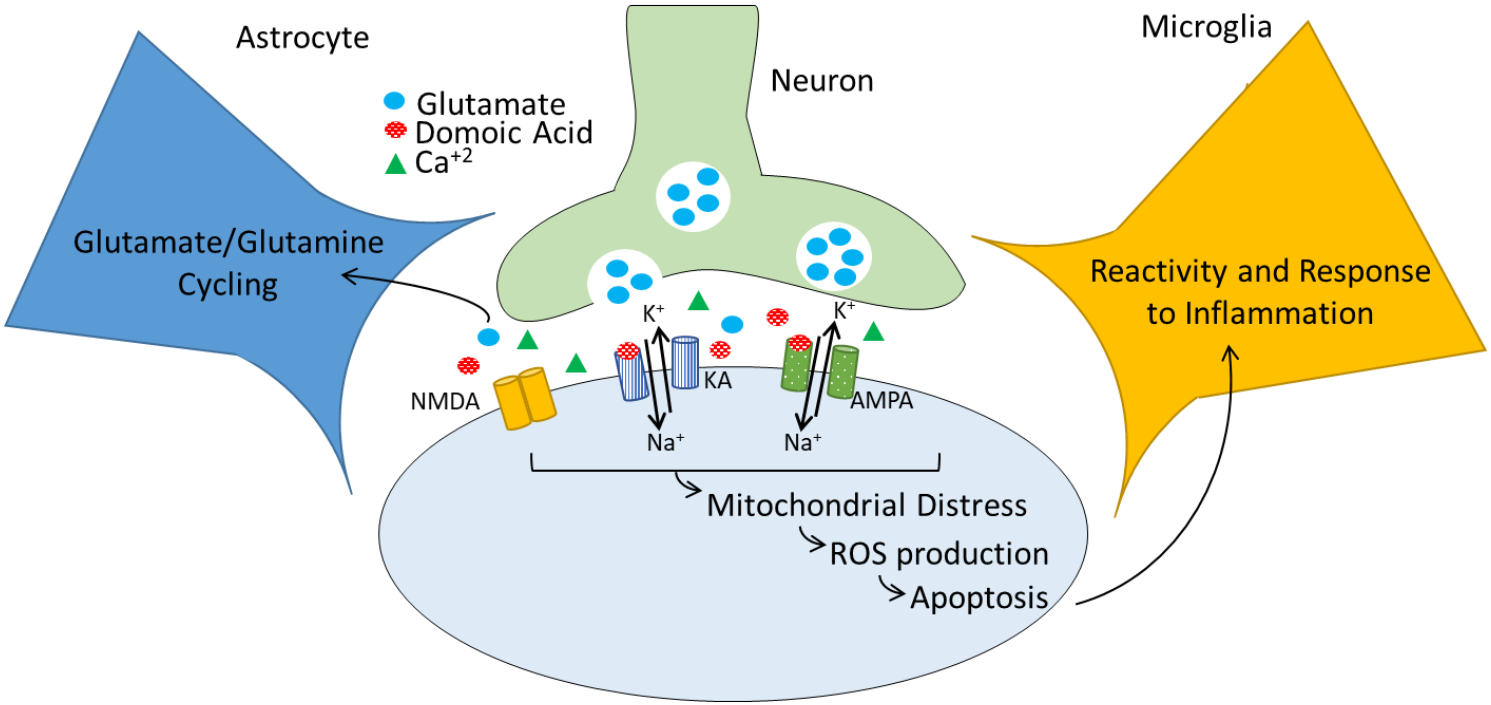


*Figure 5.1: Astrocyte and microglia involvement in low-level DA toxicity. Adapted from Figure 1.2, this shows the proposed involvement of glia cells in the neurological response to low-level and chronic DA toxicity. Astrocytes are essential in the glutamate-glutamine cycling and will uptake excess glutamate from the synapse. Microglia are responsive to ROS production and apoptosis and may help reduce neuroinflammation. Overactive microglia may also be responsible for the induction of continued neuroinflammation, which can lead to long-term and persistent effects.*